

DIFFERENTIATION AND CONTRACTILITY OF COLON SMOOTH MUSCLE
UNDER NORMAL AND DIABETIC CONDITIONS

Ketrija Touw

Submitted to the faculty of the University Graduate School
in partial fulfillment of the requirements
for the degree
Doctor of Philosophy
in the Department of Cellular and Integrative Physiology,
Indiana University

May 2011

Accepted by the Faculty of Indiana University, in partial fulfillment of the requirements for the degree of Doctor of Philosophy.

B. Paul Herring, Ph.D., Chair

Patricia J. Gallagher, Ph.D.

Doctoral Committee

Simon J. Rhodes, Ph.D.

February 15, 2011

Robert V. Considine, Ph.D.

Dedication

I would like to dedicate this dissertation to my daughter Emilia, my husband Daniel, my mom Rasma and my brother Edmunds.

To Emilia, you have been a big part of my life through my study years. You have brought a great joy to my life. I could not wish for a better daughter than my little sweet girl. With my work I hope to encourage you to do great things in your life whatever you decide to do in the future.

To Daniel, your love and support through these years have been invaluable for me. It have been comforting to know that as challenging my day can be I can always relay on your good attitude and understanding. Your passion for life, work, music and anything you do have been inspirational for me. It is a joy to be around you and share my life with you. I could not have done it without you.

To my mom, you have always been a loving and caring person. I will always appreciate your support for me. You have shown me how much hard work matters and have set standards for how to be a great working mother. I can not be more thankful for everything you have done for me.

To Edmunds, it is a great joy to have such a great brother with such big heart. I know that you will always walk an extra mile for me.

Acknowledgments

First and foremost, I would like to thank my advisor, Dr. B. Paul Herring, for the guidance through my studies. Through the years from when I was working as technician and later as a graduate student, I have received great support in my scientific work and also on a personal level. In Paul's lab I have received great mentorship and advice during the progression of my project. Paul's guidance and support through the many challenges encountered through my project have been invaluable and have helped me to become a more independent scientist. I will always be grateful for the opportunity to be part of the Herring lab.

I would also like to thank my committee members Dr. Patricia Gallagher, Dr. Simon Rhodes and Dr. Robert Considine. I appreciate the time and thoughtful advice that I have received through my studies. Your challenging questions have helped me to develop critical thinking and have been invaluable for my scientific advancement.

I would also like to thank our collaborators who have been very helpful with their expert insight and have allowed me to use their equipment. Dr. Jonathan Tune and his lab have been very helpful with contractility studies and generously allowed me to use their equipment numerous times. I would like to acknowledge Dr. Alexander Obukhov and Dr. Saikat Chakraborty for your expertise in calcium imaging and many hours spent for accomplishing this part of the study. I am also grateful for Dr. Susan Gunst's and Dr. Wenwu Zhang's help with myosin phosphorylation studies. I would also like to thank Dr. Yun Laing and Huisi Ai for performing CT scan study.

I am very honored and thankful for the financial support I have received from NIH Diabetes and Obesity T32 training program. It has been very helpful for my career through these years.

I would like to sincerely thank current and former Herring and Gallagher lab members for your collegiality and fun times shared. Especially I would like to thank Herring lab members April Hoggatt for training me when I first joined the lab, Dr. Min Zhang and Dr. Jiliang Zhou for your help and advice, Meng Chen, Dr. Jury Kim and Rebekah Jones for your contributions to my work and your friendship. I would also like to say special thanks to Dr. Ryan Widau and Dr. Emily Blue from Gallagher lab for all your advice and friendship. It has been truly great to be part of such a great work environment.

I would like to thank my husband Daniel and his family Daniel, Nancy, Jennifer, Sergio, Christopher, Ian and Sophia for all their support and acceptance of me. It has been a great pleasure to have such a wonderful new family in United States. I would like to thank my daughter Emilia for being patient at times when I have to work. I would also like to thank my Latvian family - my parents Rasma and Raimonds, my brother Edmunds, his wife Dina, and my grandparents Emilija, Katrina and Leokadija. Each of you has contributed to my growth at different times through my life and your encouragement has let me to believe in myself and achieve my goals in life.

Abstract

Ketrija Touw

DIFFERENTIATION AND CONTRACTILITY OF COLON SMOOTH MUSCLE UNDER NORMAL AND DIABETIC CONDITIONS

Intestinal smooth muscle development involves complex transcriptional regulation leading to cell differentiation of the circular, longitudinal and muscularis mucosae layers. Differentiated intestinal smooth muscle cells express high levels of smooth muscle-specific contractile and regulatory proteins, including telokin. Telokin is regulatory protein that is highly expressed in visceral smooth muscle. Analysis of cis-elements required for transcriptional regulation of the telokin promoter by using hypoxanthine-guanine phosphoribosyltransferase (*Hprt*)-targeted reporter transgenes revealed that a 10 base pair large CC(AT)₆GG cis-element, called CArG box is required for promoter activity in all tissues. We also determined that an additional 100 base pair region is necessary for transgene activity in intestinal smooth muscle cells. To examine how transcriptional regulation of intestinal smooth muscle may be altered under pathological conditions we examined the effects of diabetes on colonic smooth muscle. Approximately 76% of diabetic patients develop gastrointestinal (GI) symptoms such as constipation due to intestinal dysmotility. Mice were treated with low-dose streptozotocin to induce a type 1 diabetes-like hyperglycemia. CT scans revealed decreased overall GI tract motility after 7 weeks of hyperglycemia. Acute (1 week) and chronic (7 weeks) diabetic mice also had decreased potassium chloride (KCl)-induced colon smooth muscle contractility. We hypothesized that decreased smooth muscle contractility at least in part, was due to alteration of contractile protein gene expression. However, diabetic mice showed no changes in mRNA or protein levels of smooth muscle contractile proteins. We determined that the decreased colonic contractility was associated with an attenuated intracellular calcium increase, as measured by ratio-metric

imaging of Fura-2 fluorescence in isolated colonic smooth muscle strips. This attenuated calcium increase resulted in decreased myosin light chain phosphorylation, thus explaining the decreased contractility of the colon. Chronic diabetes was also associated with increased basal calcium levels. Western blotting and quantitative real time polymerase chain reaction (qRT-PCR) analysis revealed significant changes in calcium handling proteins in chronic diabetes that were not seen in the acute state. These changes most likely reflect compensatory mechanisms activated by the initial impaired calcium response. Overall my results suggest that type 1 diabetes in mice leads to decreased colon motility in part due to altered calcium handling without altering contractile protein expression.

B. Paul Herring Ph.D., Chair

Table of Contents

List of Tables.....	x
List of Figures.....	xi
Abbreviations	xiii
Chapter I: Introduction.....	1
Structure and functions of the colon	1
Regulation of colonic contractility	2
Differentiation and development of the colon smooth muscle.....	5
Smooth muscle contractile and regulatory proteins	7
Transcriptional regulation of smooth muscle	8
Regulation of smooth muscle-specific genes by Serum response factor (SRF).....	10
Approaches to generate transgenic mice for smooth muscle promoter analysis.....	12
Colon smooth muscle in diabetes.....	14
Diabetes overview	14
Diabetes effects on the GI tract	16
Posttranslational protein modifications and contractility	19
Inflammation and contractility.....	20
Thesis and Rationale.....	21
Chapter II: <i>Hprt</i> -targeted transgenes provide new insights into smooth muscle-restricted promoter activity.....	28
Summary	28
Introduction.....	29
Methods.....	31

Results	34	
Discussion	38	
Chapter III: Type 1 diabetes leads to altered calcium signaling in		
chronic and acute diabetic mice	55	
Introduction.....	55	
Methods.....	57	
Results	61	
Discussion	66	
Chapter IV: Conclusions and future directions		87
References.....	96	
Curriculum Vitae		

List of Tables

Table 1 Relative expression levels of β -galactosidase transgenes	53
Table 2 <i>Hprt</i> -targeted transgene expression pattern.....	54
Table 3 Primers used for qRT-PCR.....	86

List of Figures

Figure 1 Layers of the colon.....	23
Figure 2 Channels and receptors involved in colon smooth muscle calcium signaling	24
Figure 3 Structure of the mouse mylk1 gene, mylk1 transcripts and minimal telokin promoter schematics.....	25
Figure 4 Diabetes related defects of gastrointestinal tract.....	27
Figure 5 Telokin promoter <i>Hprt</i> targeting scheme	43
Figure 6 Expression of <i>Hprt</i> -targeted telokin 370AUG-LAC transgenes in adult mice.....	45
Figure 7 Expression of <i>Hprt</i> -targeted telokin (-190 to +180) transgenes during embryonic development	47
Figure 8 Expression of an <i>Hprt</i> -targeted SM22 α transgene in adult mice.....	49
Figure 9 Expression of <i>Hprt</i> -targeted SM22 α transgenes in embryonic mice	51
Figure 10 Expression of <i>Hprt</i> -targeted telokin 270bp (-94 to +180) transgenes.....	52
Figure 11 CT scan reveals decreased GI motility in chronic diabetic mice.....	71
Figure 12 Chronic diabetic mice show decreased colon contractility.....	72
Figure 13 Basal intracellular Ca ²⁺ levels are increased while the Ca ²⁺ response to 60mM KCl is decreased in the middle part of the colon in chronic diabetic mice.....	74
Figure 14 Changes in mRNA levels and protein of calcium handling proteins in chronic diabetic mice	76
Figure 15 Contractility in short term diabetic mice is decreased due to altered intracellular Ca ²⁺ signaling.....	78
Figure 16 Chronic hyperglycemic mice have increased global O-glycosylation levels while elevated O-glycosylation in vitro does not significantly affect contractility.....	81

Figure 17 Chronic diabetic mice show increased iNos mRNA levels in the colon smooth muscle layer	83
Figure 18 Defects occurring at acute state in STZ-induced diabetic mice	84
Figure 19 Defects occurring at chronic state in STZ-induced diabetic mice	85
Figure 20 Sequence alignment of the telokin promoter	95

Abbreviations

ANS	Autonomic nervous system
ATP	Adenosine-5'-triphosphate
BB/W rats	BioBreeding/Worcester type 1 diabetic rats
BMP	Bone morphogenetic protein
Ca ²⁺	Calcium ion
Cav1.2	Voltage-dependent L-type calcium channel alpha 1C subunit
CG	Celiac ganglion neurons
cGMP	Cyclic guanosine monophosphate
CICR	Calcium-induced calcium release
COX	Cyclooxygenase
c-Src	C-src tyrosine kinase
db/db mice	Diabetic mice with leptin receptor deficiency
DG	Dorsal ganglion
Egr-1	Early growth response factor 1
eNOS	Endothelial nitric oxide synthase
ENS	Enteric nervous system
ESC	Embryonic stem cells
FGF	Fibroblast growth factor
GI	Gastrointestinal
GTP	Guanosine-5'-triphosphate
HAT	Hypoxanthine-aminopterin-thymidine
HBP	Hexosamine biosynthetic pathway
Hh pathway	Hedgehog pathway
HLA	Human leukocyte antigen
<i>Hprt</i>	Hypoxanthine-guanine phosphoribosyltransferase
IBD	Inflammatory bowel disease
ICC	Interstitial cells of Cajal
IGF-1	Insulin-like growth factor 1

IL	Interleukin
IMG	Inferior mesenteric ganglion
iNOS	Inducible nitric oxide synthase
IP3	Inositol trisphosphate
KCl	Potassium chloride
MAPK	Mitogen-activated protein kinases
MLCK	Myosin light chain kinase
MLCP	Myosin light chain phosphatase
NCX	Sodium-calcium exchanger
NF κ B	Nuclear factor kappa B
nNOS	Neuronal nitric oxide synthase
NO	Nitric oxide
NOD mice	Non-obese diabetic mice
O-GlcNAc	O-linked N-acetylglucosamine
ONOO $^-$	Peroxynitrate
O $_s^-$	Superoxide
PIP2	Phosphatidylinositol 4,5-bisphosphate
PKC	Protein kinase C
PLC	Phospholipase C
PLN	Phospholamban
PMCA	Plasma membrane Ca $^{2+}$ ATPase
ROK	Rho-associated protein kinase
RyR	Ryanodine receptor
SCF	Stem cell factor
SERCA	Sarco/endoplasmic reticulum Ca $^{2+}$ -ATPase
Shh	Sonic hedgehog
SMG	Superior mesenteric ganglion
SMG-CG	Superior mesenteric and celiac ganglia
SM-MHC	Smooth muscle myosin heavy chain
SR	Sarcoplasmic reticulum

SRF	Serum response factor
STZ	Streptozotocin
TGF	Transforming growth factor
TNF	Tumor necrosis factor
UDP-GlcNAc	Uridine diphosphate N-acetylglucosamine

CHAPTER I

INTRODUCTION

Structure and functions of the colon

Digestive tract involved in food movement consists of the mouth, pharynx, esophagus, stomach, small and large intestine. The colon is a part of the large intestine and contains three smooth muscle layers – longitudinal, circular, and muscularis mucosae (Figure 1). The longitudinal and circular smooth muscle layers together are called the muscularis externa or muscularis propria and are responsible for the majority of motility in the colon. The muscularis mucosae is located at the border between the mucosal and submucosal layers, and promotes movement of the epithelial mucosa. The main functions of the external muscle layers are mixing, storage and propulsion of the colon contents. Mixing of the chyme within the colon occurs through segmenting contractions of the circular smooth muscle layer that promotes fluid and electrolyte absorption. The colon also serves as a reservoir of the chyme during water absorption process and until defecation of the residual material. Mass peristaltic contractions of colonic smooth muscle play an important role in propelling the colonic contents to the rectum for excretion. Functionally the colon is subdivided into proximal and distal regions. Mixing, storage and removal of water and electrolytes from the chyme occurs mainly in the proximal part of the colon. The distal part of the colon serves as a main storage reservoir and conduit for feces.

The main function of the smooth muscle is to provide the contractile activity for the colon's mixing and propulsive movements. To achieve this contractile activity the smooth muscle expresses a unique repertoire of contractile and regulatory proteins. Understanding how expression of these proteins is regulated under physiological and pathological conditions is important for developing appropriate

therapies for diseases that affect the contractility of the intestine. The smooth muscle contractile regulatory protein telokin is known to be highly expressed specifically in visceral smooth muscle tissues and represents a useful target for determining regulatory mechanisms that control expression of smooth muscle-specific genes in normal physiological and disease states. Thus, in my thesis research I analyzed telokin transcriptional regulation during development and in adulthood and determined if and how this is altered in the diabetic state. Previous studies have shown that diabetes in human patients and in different animal models leads to colon dysmotility. My research was aimed at determining the molecular defects that occur in colon smooth muscle during diabetes and what role telokin plays in the development of motility dysfunction associated with the disease.

Regulation of colonic contractility

Colon smooth muscle contractility is controlled by pacemaker cells within the intestinal wall and by the autonomic nervous system (ANS) and enteric nervous system (ENS). The ANS consists of sympathetic and parasympathetic nerve fibers which can either directly modulate the activity of intestinal smooth muscle or can synapse with neurons of the ENS. The ENS is subdivided into two interconnected plexuses, the myenteric (Auerbach) plexus located in the muscularis externa and the submucosal (Meissner) plexus. The neurons in the myenteric plexus primarily regulate contractility of the smooth muscle whereas the neurons in the submucosal plexus primarily regulate the activity of the mucosal epithelial cells. Interstitial cells of Cajal (ICC) are enteric pacemakers that mediate the basic electrical rhythm within the intestine [1]. The slow wave depolarization induced by the ICCs are transmitted to and through the intestinal smooth muscle cells via GAP junctions. Neurotransmission from nerves to smooth muscle can allow these slow waves to reach threshold and fire off action

potentials thus opening plasma membrane calcium channels to initiate contraction. Alternatively, neurotransmitters can direct pharmacomechanical coupling to induce intracellular calcium release via a receptor-inositol trisphosphate (IP₃) pathway. Vagal parasympathetic nerves from the medulla oblongata innervate the upper GI tract down to the proximal part of the colon. The parasympathetic nerves from sacral region of the spinal chord innervate the distal part of the colon via the pelvic nerves. In general, activation of parasympathetic nerves stimulate secretion and promotes motility. Sympathetic nerves from the superior mesenteric ganglion (SMG) and inferior mesenteric ganglion (IMG) innervate proximal and distal parts of the colon, respectively. Sympathetic nerve terminals mainly synapse with the ENS, however some of them terminate directly on smooth muscle [2]. Sympathetic nerves usually have inhibitory effects on GI smooth muscle motility.

Contraction of GI smooth muscle can be regulated by electromechanical or pharmacomechanical coupling. During electromechanical coupling GI smooth muscle contraction occurs following voltage dependent activation of L-type calcium channels facilitating calcium influx across the plasma membrane [3, 4]. In contrast, during pharmacomechanical coupling neurotransmitter or hormone binding to specific G-protein coupled receptors, stimulates phospholipase C (PLC) activity leading to catalysis of lipid phosphatidylinositol 4,5-bisphosphate (PIP₂). Catalysis of PIP₂ promotes production of two secondary messengers: inositol trisphosphate (IP₃) and diacylglycerol (DG). IP₃ binds to the IP₃R on the sarcoplasmic reticulum (SR), causing release of calcium into the cytosol. When intracellular calcium rises either as a result of electromechanical or pharmacomechanical coupling Ca²⁺ binds to calmodulin and activates myosin light chain kinase (MLCK). MLCK then phosphorylates the light chain of myosin stimulating myosin's actin-activated ATPase activity and the energy released from ATP hydrolysis results in myosin cross-bridge cycling and contraction.

When pharmacomechanical coupling occurs, the DG that is produced along with IP₃ activates PKC, which phosphorylates specific target proteins that can modulate contractility. Smooth muscle contractions can also occur in the absence of a rise in intracellular calcium through a calcium sensitization mechanism which occurs when myosin phosphatase activity is inhibited. For example, activation of Ras homolog gene A (RhoA) increases Rho kinase (ROK) activity leading to phosphorylation and inactivation of myosin phosphatase (MLCP). Conversely, phosphorylation of telokin by PKG plays role in Ca desensitization and smooth muscle relaxation. Telokin knock out mice showed increased sensitivity to Ca and decreased cyclic guanosine monophosphate (cGMP)-induced relaxation [22].

Intracellular calcium levels in smooth muscle cells are tightly regulated by channels and receptors. Smooth muscle stimulation leads to calcium influx into cytosol and relaxation causes calcium efflux out of the cell or uptake into SR. As mentioned above, voltage gated L-type channels play the major role in the influx of calcium into the cell from the extracellular fluid (Figure 2). Calcium release from intracellular stores can be mediated by either the IP₃ receptor or the ryanodine receptor (RyR). The IP₃ receptor (IP₃R) is located on the membrane of the SR and when stimulated by IP₃ triggers calcium release from the SR [4]. RyR's are stimulated by cytosolic calcium and play role in calcium induced calcium release (CIRC) from the SR into the cytosol. Following contraction it is important to eliminate calcium from the cytosol in order to facilitate relaxation. Sarco/endoplasmic reticulum Ca²⁺-ATPase (SERCA) is an ATP-dependent calcium pump located on the SR that plays a significant role in the reuptake of calcium into the SR permitting smooth muscle relaxation. SERCA activity is regulated by the protein phospholamban (PLN). When PLN is associated with SERCA calcium uptake into the SR is inhibited, while after dissociation from PLN, calcium uptake is increased. In cardiac and perhaps also in smooth muscle, phosphorylation of PLN relieves its inhibitory activity on SERCA. The plasma

membrane Ca^{2+} ATPase (PMCA) is a transporter located in the plasma membrane of the smooth muscle that also removes calcium from the cytoplasm by pumping it out of the cell. The pump is activated by the hydrolysis of adenosine triphosphate (ATP). While it has high affinity for binding calcium, the removal of calcium out of the cell by this pump occurs at slow rate. An additional mechanism of calcium extrusion is provided by the sodium-calcium exchanger (NCX), an antiporter located on the smooth muscle plasma membrane. NCX removes calcium from cells in exchange for sodium. In contrast to PMCA the $\text{Na}^+/\text{Ca}^{2+}$ exchanger does not bind very tightly to Ca^{2+} but it can transport calcium out of the cell rapidly.

Differentiation and development of the colon smooth muscle

Progenitors of colonic smooth muscle cells differentiate from the mesenchyme surrounding the primitive gut epithelial tube. At early stages the primitive gut has a tubular form and consists of undifferentiated epithelium surrounded by undifferentiated mesenchyme. Smooth muscle development follows a rostro-caudal progression starting in the esophagus at embryonic day 11 in mice and moving forward toward the foregut, midgut and finally the hindgut [5, 6]. The smooth muscle precursor cells are called myoblasts and express SM α -actin [5, 6]. In parallel to villi formation, the first layer of smooth muscle myoblasts differentiate and give rise to the inner circular smooth muscle layer. Around embryonic day 12 primitive crypts are formed and smooth muscle cells in the longitudinal layer differentiate. Coincident with longitudinal smooth muscle appearance the third smooth muscle layer muscularis mucosa forms from mesenchyme in close proximity to the epithelium. Although the muscularis mucosae represents an independent induction of smooth muscle it progresses through similar differentiation pattern as circular and longitudinal smooth muscle layers. During development, smooth muscle myoblasts rapidly differentiate into

smooth muscle myocytes that are immature smooth muscle cells that persist until birth [5, 6]. Smooth muscle myocytes, in addition to expressing SM α -actin also start to express high levels of SM γ -actin, smooth muscle myosin heavy chain (SM-MHC), telokin and calponin from embryonic day 12-13 in mice. However, the final differentiation and maturation of myocytes occurs only after birth.

Many signaling pathways are involved in smooth muscle differentiation during development of gastrointestinal tract. Hedgehog (Hh) signaling is important for radial patterning and mesenchyme differentiation into smooth muscle. Sonic hedgehog (Shh), a member of Hh family, has been implicated in the early development in the gut and plays role in the crosstalk between endoderm and mesoderm. Hh ligand is released by endoderm and induces development of smooth muscle [7, 8]. Hh is a radial morphogen and does not promote smooth muscle development if mesenchyme is located too close or too far to the source of the ligand [7, 8]. It also have been shown that inactivation of Hh signaling impairs smooth muscle development [7]. In the developing gut Shh induces expression of the Transforming growth factor β (TGF β) family member Bone morphogenetic protein 4 (BMP4) in the mesenchyme which is important factor in smooth muscle development [9, 10]. BMP family members are expressed in both mesenchyme and epithelial cells. BMP4 has been shown to play role in smooth muscle proliferation and differentiation [11]. However, BMP2 rather than BMP4 enhanced smooth muscle differentiation from embryonic stem cells in an in vitro gut differentiation model, as evidenced by enhanced formation of contracting gut-like structures that expressed SM α -actin [12]. Although Wnt signaling has been implicated in the development of epithelial cells, recent studies have also shown role of Wnt5a in the differentiation of mesenchyme. Wnt5a knock out mice have thinner muscularis propria, improper midgut closure, and a shortened midgut [13]. These findings suggest that Wnt signaling plays a role not only in epithelial cell proliferation but also mesenchyme proliferation and/or differentiation. Fibroblast growth factors (FGF) family members also have been shown to play

roles in development of smooth muscle of the colon. For example, FGF-9 has been implicated in signaling pathway that controls gut length through proliferation and differentiation of fibroblasts [14].

Smooth muscle contractile and regulatory proteins

All differentiated smooth muscle is characterized by the presence of unique isoforms of contractile proteins that are not expressed in other tissue types. Examples of smooth muscle-specific proteins include smooth muscle α and γ - actin, SM-MHC, caldesmon, SM22 α , telokin and calponin. Although all of these proteins are expressed in smooth muscle some of them are more abundant in visceral smooth muscle while others are more abundant in vascular smooth muscle tissue. For example, telokin and SM γ -actin are particularly abundant in visceral smooth muscle cells [15-17] while SM22 α is highly expressed in vascular and visceral smooth muscle in adult animals [18-20]. While the physiological functions of myosin and actin are well defined the functions of other smooth muscle restricted proteins are less clear. The amino acid sequence of telokin is identical to the carboxyl-terminus of the 130kDa “smooth muscle” MLCK and the 220kDa “non-muscle” form of MLCK (Figure 3). However, telokin does not contain the kinase domain of the MLCKs and functions rather to regulate the activity of the myosin light chain phosphatase. Telokin has been shown to activate myosin light chain phosphatase and to be important for cGMP mediated calcium desensitization of phasic smooth muscle tissues [21-25]. Telokin knockout mice, generated by deleting an AT-rich region and the CArG box from the core of the telokin promoter, exhibit increased myosin phosphatase activity, resulting in a leftward shift in the calcium-force relationship in visceral but not vascular smooth muscle tissues [22]. The higher level of expression of telokin in visceral as compared to vascular and smooth muscle cells can thus account for the lower calcium sensitivity of contraction in visceral as compared to vascular

tissues [21]. These findings demonstrate that differential expression of telokin in distinct smooth muscle tissues plays an important role in regulating the physiological properties of the tissue.

SM22 α is a smooth muscle-specific protein that binds cytoskeletal actin filaments in smooth muscle cells. SM22 α knock out mice develop normally and do not develop any cardiovascular or visceral organ problems suggesting that it is not required for basal homeostatic functions in these tissues [26]. However, when SM22 α knock out mice were crossed into hypercholesterolemic ApoE-deficient mice, mice developed more pronounced atherosclerotic lesions suggesting that SM22 α plays a role in smooth muscle phenotype regulation during atherogenesis [27]. SM22 α also have been implicated in calcium-independent vascular smooth muscle contractility [28]. Similar to SM22 α , calponin has been implicated in the regulation of smooth muscle contraction through its interaction with actin and inhibition of phosphorylated myosin [29]. Calponin acts as an actin filament-stabilizing molecule that contributes to physiological thin filament turnover rates in different cell types. Another actin-binding protein, caldesmon also binds myosin, calmodulin and tropomyosin and plays a significant role in regulating contractility by inhibiting the actomyosin ATPase activity. Caldesmon's activity is regulated by calcium levels and phosphorylation [30].

Transcriptional regulation in smooth muscle

Analysis of the transcriptional regulation of smooth muscle restricted genes such as telokin and SM22 α has provided important insights into the molecular mechanisms that control smooth muscle differentiation.

We have previously shown that telokin mRNA is transcribed from a promoter located within an intron that interrupts the exon encoding the calmodulin binding

domain of the MLCKs (Figure 3) [16]. Unlike the 130kDa MLCK, which has been detected in all adult tissues examined thus far, telokin protein and mRNA expression is restricted to adult and embryonic smooth muscle tissues and cultured smooth muscle cells [31, 32]. Both, in adult and in embryonic mice, telokin is expressed at higher levels in most visceral smooth muscle tissues compared to vascular smooth muscle tissues [31]. In situ hybridization analysis revealed that telokin expression is first detected in the gut at embryonic day 11.5. Expression is then detected in airway and urinary smooth muscle between day 13.5 and 15.5. Induction of telokin expression during the postnatal differentiation of the reproductive tract parallels the induction of other smooth muscle-specific proteins. The variable levels of telokin expression, in different vascular smooth muscle tissues, likely reflect the diverse origins of smooth muscle cells throughout the vasculature. For example, although no telokin could be detected in the dorsal aorta of a 14.5 day embryonic mouse, high levels of expression could be detected in the umbilical artery [31]. The cis-acting regulatory elements necessary to direct this pattern of telokin expression are contained within a 370bp proximal promoter region, as a reporter gene driven by this fragment was also restricted largely to visceral smooth muscle in adult animals in vivo [33].

Analysis of SM22 α gene expression revealed that endogenous SM22 α is expressed in skeletal, smooth and cardiac muscle during embryonic development but postnatally becomes restricted to smooth muscle only [34]. SM22 α is first detected in the primitive heart tube at embryonic day 8, after embryonic day 13.5 mRNA levels decline in the heart such that no expression can be detected in adults. Similarly, transient SM22 α expression was also observed in developing skeletal muscle between embryonic days 9.5 and 12.5. Postnatally SM22 α expression is restricted to smooth muscle tissues, although in contrast to the endogenous SM22 α which is expressed in all smooth muscle tissues, SM22 α promoter driven transgenes are restricted to vascular smooth muscle tissues [26, 35, 36]. Several reports have shown that a -441 to +62 SM22 α promoter directs

reporter gene expression specifically to arterial smooth and not to venous or visceral smooth muscle cells in transgenic mice [18-20, 33]. Longer promoter fragments exhibited a similar pattern of transgene expression but a BAC clone encompassing the entire SM22 α gene was found to be expressed in all smooth muscle tissues in transgenic mice [18, 19, 36]. These data suggest that additional distal regulatory elements are required for SM22 α promoter activity in veins and visceral tissue.

Regulation of smooth muscle-specific genes by serum response factor (SRF)

Serum response factor (SRF) is a widely expressed transcription factor that plays roles in differentiation of cardiac, skeletal and smooth muscles. SRF regulates genes by binding to a 10 bp *cis*-element, CC(AT)₆GG, called the CArG box [37]. SRF have been shown to play a role in smooth muscle differentiation and smooth muscle-specific gene expression. Mouse knockout studies have shown that SRF is important in mesoderm differentiation during mouse embryogenesis [38]. Although SRF knock out embryonic stem (ES) cells could form mesoderm in vitro, by an unknown mechanism, they were not able to express smooth muscle markers [39]. These data suggest that, in addition to regulating mesoderm from which most smooth muscle cells are derived, SRF also plays a direct role in regulating smooth muscle differentiation. This is supported by studies which generated a smooth muscle-specific knockout of SRF in adult tissues [40-42]. Knocking out SRF in adult smooth muscle tissues resulted in a dilated GI tract with decreased contractility due to attenuated expression of smooth muscle contractile proteins and a thinning of the muscularis externa. These defects led to severe intestinal obstruction [40, 41].

The promoter regions of most smooth muscle restricted genes contain one or more CArG elements that bind (SRF). SM-MHC, α and γ -actin, and calponin each have multiple CArG boxes, smoothelin A and SM22 α - two CArG boxes and telokin only one [18, 32, 43-47]. Combinations of one or two CArG box mutations have shown inhibited promoter activity in different smooth muscle subtypes. For example, mutations in both CArG elements in the SM22 α abolished promoter activity in arterial smooth muscle cells [18, 48]. A study using mutation analysis of CArG elements within the smooth muscle myosin heavy chain promoter in vivo showed that transcriptional regulation of SRF differs among smooth muscle subtypes [49]. For example, the CArG box located in the 5'-flanking sequence (CArG1) was required for promoter activity in all smooth muscle cells, while the CArG box located in the intronic region (CArG2) was important for expression more specifically in arteries. Mutation of CArG2 resulted in decreased promoter activity in the GI tract, abolished expression in large blood vessels, trachea and bronchi while showing weak expression in small vessels and was not affected in bladder. Our in vitro studies have also shown that the CArG element within the telokin promoter is necessary for telokin expression in smooth muscle cells [32]. These findings suggest that CArG elements play a central role in regulating smooth muscle gene expression, however these elements alone cannot explain the unique expression patterns of genes within different smooth muscle tissues. It is likely that different genes may require distinct additional factors to direct expression in different smooth muscle tissues. One of the goals of my thesis was to identify these additional elements within the telokin promoter.

In addition to its important role in smooth muscle development, SRF also controls expression of cardiac and skeletal muscle-specific genes as well as genes involved in growth and proliferation. SRF's ability to regulate this disparate group of genes is regulated through several mechanisms such as regulated SRF expression levels, altered DNA binding or alternative splicing of SRF and association with cell-restricted cofactors [37]. For example SRF's interaction with

the myocardin family of cofactors allows it to potently activate smooth muscle-specific genes selectively [50, 51]. Whereas SRF's interaction with the ETS family of cofactors allow it to selectively activate growth and proliferation genes [37]. Although selective cofactor interactions can at least partly explain the gene specificity of SRF these interactions still do not explain the unique tissue distribution of genes in distinct smooth muscle tissues.

Approaches to generate transgenic mice for smooth muscle promoter analysis

To understand the mechanisms regulating expression of genes in distinct smooth muscle tissues, it is necessary to analyze *cis*-acting regulatory elements and their role in regulating expression of these genes in vivo. Previously we and other labs have analyzed the activity of smooth muscle-specific promoters in transgenic mice in vivo by utilizing standard transgenic approaches. In this procedure the transgene construct is injected into pronucleus of a fertilized egg where it randomly integrates into the genome at a variable copy number. The expression pattern and level of these transgenes is dependant on copy number of the transgene and the chromatin structure at the site of integration leading to significant variability in the patterns and levels of expression in different founder lines [52]. Depending on the site of integration one can observe ectopic non-specific expression due to the activity of nearby promoters or silencing of expression due to nearby silencer elements. For example, during our analysis of telokin promoter transgenes, we observed that the majority of transgenic lines exhibited no detectable transgene expression [33]. In addition, the pattern of transgene expression driven by an SM22 α promoter was distinct in different transgenic lines, with most lines exhibiting artery-specific expression, whereas some showed additional expression in veins and in heart [33]. Variability in the expression patterns of these founder lines can make analysis of *cis*-acting

elements within these promoters difficult. Although generation of these transgenes is relatively fast it requires analysis of large numbers of independent founder lines. To be able to determine the relative importance of regulatory elements in different smooth muscle tissues, it is necessary to generate transgenic mice in which the activity of wild-type promoters are highly reproducible in terms of both their levels and tissue-specific patterns of activity. One way to improve transgene expression is to place insulator elements around the transgene. Although constructs still integrate randomly, with variable copy number, the insulator element protects the transgene from the effects of exogenous enhancers and silencers leading to more reproducible expression pattern. Studies have shown that insulator from H19 gene can be used for transgene studies [53, 54]. A second approach to minimize variability of transgene expression is to target single copy transgenes to a specific region of open chromatin structure by placing it adjacent to a housekeeping gene, such as hypoxanthine phosphoribosyltransferase (*Hprt*) [55]. Although this approach has previously not been utilized for smooth muscle-specific promoters, previous studies using endothelial cell-specific promoters demonstrated that, when targeted to this locus, these promoters exhibit very reproducible endothelium-specific expression [56-59]. Similarly, the myogenin promoter also exhibited appropriate skeletal muscle-specific expression when targeted to the *Hprt* locus [60]. In this method mutated ES cells with a partial *Hprt* locus deletion are transfected with a targeting construct containing a LACz reporter gene and homology arms complementary to the *Hprt* locus [52, 61]. When homologous recombination occurs it restores *Hprt* function and cells can be selected by hypoxanthine-aminopterin-thymidine (HAT) media. The advantage using this approach is that it avoids the necessity of introduction of selectable markers. The HAT selection is very efficient with more than 80% of selected cells usually exhibiting the correct integration of the transgene. In my thesis studies I have utilized this approach to identify key regulatory regions and elements within the

telokin promoter that are required for expression in different smooth muscle tissues.

Colon smooth muscle in diabetes

Smooth muscle phenotypic changes occur during the development of atherosclerosis, asthma, and bladder and GI obstruction. In atherosclerotic plaques dedifferentiated smooth muscle cells exhibit a proliferative and synthetic phenotype. SM α -actin, MHC, calponin and SM22 α genes are highly expressed in differentiated cells while they are downregulated in dedifferentiated atherosclerotic smooth muscle [62]. Smooth muscle contractile gene expression is also altered in asthma and diseases involving visceral smooth muscle obstruction where these genes are downregulated and in some cases distinct nonmuscle isoforms of the genes are expressed [63-66]. These disease-related phenotypic changes in different tissues lead to decreased contractility. Although diabetes has been shown to affect GI motility, whether it occurs through smooth muscle phenotypic changes have not been studied. In my thesis work I was interested to investigate the effects of diabetes on colon smooth muscle and determine whether altered GI motility occurs through mechanisms leading to smooth muscle dedifferentiation.

Diabetes overview

Based on data from the Center for Disease Control and Prevention, 23.6 million people (7.8%) in United States have diabetes. The two main types of diabetes are type 1 and type 2 diabetes. Type 1 diabetes is an autoimmune disease triggered by genetic and environmental factors leading to destruction of insulin producing β -cells resulting in impaired or abolished insulin secretion and

hyperglycemia. Approximately 50% of the genetic risk for type 1 diabetes is attributed to the human leukocyte antigen (HLA) region. Islet cell auto-antibodies (ICA), antibodies to insulin (IAA), glutamic acid decarboxylase (GAD) and protein tyrosine phosphatase (IA2) have all been implicated in the development of type 1 diabetes [67]. A combination of many genes rather than a single gene play a role in development of the disease, thus it is a polygenic disease which accounts for about 5% of all cases of diabetes.

Type 2 diabetes is a metabolic disorder and occurs because of insulin resistance. Unknown primary defects leading to insulin resistance in metabolic tissues cause elevated blood glucose. In response to this elevated blood glucose the body increases insulin production in an attempt decrease glucose levels [68]. Thus, early stage of type 2 diabetes is marked with hyperglycemia and hyperinsulinemia. In the later stages, insulin levels are reduced because of β -cell depletion, and blood glucose levels are elevated. Risk factors for type 2 diabetes include obesity, genetic predisposition, physical inactivity, and impaired glucose metabolism. Type 2 diabetes can develop over a long period of time from a preclinical insulin resistance to a more significant insulin resistance that is associated with, hypertension, dislipidemia and being overweight (metabolic syndrome) to full blown diabetes associated with β -cell failure. Type 2 is the most common and increasing form of diabetes and accounts for 90% of all diabetes cases. Therapy for type 2 diabetes is usually tailored toward obtaining glycemic control at each stage of the disease. Important step in prevention of complications of type 1 and type 2 diabetes is maintenance of normal glucose levels. The consequences of uncontrolled diabetes and persistent high glucose levels include peripheral neuropathy, cardiovascular and kidney disease and gastrointestinal motility problems [69-73].

Diabetes effects on the GI tract

As many as 76% of diabetic patients at some point in the course of their disease develop gastrointestinal (GI) symptoms [74]. The entire GI tract motility from esophagus to anorectal area is affected by diabetes (Figure 4). Common symptoms in diabetic patients include dysphagia, gastroparesis, vomiting, early satiety, abdominal pain, constipation, diarrhea or fecal incontinence [74]. Constipation and gastroparesis are the most common symptoms and affect approximately 60% and 30-60% of the diabetic patients, respectively [74, 75].

Gastroparesis is a condition where food is retained in the stomach because of decreased stomach motility. It leads to bloating, feeling of early satiety, abdominal pain, nausea and vomiting. Diabetic patients also develop small and large intestine motility problems leading to abnormal motility, impaired intestinal secretion or absorption problems [74]. These defects also lead to abdominal bloating, diarrhea or constipation. GI complications are mostly related and studied in respect to neuronal damage leading to neuropathy. Gastrointestinal neuropathies are known to affect GI tract motility, sensation, secretion and absorption. Different autonomic neurons stimulate or inhibit GI motility in different regions of the GI tract and neuropathies can lead to accelerated or delayed motility depending on which neurons are most affected. Study of diabetic patients have shown enlarged dystrophic axons and nerve terminals in prevertebral superior mesenteric (SMG) and celiac sympathetic ganglia (CG) [76]. Animal models of streptozotocin (STZ)-induced diabetes and diabetic BBW rats also show dystrophic axons of prevertebral sympathetic ganglia innervating the small intestine [77]. Recent study show that non-obese diabetic (NOD) mice also develop swollen axons and dendrites in the prevertebral superior mesenteric and celiac ganglia (SMG-CG) while STZ-induced diabetic mice developed less severe changes even after longer periods of time [78].

There is emerging evidence that the intrinsic ENS also play a role in diabetic neuropathy [78-83]. For example, STZ-induced diabetic rats show decreased number of enteric neurons in colon and stomach after only 7 days of hyperglycemia [84, 85]. Recent evidence also suggests that disrupted insulin/(insulin-like growth factor) IGF1 signaling might play a role in ENS apoptosis causing motility problems [86, 87]. Decreases in number and alterations in structure of ICC, (the pacemaker cells in the intestine) have also been observed in patients as well in different parts of the gastrointestinal tract of mice and rats with type 1 and type 2 diabetes [79, 82, 88, 89]. These changes have been associated with dysrhythmias and motility problems of gastrointestinal tract suggesting the role of the ENS and the pacemaker network in development of disease [90]. The loss of ICC has mostly been attributed to hyperglycemia [86, 87]. Although diabetic GI dysmotility often is associated with neuronal damage studies suggest that it is most likely a multifactorial disease also involving direct defects in smooth muscle and epithelial cells. Studies have shown that diabetes can lead to distinct smooth muscle alterations depending on the animal model used and the specific parts of the GI tract tested. Studies in an STZ-induced diabetic rat model revealed increased small intestine smooth muscle mass [91, 92]. The diabetic small intestine was longer with increased diameter when compared to control animals, although these changes did not affect contractile response to cholinergic stimulation. Other studies have shown increased colon contractility in rats [91, 92]. In diabetic rats the frequency of spontaneous contractions in the colon was not affected while the amplitude was increased. Conversely in STZ-induced diabetic mice the smooth muscle contractile response to carbachol in colon was weaker when compared to control animals at 4 and 8 weeks following STZ treatment [93]. This was also associated with delayed gastric emptying and increased intestinal transit time [86]. Diabetic db/db mice with leptin receptor activity deficiency also show lower gastric emptying and prolonged whole gut transit time as compared to wild type mice [79]. These studies together with the

hypercontractile and hypocontractile defects seen in human patients highlight the differing effects of diabetes on the GI tract.

The molecular mechanisms leading to these different pathologies in GI smooth muscle of diabetic patients and animals are complex and are not well described. Altered GI contractility has been associated with altered calcium signaling. Studies in diabetic rats showed decreased intracellular Ca^{2+} handling in ileum but found no changes in colon [94]. Studies showing impaired smooth muscle contractility in the stomach of STZ-induced and db/db mice demonstrated that these changes were due to alterations in muscarinic receptor coupling through Guanosine-5'-triphosphate (GTP)-binding proteins [95]. Diabetic BB/W rats show no changes in KCl induced contractile responses compared to control animals, indicating that there are likely no defects in voltage gated L-type calcium channels in these animals. In contrast, a decreased contractile response of stomach smooth muscle that resulted from altered intracellular signal transduction through IP3 and PKC pathways was observed in these animals. [96]. In some severe cases of gastroparesis with poor glycemic control, dysmotility is associated with gastric smooth muscle myopathy [96, 97]. Diabetic patients with type 1 diabetes show atrophic smooth muscle cells and increased collagen production in muscularis propria layer likely related to the absence of insulin signaling [96, 97]. Diabetes related GI symptoms have been largely linked to hyperglycemia. Poor glycemic control rather than the duration of the disease seems to be associated with more severe GI problems [98]. However, recently it has been shown that that reduction in insulin/IGF-I in diabetic mice causes decreased stem cell factor (SCF) production and smooth muscle atrophy that eventually leads to ICC depletion [87]. These studies stress that myopathy may play a more central role in diabetic gastroenteropathies than previously recognized. It also emphasizes the role of insulin depletion rather than hyperglycemia in progression of the smooth muscle dysfunction.

Posttranslational protein modifications and contractility

High glucose and oxidative stress lead to many diabetes related complications because of increased free radical formation. These changes can lead to posttranslational modification of proteins altering their physiological function through several different pathways. Two well recognized posttranslational modifications related to diabetes are O-linked glycosylation (O-glycosylation) and nitration. These modifications also have been shown to alter muscle contractility. Glucose mostly is metabolized through glycolysis; however, when there is a glucose overload it can also be metabolized via the hexosamine biosynthesis pathway (HBP). The end product of this pathway is uridine diphosphate *N*-acetylglucosamine (UDP-GlcNAc), which is a substrate for protein O-glycosylation (O-GlcNAc-modification) on serine and threonine residues. Hyperglycemia and oxidative stress lead to increased levels of UDP-GlcNAc and elevated O-glycosylation of nuclear, cytoplasmic and membrane proteins. O-glycosylation is a posttranslational modification that has been implicated in development of diabetic complications. Many transcription factors, cytoskeletal proteins, nuclear pore and signal transduction molecules are known to be O-glycosylated [99, 100]. Moreover, diabetes have been shown to contribute to complications of diabetes in many tissues, including pancreatic β -cells, cardiomyocytes and skeletal muscle [101-104]. Although O-glycosylation can alter protein function in several ways one effect it has is to prevent the modified site from being phosphorylated [99]. Increased global O-glycosylation in cardiac and skeletal muscles have been shown to decreased Ca^{2+} sensitivity in these tissues and alter contractility [101, 102, 104]. This occurred through increased O-glycosylation of the microfilaments thus leading to altered contractility. Although O-glycosylation has been shown to affect cardiac and skeletal muscle contractility, it's effects on contractility have not been explored in regard to colon smooth muscle in STZ-induced diabetic animals.

Nitration of tyrosine on different functionally important proteins is implicated in pathophysiology of many diseases such as Alzheimer's, Parkinson's, endothelial dysfunction, inflammatory bowel disease (IBD) and diabetes [105-110]. Studies show that nitration of tyrosine residues can affect protein function by preventing these residues from being phosphorylated. Nitric oxide (NO) production in cells is regulated by enzymes neuronal NOS (nNOS), endothelial (eNOS) and inducible NOS (iNos). High iNos production occurs in an oxidative environment and once induced can produce large amounts of NO. In an oxidative environment, such as diabetes, NO can interact with superoxide (O_2^-) to form peroxynitrite ($ONOO^-$) leading to nitration of tyrosine residues [111]. Studies in experimental colitis have shown that nitration attenuates L-type channel function in colon smooth muscle leading to decreased calcium influx into the cell and decreased contractility [112]. This study showed that L-type calcium channel mRNA and protein levels were not changed while calcium influx was decreased due to L-type calcium channel nitration and its subsequent inability to interact with c-src tyrosine kinase (c-Src) [113].

Inflammation and contractility

Recent studies in colitis and postoperative ileus models have indicated that inflammation can lead to decreased gut motility. It is believed that macrophages residing in the muscularis layer in gastrointestinal tract play a significant role in inflammatory response [114]. Studies using macrophage-deficient osteopetrotic mice showed decreased levels of pro-inflammatory cytokine release and improved gastrointestinal transit after postoperative ileus manipulation [115]. It has been shown that surgical manipulation activates macrophages by activating Mitogen-activated protein kinase (MAPK) signaling pathway resulting in activation of early growth response (Egr)-1, nuclear factor kappa B ($NF\kappa$ -B) and interleukin (IL)-6 [116-118]. These signaling pathways lead to secretion of pro-

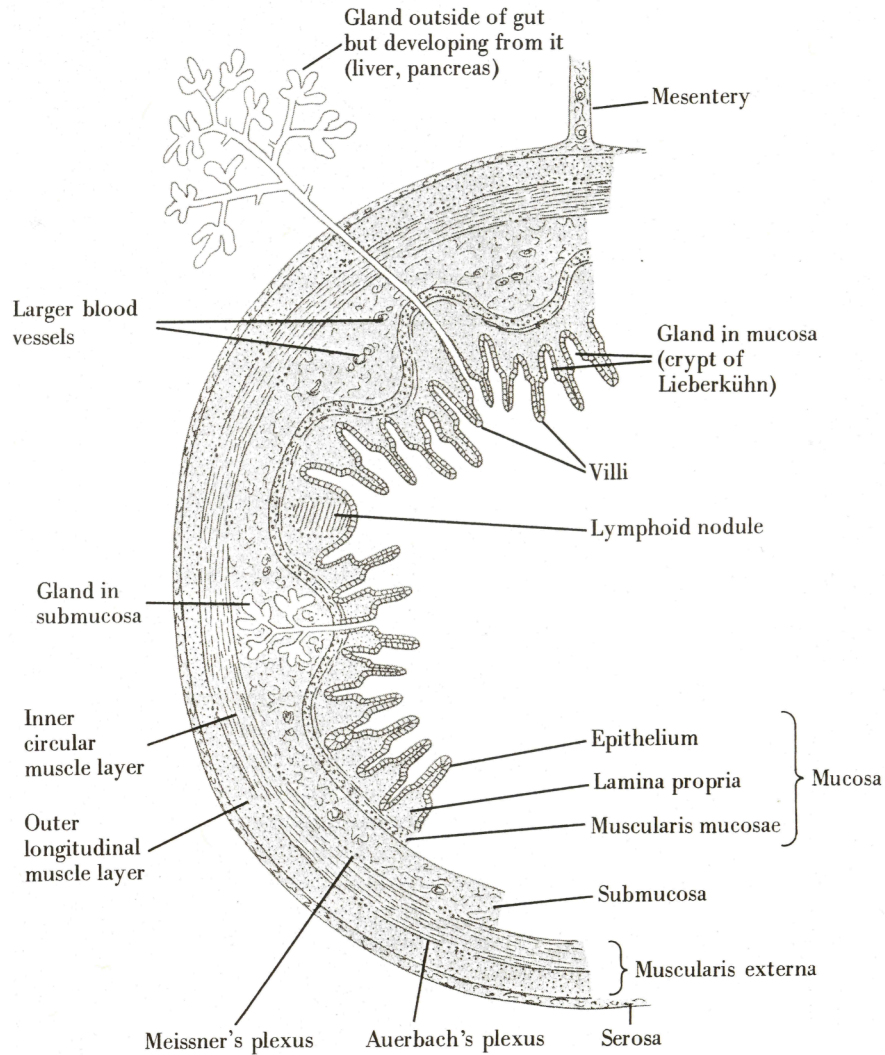
inflammatory cytokines tumor necrosis factor (TNF) α , IL-1, IL-6 as well as NO and cyclooxygenase (COX)-2 production in macrophages of the muscular layer [116-118]. Further studies showed that direct TNF α treatment decrease gastrointestinal smooth muscle contractility [117]. iNos knockout mice also showed decreased neutrophil infiltration in muscularis after intestinal manipulation and normal contractile response when compared to the attenuated response seen in wild type animals. These studies suggest that iNos can play an important role in inhibiting GI smooth muscle contractility [119]. Studies using bone marrow transplants from iNOS KO mice suggest that the biologically important iNOS that attenuates contractility after surgical manipulation is derived from blood cells [120]. These data highlight the importance of macrophages at the first steps of inflammation-induced impairments in GI smooth muscle contractility.

Thesis Rationale

The overall goal of my study was to identify molecular mechanisms that regulate gene expression specifically in GI smooth muscle cells and determine how these mechanisms are altered under pathological conditions. As the smooth muscle contractile regulatory protein telokin is highly and specifically expressed in visceral smooth muscle in vivo, I utilized this gene to dissect the transcriptional pathways that control gene expression in GI smooth muscle. Specifically I set out to determine whether *Hprt*-targeted transgenes would give reproducible transgene expression patterns suitable for the analysis of cis-acting gene regulatory elements.

As diabetes have been shown to affect GI tract motility in human patients and animal models the second goal of my studies was to determine whether colon smooth muscle undergoes dedifferentiation in a mouse model of type 1 diabetes.

As part of this goal I examined the effects of diabetes on colon smooth muscle contractility. Previous studies in diabetic rats implied that altered GI contractility possibly occurs through altered sensitivity to calcium in smooth muscle [94]. As telokin is known to play a role in smooth muscle calcium desensitization, the other part of my goal was to determine whether telokin expression is altered in colon smooth muscle of diabetic mice.



Ross and Romrell, Hystology. A text and atlas. Second edition, 1989.

Figure 1. Layers of the colon. The colon is lined with mucosa layer consisting of epithelial cell layer, lamina propria and muscularis mucosae. The mucosa layer forms invaginations called villi that are supplied with glands and contain lymphoid nodules. The next is the submucosa layer located between mucosa and smooth muscle layers. The outer muscle layer muscularis externa consists of inner circular layer and outer longitudinal layer. The outermost layer is the serosa. The nervous Meissner's plexus is located between muscularis mucosae and submucosa. Another nervous Auerbach's plexus is located between two smooth muscle layers. Mesenteric vessels reach the wall of the colon for blood supply.

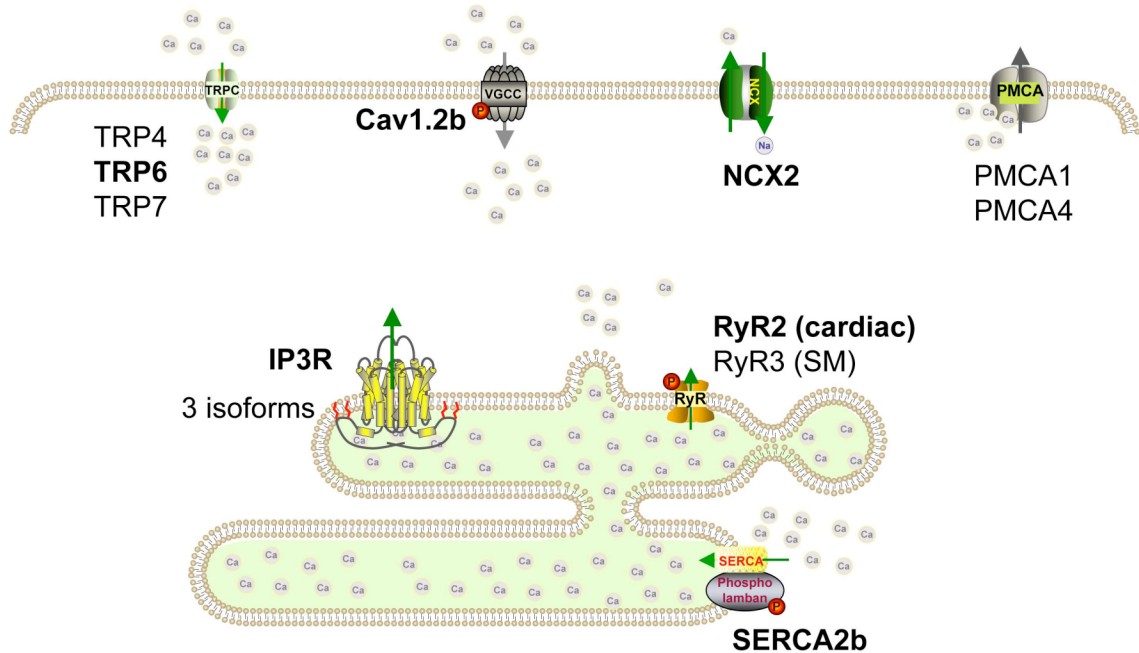


Figure 2. Channels and receptors involved in colon smooth muscle calcium signaling. L-type channels (Cav1.2) and TRP channels are located in the cell membrane and are involved in calcium influx. PMCA and NCX are transporters located in the plasma membrane and play roles in calcium export out of the cell. IP3R is located on the membrane of SR and triggers calcium release from SR. RyR are also located on SR and play role in calcium-induced calcium release (CICR). SERCA is Ca ATP-ase located on the SR and plays role in the calcium uptake to SR and smooth muscle relaxation. SERCA activity is regulated by phospholamban (PLB). PLB binding to SERCA inhibits calcium uptake while PLB release activates calcium uptake into SR.

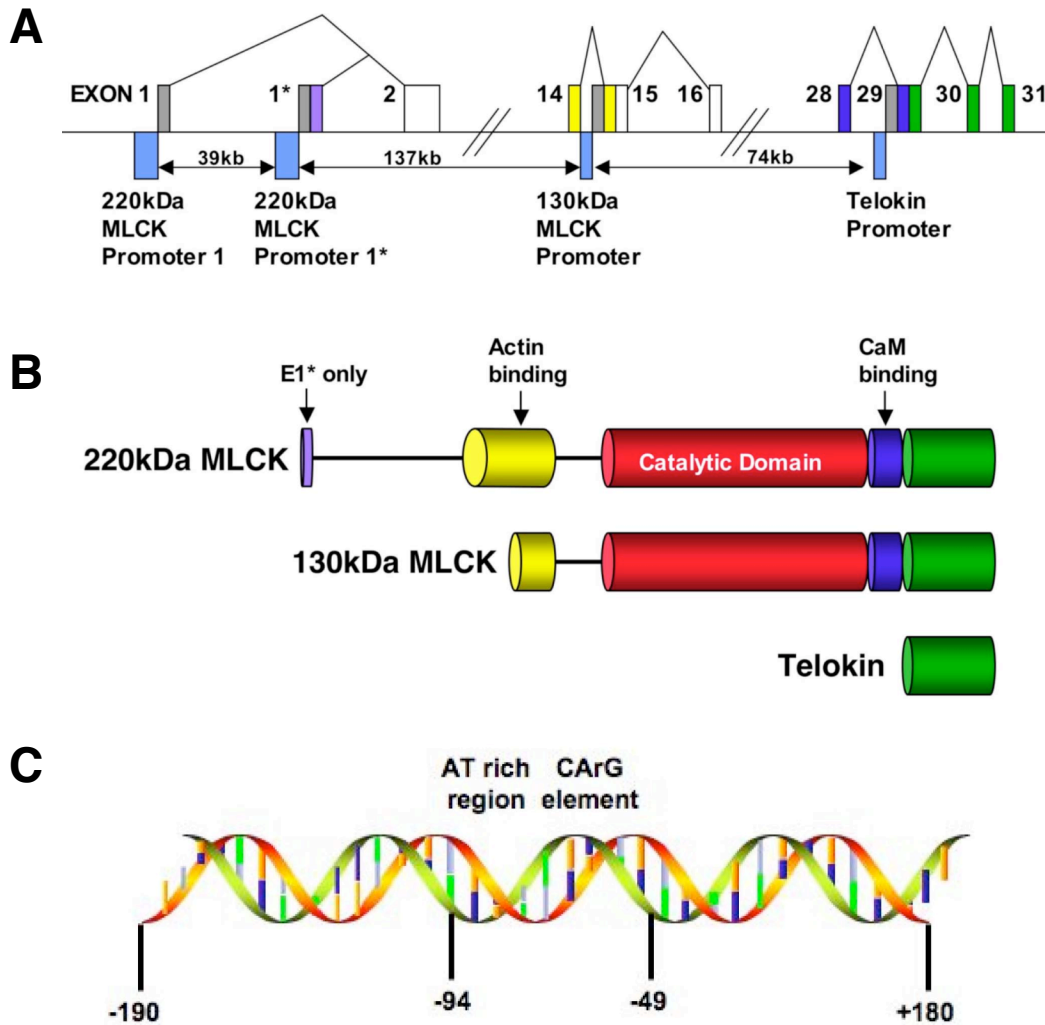


Figure 3. Structure of the mouse mylk1 gene, mylk1 transcripts and minimal telokin promoter schematics. (A) Representation of a portion of the mouse mylk1 gene. Exons are indicated by boxes and are color coded to match the domains in the (B) schematics. The dark gray boxes represent the unique 5'-untranslated region (UTR) segments of each transcript. Promoter regions are indicated by the blue boxes below the line. Genomic sequence predicts that two 5' promoters direct the expression of the two isoforms of the 220-kDa MLCK that differ from each other only in the sequence encoded by exon 1* of the 220-kDa MLCK E1*. The protein produced from usage of exon 1* is predicted to be 9 amino acids longer than the protein resulting from usage of exon 1. Two internal

promoters direct the expression of transcripts encoding the 130-kDa MLCK and telokin. (B) Representation of the mylk1 transcripts. The amino acid sequence of telokin is identical to the COOH terminus of the MLCK molecules. The amino acid sequence of the 130-kDa MLCK is identical to the common COOH-terminal portion of the 220-kDa MLCK. (C) Telokin minimal promoter schematics. Numbers assigned are relative to transcription start site. Analysis of promoter fragments in transgenic mice has suggested that the core of the telokin promoter, which includes a CArG box and adjacent AT-rich region, is required for expression in smooth muscle cells.

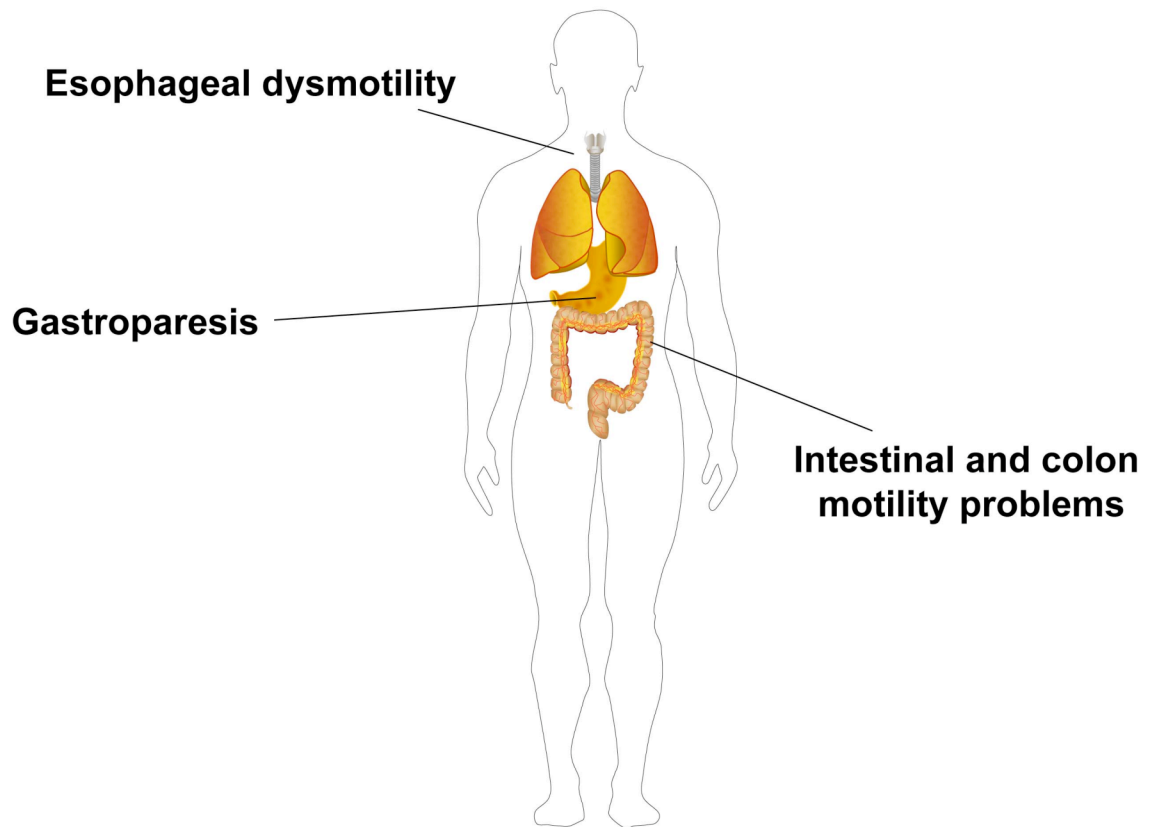


Figure 4. Diabetes-related defects of gastrointestinal tract. Type 1 and type 2 diabetes leads to defective motility in upper and lower GI tract. Diabetic patients develop dysmotility of the esophagus, stomach and intestine.

CHAPTER II

***HPRT*-TARGETED TRANSGENES PROVIDE NEW INSIGHTS INTO SMOOTH MUSCLE-RESTRICTED PROMOTER ACTIVITY**

Summary

Mouse telokin and SM22 α promoters have previously been shown to direct smooth muscle cell-specific expression of transgenes in vivo in adult mice. However, the activity of these promoters is highly dependent on the integration site of the transgene. In the current study, we found that although the ectopic expression of these transgenes could be abolished by flanking the transgene with insulator elements from the H19 gene. However, the insulator elements did not increase the proportion of mouse lines that exhibited consistent, detectable levels of transgene expression. In contrast, when transgenes were targeted to the *Hprt* locus both telokin and SM22 α promoters resulted in reproducible patterns and levels of transgene expression in all lines of mice examined. Telokin promoter transgene expression was restricted to smooth muscle tissues in adult and embryonic mice. As reported previously, SM22 α transgenes were expressed at high levels specifically in arterial smooth muscle cells; however, in contrast to randomly integrated transgenes, the *Hprt*-targeted SM22 α transgenes were also expressed at high levels in smooth muscle cells in veins, bladder and gallbladder. Using *Hprt*-targeted transgenes we further analyzed elements within the telokin promoter required for tissue specific activity in vivo. Analysis of these transgenes revealed that the CArG element in the telokin promoter is required for promoter activity in all tissues and that the CArG element and adjacent AT-rich region are sufficient to drive transgene expression in bladder, but not intestinal smooth muscle cells.

Introduction

Analysis of transgene expression driven by various fragments of smooth muscle-specific promoters has suggested that distinct cis-acting regulatory elements are required to direct expression of genes in different smooth muscle tissues [18, 20, 33, 49, 121, 122]. It is thus likely that distinct transcription regulatory pathways control the expression of genes in different smooth muscle tissues. This hypothesis is supported by several observations; for example differentiation of coronary artery smooth muscle cells is dependent on a complex of SRF, GATA4/6 and CRP [123]. In contrast, differentiation of aortic smooth muscle cells is dependent on myocardin [124], whereas myocardin-related transcription factor B (MRTF-B) plays a specific role in the differentiation of cardiac neural crest-derived smooth muscle cells [125, 126].

To better understand the mechanisms regulating expression of genes in distinct smooth muscle tissues, it is necessary to carefully analyze the relative importance of individual cis-acting regulatory elements in regulating expression of these genes in each tissue *in vivo*. Previous studies that have analyzed the activity of smooth muscle-specific promoters, in transgenic mice *in vivo*, have utilized standard transgenic approaches. One of the limitations of this approach is that the site of integration of the transgene and the transgene copy number can greatly affect both the pattern and level of transgene expression. For example, in our analysis of telokin promoter transgenes, we observed that the majority of transgenic lines exhibited no detectable transgene expression [33]. In addition, the pattern of transgene expression driven by an SM22 α promoter was distinct in different transgenic lines, with most lines exhibiting arterial-specific expression while some showed additional expression in veins and in heart [33]. In general, telokin promoter transgenes are expressed at highest levels in visceral smooth muscle tissues [33], by contrast, SM22 α transgenes are most highly expressed in vascular smooth muscle tissues [18, 20, 122]. The reciprocal expression of

telokin and SM22 α transgenes, make these two promoters good tools for identifying regulatory elements that direct transcription to distinct smooth muscle tissues. However, the variable patterns and levels of expression of these transgenes makes analysis of regulatory elements within these promoters difficult, requiring the analysis of large numbers of independent founder lines. In order to be able to determine the relative importance of regulatory elements in different smooth muscle tissues it is necessary to generate transgenic mice in which the activity of wild type promoters are highly reproducible both in terms of their levels and tissue-specific patterns of activity.

In the current study we used two different approaches to decrease the variability in the pattern and level of transgene expression. In the first, we used a transgene cassette in which the transgene is flanked by insulator elements from the H19 gene. In a second approach, we targeted single copy transgenes adjacent to the hypoxanthine phospho-ribosyltransferase (*Hprt*) locus using homologous recombination in ES cells. *Hprt* is a housekeeping gene expressed in all cell types, hence it would be anticipated that this locus would be transcriptionally favorable. Although this approach has not been utilized for smooth muscle-specific promoters, previous studies using endothelial cell-specific promoters demonstrated that, when targeted to this locus, these promoters exhibit very reproducible endothelial-specific expression [56-59]. Similarly, the myogenin promoter also exhibited appropriate skeletal muscle-specific expression when targeted to the *Hprt* locus [60]. Results from the current studies demonstrate that telokin promoter-driven transgenes exhibited greatly reduced ectopic expression when flanked by insulator elements. However, the levels of transgene expression still remained highly variable between transgenic lines. In contrast, *Hprt*-targeted telokin promoter transgenes exhibited faithful, reproducible patterns and levels of transgene expression, in all animals examined. In *Hprt*-targeted telokin promoter transgenes, similar to endogenous telokin, expression was restricted to visceral and to a lesser extent vascular smooth muscle tissues. The reproducible patterns

and levels of transgene expression allowed us to begin to determine the importance of specific regulatory elements within the telokin promoter. We found that although mutation of the CArG box was sufficient to abolish transgene expression in all smooth muscle tissues, a core promoter extending from -90 to +180 relative to transcription start site, that included an AT-rich region and the CArG box, was not sufficient for high levels of transgene expression in most smooth muscle tissues. Analysis of *Hprt*-targeted SM22 α promoter transgenes demonstrated that the *Hprt*-targeting system is universally applicable to smooth muscle-restricted promoters. These transgenes also exhibited a very reproducible pattern of transgene expression in all animals analyzed. *Hprt*-targeted SM22 α transgenes were transiently expressed in embryonic skeletal and cardiac muscle and robustly expressed specifically in embryonic and adult arterial, venous and bladder smooth muscle tissues.

Methods

Transgenic mouse production. The 370bp telokin promoter-AUG LAC transgenes, contained the -180 to +190 fragment of the mouse telokin promoter fused to a modified b-galactosidase transgene, followed by an SV40 large T-antigen polyadenylation sequence, as described previously [33]. To generate a transgene that is flanked by insulator elements, the 370bp mouse telokin promoter fragment extending from -180 to +190 relative to transcription start site was amplified by PCR, digested with XhoI and ligated into the pWhere vector (InvivoGen, San Diego, CA). Restriction digestion and DNA sequencing were performed to confirm the orientation and integrity of the resultant plasmid such that the promoter is located in the 5'-3' orientation 5' of a modified LACz gene in which all CpG sequences are mutated and a SV40 nuclear localization added (T370-pWhere). The Indiana University Transgenic Facility generated all standard transgenic lines in C3H mice; founders were then bred with DBA/2 mice

to establish stable lines. Transgenic animals were identified by PCR. To generate *Hprt*-targeted transgenes, telokin promoter fragments extending from -190 to +180 (T370), -90 to +180 (T270), a -180 to +190 telokin promoter harboring a mutation in the CArG element and a -475 to +61 SM22 α promoter were cloned into the AUG-LAC β -galactosidase vector. The AUG-LAC transgene vectors, were then digested with appropriate restriction enzymes and cloned into the pMP8SKB *Hprt* targeting vector, kindly provided by Dr. Sara Bronson [55]. This resulted in the placement of the promoter, LAC cDNA and SV40 poly A sequence 5' of the *Hprt* promoter (Figure 5). The resultant targeting constructs were linearized by digestion with Sal I and electroporated into BK4 embryonic stem cells by the Indiana University Transgenic Mouse facility [55]. Correctly targeted embryonic stem cells have repaired the mutant *Hprt* gene in BK4 ES cells and can therefore be selected using HAT media. HAT resistant clones were expanded and genomic DNA isolated (Puregene, Genra Systems, Minneapolis, MN). Homologous recombination was then confirmed by southern blot analysis of genomic DNA digested with Bam HI. Wild type BK4 cells have a 9kb Bam HI fragment, that hybridizes to an exon 3 derived probe, whereas cells harboring the targeted telokin transgene have an approximately 12kb fragment (Figure 5). For all *Hprt*-targeted transgenes (except T370 AUG LAC, in which chimeras derived from only 1 ES line transmitted the transgene) lines of mice were established from two independently targeted ES clones. As the *Hprt* gene is on the X chromosome, transgene expression was analyzed in hemizygous male mice or in homozygous female mice.

Transgenic mice were genotyped by PCR using transgene specific primers. Primers used were: Telokin 370 AUG-LAC, Telokin 370-*Hprt* and Telokin 370 CArG mutant-*Hprt*, S- ACTGTCTCTTTGACCACTTGAAATCC, AS-GGCAGGGTTTTCCAGTCACGACG TTG; Telokin 370-pWhere S, same as T370 AUG-LAC, and AS- CAACCCACCTG CCATTGCACCAAGAGGTG; Telokin 270-*Hprt*, S-GAAGTAGGCTAAAGAGTTGAACGCAAAG, AS-

GGCAGGGTTTTCCAGTCACGACGTTG; SM22 α -*Hprt*, S-GCACAGACTGCTCCAAGTGGTGTCTTTC, AS-CAACCCACCTGCCATTGCACCAGAGGTG. Male embryos were identified by using PCR primers S-GTACAAGTCTGCAGACTCTTCCAAC and AS-CCGAGGGTCTCCGGAATCCTTTCTTG that were designed to amplify the ZFY region on the Y chromosome.

β -galactosidase staining and histology. For whole mount analysis of β -galactosidase expression in neonatal F1 mice and adult founder mice, tissues were rapidly excised and fixed for one hour on ice in 2% paraformaldehyde/ 0.2% gluteraldehyde in phosphate buffered saline (PBS). For analysis of expression in whole embryos, embryos were dissected free of the yolk sac and then treated as described for tissues. Following fixation, tissues or embryos were washed 4-6 times with PBS and stained with X-gal staining solution overnight at room temperature. X-gal staining solution is comprised of 0.5mg/ml X-Gal, 5mM K₃Fe(CN)₆, 5mM K₃Fe(CN)₆, 2mM MgCl₂, 0.2% NP40, 0.2% Tween 20, 0.2% Triton X-100 in PBS. Tissues are then washed in PBS and further fixed in 4.0% paraformaldehyde overnight. Following fixation, tissues were either directly photographed using a dissecting microscope and digital camera (Kodak MDS290) or were dehydrated in increasing concentrations of ethanol and cleared in methyl salicylate prior to photography. Tissues for histological sections were excised, equilibrated in 20% sucrose in PBS overnight, frozen in tissue freezing medium (Triangle Biomedical Sciences) and sectioned at 8-12 μ m. For analysis of β -galactosidase expression slides were fixed in 0.5% gluteraldehyde in PBS for 10 minutes at room temperature, washed in PBS, stained overnight with X-gal staining solution, washed 3 times in PBS and then counterstained with Hematoxylin and Eosin according to standard procedures. For analysis of smooth muscle myosin expression, sections were fixed in 3.7% formaldehyde and incubated with antibodies directed against SM1 smooth muscle myosin heavy

chain, primary antibody was detected using fluorescein conjugated anti-rabbit IgG, as described previously [127].

Results

Addition of insulator elements decreases ectopic expression of transgenes driven by the telokin promoter in embryos. Previously we have shown that a 370bp mouse telokin promoter fragment can direct β -galactosidase expression specifically to smooth muscle tissues in neonatal and adult mice [33]. However, only 4 out of 14 lines of transgenic mice harboring this transgene had detectable levels of transgene expression. In addition, we observed significant ectopic expression of the transgene at embryonic days 12.5 and 14.5 in these mice (Table 1 and data not shown). To determine if the ectopic expression of telokin promoter-driven transgenes during embryonic development results from the influence of exogenous enhancer elements, transgenic mice were generated in which the transgene was flanked by insulator elements (Methods). Of the 6 positive transgenic lines obtained using this transgene cassette, only three lines had detectable levels of β -galactosidase expression. In one of these three lines (line #3) expression levels were very low with only a few smooth muscle cells staining in the gut and bladder (Table 1). The other two lines (lines #1,2) showed robust β -galactosidase staining that was restricted to smooth muscle cells of the gastrointestinal, genitourinary and respiratory tracts, in adult mice (Table 1). Low levels of expression were also observed in the abdominal aorta and mesenteric vessels. There was no detectable β -galactosidase expression in the aortic arch, coronary or pulmonary vasculature, in the brain, cardiac muscle or any other tissue examined (including liver, kidney and skeletal muscle, data not shown). Only one of these lines (#1) passed the transgene to the F1 generation, permitting analysis of embryonic expression. In embryos from this line, transgene expression was restricted to smooth muscle cells (Table 1). This pattern of

expression mimics endogenous telokin, which is also restricted to smooth muscle cells throughout development.

***Hprt*-targeted transgenes recapitulate endogenous telokin expression in adult mice and during embryonic development.** As addition of insulator elements did not lead to increased numbers of mice exhibiting detectable levels of transgene expression, we next targeted transgenes to the X-linked hypoxanthine phosphoribosyltransferase (*Hprt*) locus. *Hprt* is a housekeeping gene expressed in all cell types, hence it would be anticipated that this locus would be transcriptionally favorable. The 370bp AUG-LAC transgene, described previously [33], was introduced into the *Hprt* targeting vector pMP8SKB as shown in Figure 5. Six chimeric male mice were generated from a telokin promoter transgene ES clone (clone #6, Figure 5), and bred with C57/BL6J female mice. Five of these chimeras transmitted the transgene, three were used to establish transgenic lines. Four male hemizygous animals (F2-4) were analyzed from each line. To obtain homozygous transgenic female mice, hemizygous male mice were bred with heterozygous transgenic females. In all mice analyzed, β -galactosidase was expressed at high levels in visceral smooth muscle cells throughout the GI tract, bladder and bronchi. Low levels of expression were seen in gallbladder, vascular smooth muscle cells of mesenteric vessels, in vessels on the surface of the brain, in the abdominal aorta, vena cava and in the renal vessels (Figure 6, Table 2). No transgene expression was detected in the thoracic aorta, pulmonary or coronary vasculature or in any other tissue, such as heart, skeletal muscle, liver or kidney. Within these tissues transgene expression was restricted to smooth muscle cells (Figure 6 and data not shown). The pattern of expression of this transgene mirrors that of endogenous telokin, which is expressed at high levels in visceral smooth muscle tissues and lower levels in vascular smooth muscle (Table 2 and references 5,14). In contrast to endogenous telokin and transgene expression in T370 AUG-LAC and T370 pWhere mice, no β -

galactosidase activity was detected in the reproductive tract smooth muscle of the *Hprt*-targeted mice.

The smooth muscle-specific pattern of transgene expression in T370-*Hprt* mice was maintained throughout embryonic development. Expression was first detected at E11.5 in the umbilical artery (Figure 7). By day 12.5 expression could also be seen in the intestine and in a small group of cells at the apex of the heart. In E14.5 mice, robust expression was seen in the herniated gut and umbilical artery and lower levels of expression could be seen in the bronchi, abdominal aorta, cerebral vasculature and at the apex of the heart (Figure 7). In sections obtained from E14.5 and E15.5 mice β -galactosidase expression was shown to be restricted to the smooth muscle cells in the bladder, gut and umbilical vessels (Figure 7 and data not shown). We were not able to detect the β -galactosidase positive cells at the apex of the heart in histological sections, hence the identity of these cells could not be determined.

***Hprt*-targeted SM22 α -promoter driven transgenes are expressed in venous and bladder smooth muscle cells in addition to arterial smooth muscle cells.** To determine if the *Hprt*-targeting system would be generally applicable to other smooth muscle-specific promoters we also generated and characterized *Hprt* transgenes driven by a -475 to +61 fragment of the SM22 α promoter. Previously, we noted that transgenes driven by this SM22 α promoter also exhibited variable patterns of expression in different lines of mice [33]. In all of the *Hprt*-targeted SM22 α promoter-driven transgenic mice, derived from two independent ES clones, we observed an identical pattern of transgene expression. High levels of β -galactosidase activity were detected in arteries and veins in small and large blood vessels, including mesenteric, abdominal, renal, thoracic, pulmonary, coronary, femoral and brain vasculature. Little or no staining was observed in visceral smooth muscle tissues except in the bladder and gallbladder, which exhibited high levels of β -galactosidase activity (Figure 8,

Table 2). Some staining was also observed in the main branches of bronchi at the entrance to the lung, but was not detected in trachea or further along the bronchi or bronchioles. In E12.5 mice we observed strong β -galactosidase staining in dorsal aorta, umbilical artery and vein, vitelline vessels, heart and somites. By E14.5 expression in heart and somites had declined and expression in small blood vessels throughout the head and limbs increased (Figure 9).

***Cis*-acting elements located 5' of the AT-rich/CArG core of the mouse telokin promoter are necessary for driving expression in GI smooth muscle cells.** Previously, we showed that the -94 to -49 core of the telokin promoter, that includes an AT-rich region and CArG box, is required for telokin transcription in vivo [22]. To determine if this region is sufficient to drive telokin promoter activity, an *Hprt*-targeted transgene was generated containing a fragment of the telokin promoter extending from -90 to +180. In all neonatal mice harboring this transgene there was almost no transgene expression detected in intestinal smooth muscle cells (Figure 10, Table 2). Although expression in bladder smooth muscle cells was also reduced, as compared to expression in transgenes driven by the larger -190 to +180 telokin promoter fragment, (compare Figure 2 to Figure 10) it remained significantly higher than in intestinal smooth muscle cells (Figure 10). Expression levels in mesenteric, renal and brain vasculature also decreased slightly, and expression in bronchi, abdominal aorta and vena cava was not detectable.

The CArG box in the mouse telokin promoter is required for telokin promoter activity in all smooth muscle tissues. Our previous in vitro results suggest that a CArG element is crucial for telokin promoter activity [32]. In addition, deletion of the CArG element together with the adjacent AT-rich region abolished the activity of the endogenous telokin promoter [22]. To determine if CArG element alone is required for telokin promoter activity this element was mutated to ablate SRF binding within the context of the 370bp, -190 to +180

telokin promoter. Two lines of *Hprt*-targeted transgenes were generated from independently targeted ES clones. In all adult and embryonic mice harboring this transgene no specific β -galactosidase expression was detected in any tissue (Table 2).

Discussion

These results demonstrate that a single copy of the telokin promoter targeted to the *Hprt* locus is able to reproducibly drive high levels of transgene expression specifically in smooth muscle tissues throughout mouse development. Most importantly, the pattern of expression of this transgene largely recapitulated the expression of the endogenous telokin. Although flanking telokin promoter driven transgenes with insulator elements abolished ectopic transgene expression, 50% of the lines of mice harboring these transgenes still did not exhibit detectable levels of transgene expression (Table 1). As the insulators should block the activity of repressor elements, the lack of expression in many lines may be due to the integration of the transgene at sites of compact, inactive chromatin. If transgenes integrate into sites of compact chromatin structure, then the activity of the transgene will depend on the ability of the regulatory elements within the transgene to modify chromatin structure, allowing appropriate transcription factors to bind and activate the promoter. All of the telokin promoter-driven transgenic lines, derived from a single ES clone in which the transgene was targeted to the *Hprt* locus, exhibited high levels of transgene expression. We also observed a similar pattern of expression when this promoter was used to drive expression of an EGFP transgene targeted to the *Hprt* locus (data not shown). Thus, when placed in a region of relaxed, open chromatin structure, such as the *Hprt* locus, the 370bp telokin promoter is able to mediate high levels of tissue-restricted transgene expression. This then raises the question of how the telokin promoter is active in its endogenous location if it is not able to remodel chromatin

structure. The telokin gene locus is, however, rather unusual in that the telokin promoter is located within an intron of the larger mylk1 gene [16, 17, 131]. In addition to telokin, the mylk1 gene encodes at least two myosin light chain kinase (MLCK) isoforms, the 220kDa and 130kDa MLCK [131]. Each of these protein kinases is transcribed from its own independent promoter within the mylk1 gene, rather than arising from alternative splicing [131, 132]. Myosin light chain kinases are expressed in most if not all tissues in adult and embryonic mice [133], hence it would be anticipated that the MLCK/telokin locus would be expected to have a transcriptionally active, open chromatin configuration in most cells, throughout development. This proposal suggests that upstream elements in the mylk1 gene exist, that are responsible for maintaining the chromatin structure of the telokin promoter in a relatively open conformation. Further studies will be required to confirm this possibility.

The visceral smooth muscle-selective pattern of expression of *Hprt*-targeted telokin promoter-driven transgenes parallels endogenous telokin expression. Both in adult and in embryonic mice, endogenous telokin is expressed at higher levels in most visceral smooth muscle tissues compared to vascular smooth muscle tissues [21, 31]. *Hprt*-targeted telokin promoter transgene expression was observed in cells on the surface of the apex of the heart in E12.5-E14.5 mice (Figure 7). This may reflect ectopic expression, resulting from an influence of the *Hprt* locus on the transgene, as endogenous telokin expression has not been observed in embryonic mouse heart [31]. However, as β -galactosidase expression in these cells is low and could not be detected in tissue sections, it is possible that expression of endogenous telokin in these cells may also not have been detected in our previous in situ hybridization study [31]. Our inability to detect β -galactosidase expression in these cells on tissue sections has prevented us from further characterizing these cells to determine their identity. In contrast to endogenous telokin, *Hprt*-targeted telokin promoter transgene expression was not observed in smooth muscles of the male or female

reproductive tract (Table 2). As both telokin promoter pWhere and AUG-LAC transgenes exhibit transgene expression in uterine smooth muscle (Table 1) this would suggest that the lack of expression of *Hprt*-targeted transgene expression in uterine smooth muscle most likely results from ectopic influences of the *Hprt* locus.

Although previous studies have shown that *SM22 α* promoter transgenes are restricted to arterial smooth muscle we also observed high levels of expression in bladder, gallbladder and veins when the transgene was targeted to the *Hprt* locus (Figure 8). Moreover, venous expression was observed not only in adult animals but also through embryonic development at E12.5 and E14.5 (Figure 9). Although the *Hprt*-targeted *SM22 α* transgenes more closely recapitulate endogenous *SM22 α* expression, which is expressed in all smooth muscle tissues [35, 129, 134], the lack of transgene expression in GI and reproductive tract smooth muscle cells suggest that additional more distal regulatory elements are required to drive *SM22 α* expression in these tissues. In support of this proposal, a BAC clone encompassing the *SM22 α* gene was expressed in all smooth muscle tissues in transgenic mice [36]. The expression of the *Hprt*-targeted *SM22 α* transgenes in bladder and veins also suggest that tissue-specific chromatin remodeling complexes may be important for regulating *SM22 α* expression. Alternatively, it is possible that regulatory elements within the *Hprt* locus are affecting the activity of the *SM22 α* promoter to increase expression in veins and bladder smooth muscle.

The reproducible pattern of expression of telokin- and *SM22 α* -driven transgenes targeted to the *Hprt* locus permitted us to begin to dissect the role of individual elements within these promoters. A telokin promoter fragment extending from -90 to +180 exhibited a marked decrease in expression when compared to a -190 to +180 transgene (Figure 10). Transgene expression in the GI tract was

particularly affected with only a few isolated cells staining positive for β -galactosidase activity (Figure 10). This result is in contrast to in vitro data in which deletion of the -190 to -94 region resulted in only a 30% decrease in reporter gene activity in A10 smooth muscle cells [33]. However, the small change in activity in A10 cells may reflect cell-specific differences, as the low levels of transgene expression seen in the vasculature did not appear to be as significantly affected by deletion of the -190 to -90 region as transgene expression in the GI tract (Figure 10). Together these data suggest that the -190 to -90 region of the telokin promoter is required for high levels of telokin expression, and that this fragment is particularly important in smooth muscle cells of the GI tract. Although we do not yet know which transcription factors bind to this region, analysis of the sequence of the -190 to -90 region using rVISTA revealed the presence of a conserved Sox binding site. As Sox family members have been shown to play a role in GI tract development it is tempting to propose that they may be contributing to telokin expression in the GI tract [135].

Previous studies have demonstrated that SRF binds to this CArG box in the telokin promoter, in intact chromatin, in smooth muscle cells and that myocardin can strongly activate the promoter through its interaction with SRF bound to this site [136]. Myocardin has been shown to be a powerful co-activator of SRF on smooth muscle specific genes and to be required for vascular smooth muscle development [50, 51, 124, 130, 137]. In the current study we have also shown that the CArG box is required for telokin expression in all smooth muscle tissues in vivo (Table 2). However, the CArG box and adjacent AT-rich region are not sufficient for telokin promoter activity in vivo, in most smooth muscle tissues, as a -90 to +180 telokin transgene was not expressed at significant levels in the GI tract, reproductive tract or in airway smooth muscle. Together these data suggest that, in these smooth muscle tissues, myocardin must cooperate with other factors to drive telokin expression.

In summary, the reproducibility of *Hprt*-targeted telokin and SM22 α promoter transgene expression will greatly facilitate analysis of the tissue-specific roles of cis-acting elements within these promoters. The advantage of this approach, is that a single copy of the transgene integrates at a defined locus, this thus permits, quantitative comparison of transgene expression driven by wild type and mutant promoters.

Further we were interested to investigate whether telokin transcriptional regulation is altered in disease state. Previous studies in diabetic rats showed that impaired GI contractility possibly occurs through altered sensitivity to calcium in colon smooth muscle [94]. As telokin is known to play a role in smooth muscle calcium desensitization, it could possibly play a role in motility defect detected in diabetic patients and animal models. Thus, I was interested to determine whether colon smooth muscle in diabetic state undergoes dedifferentiation leading to decreased telokin expression.

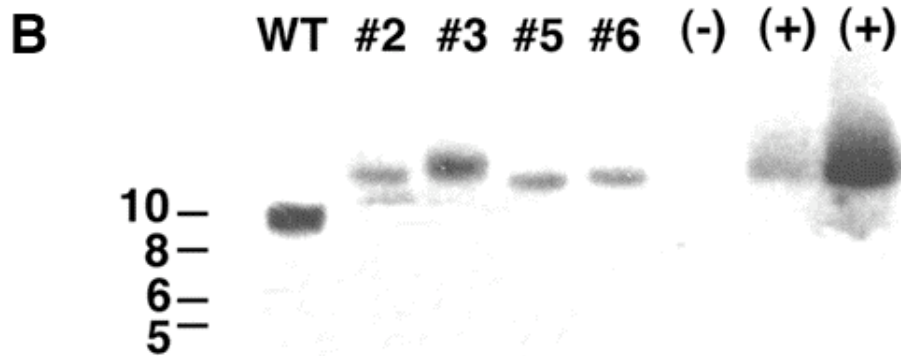
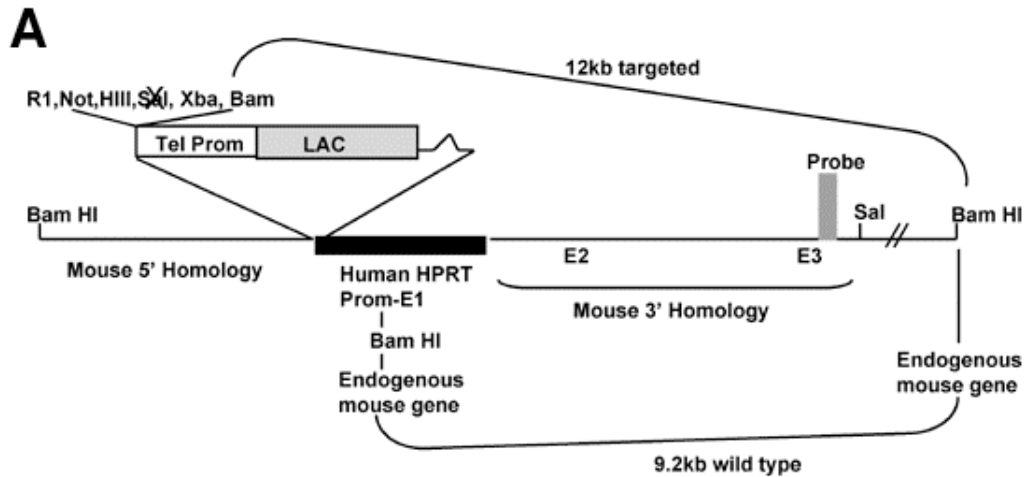
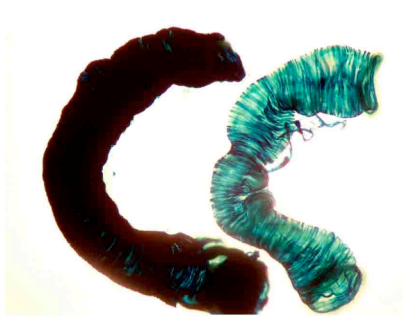


Figure 5. Telokin promoter *Hprt* targeting scheme. (A) Schematic representation of the *Hprt* targeting vector. (B) Southern blot analysis of genomic DNA extracted from targeted HAT resistant embryonic stem cell clones. Genomic DNA was digested with BamHI, separated on a 0.8% agarose gel, transferred to a nylon membrane and then reacted with a probe to exon 3 of the mouse *Hprt* gene (shown in A). A 9 kb band corresponding to the endogenous mouse *Hprt* gene fragment was seen in wild type cells and bands of approximately 12 kb were seen in clones 2, 5 and 6 corresponding to the correctly targeted locus. The band obtained from clone #5 was slightly smaller than the bands obtained from clones 2 and 6, additional PCR and sequence analysis revealed that this clone contained a small deletion within the β -galactosidase cDNA. ES clones #2 and #6 were used to generate chimeric mice. Chimeric mice derived from ES clone #2

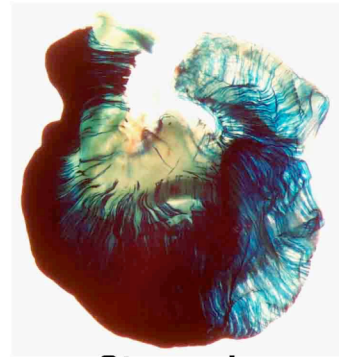
did not transmit the transgene, hence data presented are from mice derived from ES clone #6. Clone #3 contained a band significantly larger than 12 kb and likely represents an insertional event rather than a replacement as described previously [55].



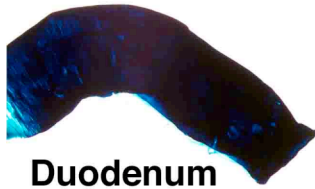
Bladder



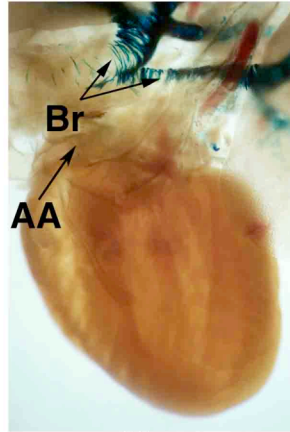
Colon



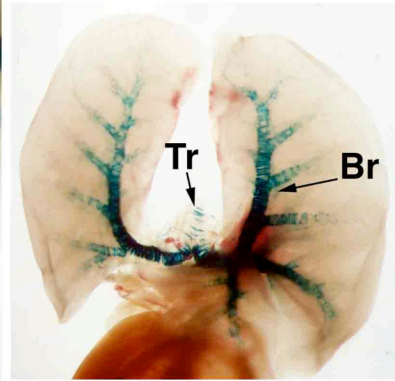
Stomach



Duodenum



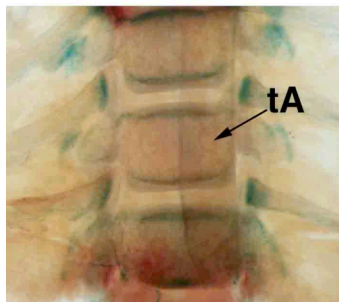
Heart



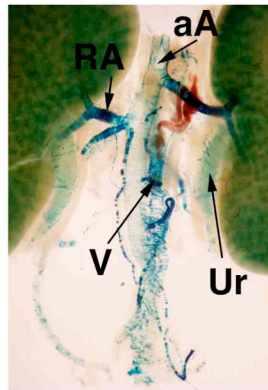
Lungs



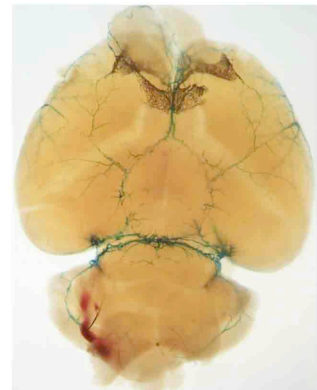
Skeletal Muscle



Spinal Cord

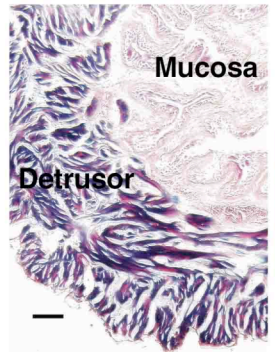


Kidney



Brain

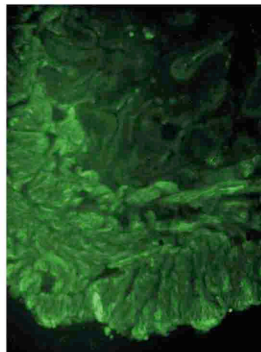
X-Gal/H&E



Mucosa

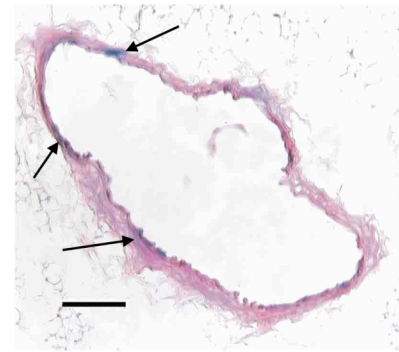
Detrusor

SM1



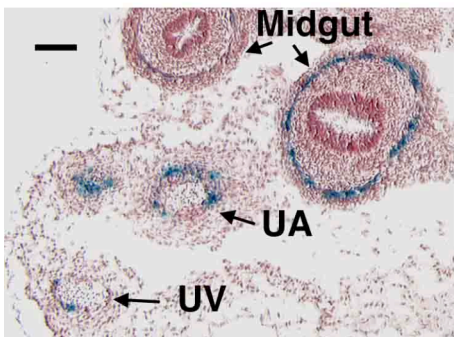
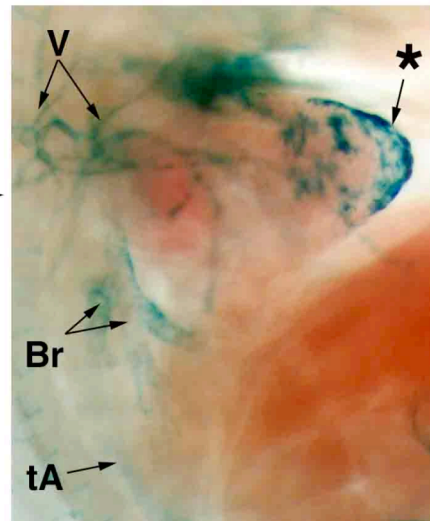
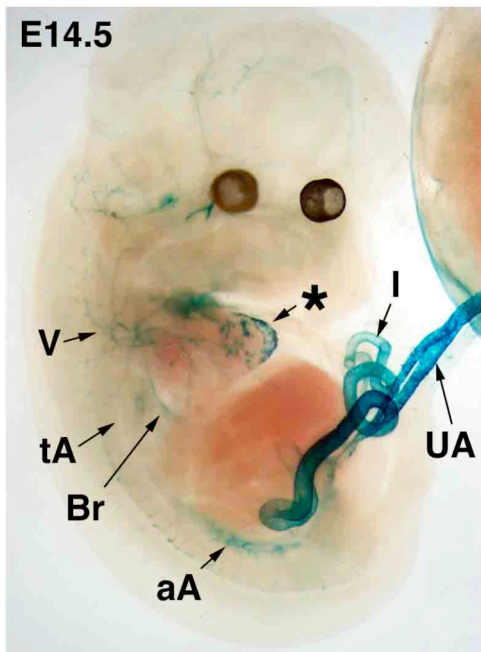
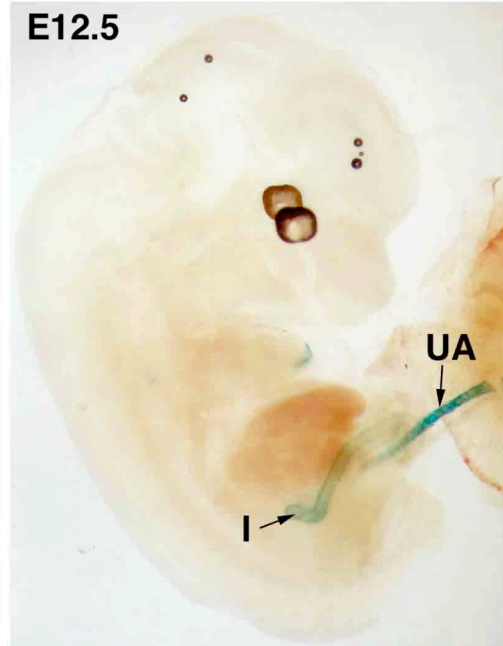
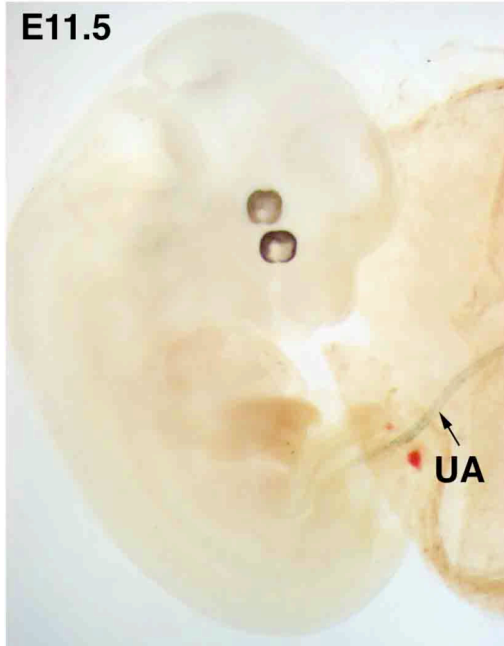
Bladder

X-Gal/H&E

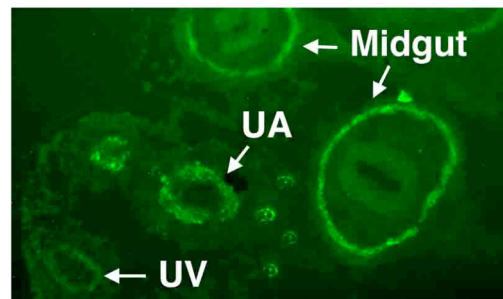


Aorta

Figure 6. Expression of *Hprt*-targeted telokin 370AUG-LAC transgenes in adult mice. Tissues were rapidly dissected from a positive hemizygous male *Hprt*-targeted telokin promoter 370bp AUG-LAC transgenic mouse, fixed and stained for β -galactosidase expression as described in 'Methods'. This transgene resulted in high levels of β -galactosidase expression in smooth muscle tissues of the bladder, colon, stomach, duodenum, bronchi (Br), trachea (Tr) and renal artery (RA) and low levels of expression in the abdominal aorta (aA), vena cava (V), ureter (Ur) but no expression in the aortic arch (AA) or thoracic aorta (tA) as indicated. In the bottom three panels tissues were frozen, and serial sections were stained for β -galactosidase (blue stain), hematoxylin and eosin (X-Gal/H&E) and smooth muscle myosin heavy chain (SM1, green). The arrows on the abdominal aorta section indicates β -galactosidase positive smooth muscle cells. The scale bars represent 100 μ m.



X-Gal/H&E



SM1

Figure 7. Expression of *Hprt*-targeted telokin (-190 to +180) transgenes during embryonic development. Timed embryos were obtained from *Hprt*-targeted 370 bp telokin promoter (-190 to +180) AUG-LAC transgenic mice as indicated. Positive male mice were identified by PCR using transgene specific primers and primers to the ZFY locus which is located on the Y chromosome. Male embryos were processed for histochemical detection of β -galactosidase expression as described in 'Methods'. Blue staining representing β -galactosidase expression can be first seen at E11.5 in the umbilical artery (UA). This staining is more pronounced at E12.5 and can also be seen in the intestine (I). Expression is further increased by E14.5 where staining can be seen in the intestine (I), umbilical artery (UA), bronchi (Br) abdominal aorta (aA), cerebral and trunk vasculature (V) and on the surface of the apex of the heart (*). No staining was detected in the thoracic aorta (tA), liver or any other organ. The bottom two panels are serial sections through an E14.5 embryo that were stained for β -galactosidase (blue stain) and hematoxylin and eosin (X-Gal/H&E) or smooth muscle myosin heavy chain (SM1, green), as described in 'Methods'. Scale bar represents 100 μ m. β -galactosidase and SM1 staining can be seen in the midgut, umbilical artery (UA) and umbilical vein (UV).

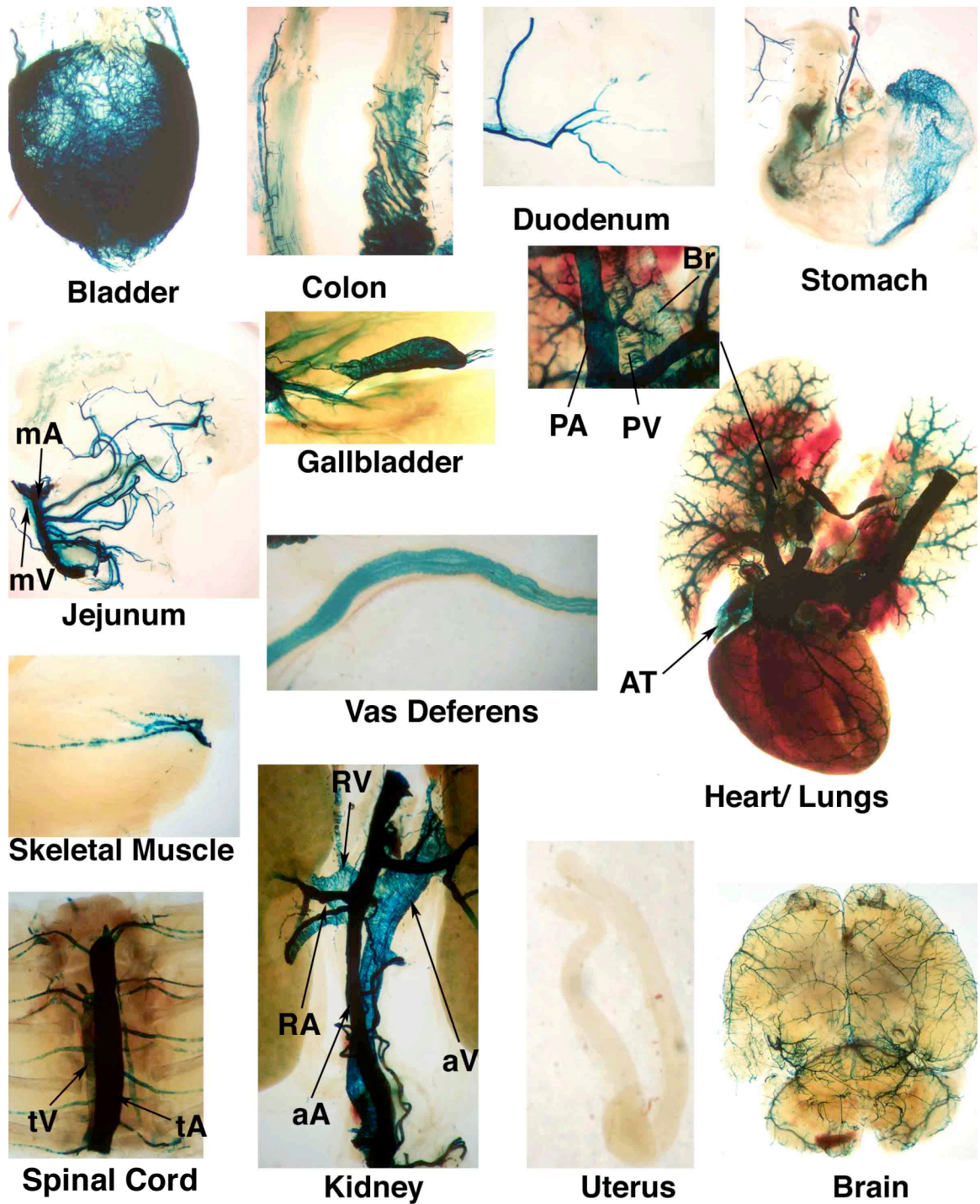


Figure 8. Expression of an *Hprt*-targeted SM22 α transgene in adult mice. Tissues were rapidly dissected from a positive hemizygous male *Hprt*-targeted 536bp SM22 α promoter (-475 to +61) AUG-LAC transgenic mouse, fixed and

stained for β -galactosidase expression as described in 'Methods'. This transgene resulted in high levels of β -galactosidase expression in smooth muscle tissues of the mesenteric arteries (mA) and veins (mV), renal artery (RA) and vein (RV), abdominal aorta (aA), and vena cava (aV), thoracic aorta (tA) and vena cava (tV), pulmonary artery (PA) and vein (PV), bronchi (Br), atria (AT), coronary and brain vessels, bladder and gallbladder. No expression was detected in colon, duodenum, stomach, jejunum, uterus or in skeletal muscle cells. Identical patterns of transgene expression were observed in two hemizygous male and 2 homozygous female mice obtained from each of two SM22 α transgenic lines. Each of these lines was generated from an independently targeted ES cell clone.

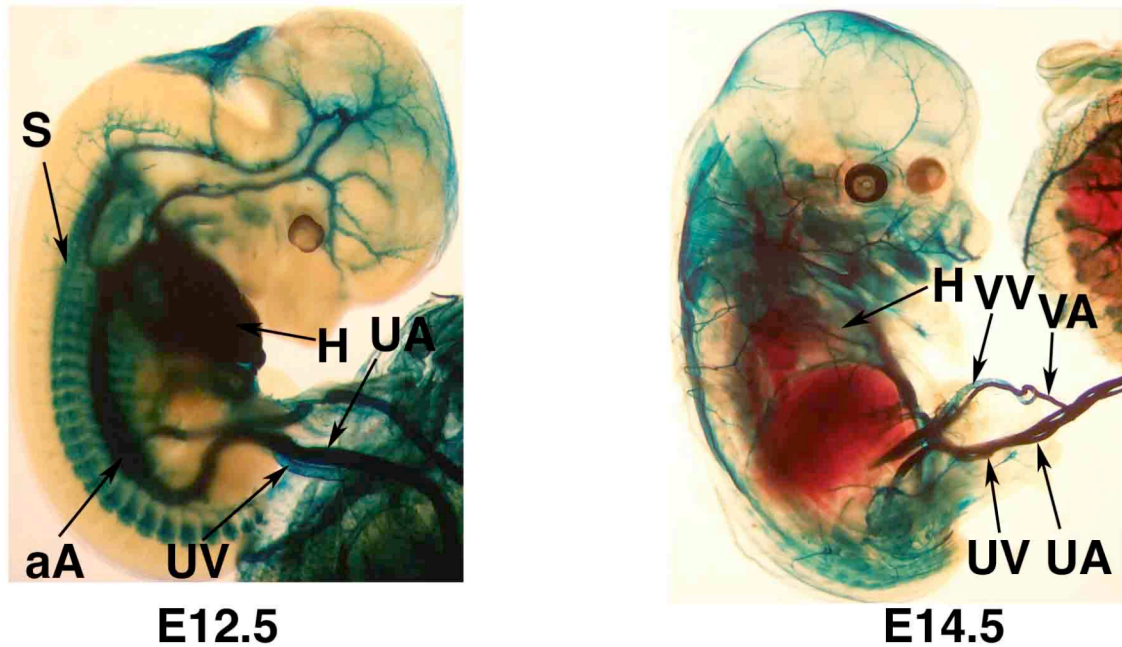


Figure 9. Expression of *Hprt*-targeted SM22 α transgenes in embryonic mice. Timed embryos were obtained from *Hprt*-targeted 536bp SM22 α promoter (-475 to +61) AUG-LAC transgenic mice as indicated. Positive male mice were identified by PCR using transgene specific primers and primers to the ZFY locus which is located on the Y chromosome. Embryos were processed for histochemical detection of β -galactosidase expression as described in 'Methods'. Blue staining representing β -galactosidase expression can be seen in umbilical artery (UA) and vein (UV), vitelline artery (VA) and vein (VV), abdominal aorta (aA), heart (H) and somites (S) at E12.5. By day 14.5 expression decreased in the heart, somites and abdominal aorta.

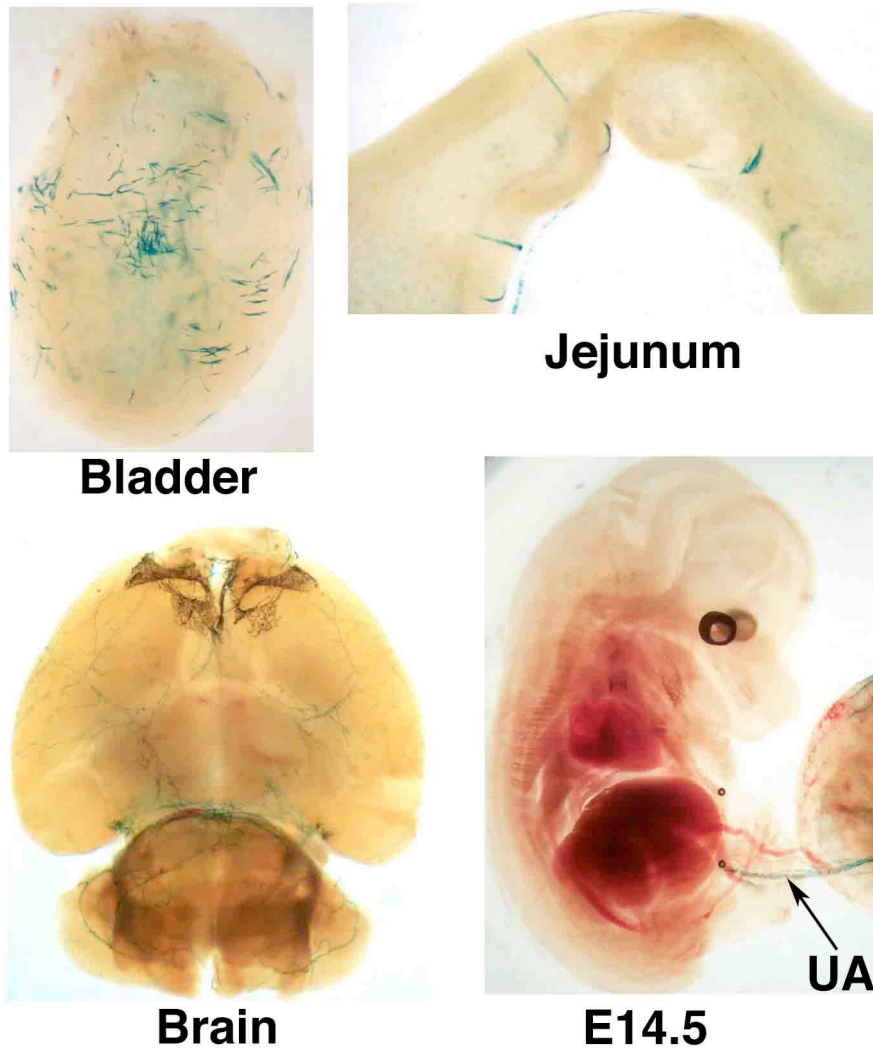


Figure 10. Expression of *Hprt*-targeted telokin 270bp (-94 to +180) transgenes. Tissues were collected from a positive hemizygous neonatal male *Hprt*-targeted 270bp telokin promoter (-94 to +180) AUG-LAC transgenic mouse or from an E14.5 transgenic mouse. Tissues and embryos were processed for histochemical detection of β -galactosidase expression as described in 'Methods'. Blue staining representing β -galactosidase expression adult mice can be seen at low levels in bladder, mesenteric vessels and brain vasculature. Blue staining in E14.5 is seen in umbilical artery (UA). An identical staining pattern was also observed in hemizygous male mice obtained from an independently targeted ES clone.

Table 1. Relative expression levels of β -galactosidase transgenes

Transgene	Expressing/ Total Lines		Relative Expression Levels									
			Blad	Gut	Brai n	Uterus	Aor. Arch	Ab. Aorta	E14 Vasc	E14 Gut	E14 Ect	
T370 (-190 to +180) AUG LAC	4/14	Line										
		1	++	++	-	+	-	+/-	-	-	+++	
		2	+/-	+/-	-	+	-	-	-	-	-	
		3	+	+	-	+++	-	+	nd ¹	nd ¹	nd ¹	
		4	+++	+++	-	male	-	+	nd ¹	nd ¹	nd ¹	
T370 (-190 to +180) pWhere	3/6	Line										
		1	+++	+++	-	+++	-	+	-/+	++	-	
		2	+++	+++	-	male	-	-	nd ¹	nd ¹	nd ¹	
		3	+	+/-	-	male	-	-	nd ¹	nd ¹	nd ¹	
T370 (-190 to +180) <i>Hprt</i>	3/3	Chimeras										
		1	+++	+++	-	-	-	+	+	++	-	
		2	+++	+++	-	nd	-	+	+	++	-	
		3	+++	+++	-	nd	-	+	nd	nd	nd	

Blad, Bladder; Aor.Arch, aortic arch; Ab.Aorta, abdominal aorta, E14 Vasc, E14 vasculature, E14 Ect, E14 ectopic expression (none smooth muscle).

nd, not determined

nd¹, no embryos analyzed, as founder produced no pups.

Table 2. *Hprt*-targeted transgene expression pattern

Mice Tissue	Endogenous Telokin	T370 (-190 to +180)	T270 (-90 to +180)	T CArG mut. (-190 to +180)	Endogenous SM22a	SM22 (-475 to +61)
Bladder	+++	+++	+	-	+++	+++
Colon	+++	+++	-	-	+++	-
Ileum	+++	+++	-	-	+++	-
Jejunum	+++	+++	-	-	+++	-
Duodenum	+++	+++	-	-	+++	-
Stomach	+++	+++	-	-	+++	-
Gallbladder	+	+	-	-	N	+++
Ureter	++	+++	-	-	N	-
Vas Deferens	+++	-	-	-	N	-
Bronchi	+++	+++	-	-	+++	+
Uterus	+++	-	N	N	+++	-
Mesenteric vessels	N	++	+	-	+++	+++
Renal vessels	+	++	+	-	N	+++
Thoracic aorta	-	-	-	-	+++	+++
Coronary vessels	-	-	-	-	+++	+++
Brain vessels	N	++	+	-	+++	+++
Skeletal muscle	-	-	-	-	- (adult)	- (adult)

N, not analyzed

CHAPTER III

TYPE 1 DIABETES LEADS TO ALTERED CALCIUM SIGNALING IN CHRONIC AND ACUTE DIABETIC MICE

Introduction

As many as 76% of diabetic patients at some point in the course of their disease develop gastrointestinal (GI) symptoms such as dysphagia, vomiting, constipation, diarrhea or fecal incontinence [74]. Constipation is the most common symptom and affects approximately 60% of patients [74, 75]. GI symptoms have been linked to poor glycemic control rather than duration of the disease [98]. Animal studies have shown that diabetes can lead to accelerated or delayed GI motility depending on the animal model used and the specific parts of the GI tract tested. Studies in an STZ-induced diabetic rat model revealed increased small intestine smooth muscle mass and increased colon contractility [91, 92]. The spontaneous contractile activity in STZ-induced diabetic rat colon smooth muscle was increased [138] without a change in intracellular Ca^{2+} handling [94] while in ileum intracellular Ca^{2+} handling was decreased [94]. Conversely in STZ-induced diabetic mice the colon smooth muscle contractile response to carbachol stimulation was weaker when compared to control animals at 4 and 8 weeks following STZ treatment [93]. In these mice this was also associated with delayed gastric emptying and increased intestinal transit time [86]. Diabetic db/db mice also show slower gastric emptying and prolonged whole gut transit time as compared to wild type mice [79]. These mouse models are consistent with human studies that demonstrated impaired colonic smooth muscle contractility in diabetic patients [139].

Most studies attribute GI motility changes to autonomic or enteric nervous system (ENS) neuropathy [78-83, 139]. A study using non-obese diabetic (NOD), STZ-

induced diabetic and db/db mice models demonstrated that NOD and STZ mice develop autonomic neuropathy while chronically diabetic db/db mice fail to develop neuritic dystrophy [78]. STZ-induced diabetic rats have been reported to show decreased number of enteric neurons in colon and stomach after only 7 days of hyperglycemia [84, 85]. Human studies have also demonstrated a loss of enteric neurons in colons from diabetic patients [139]. However, few studies have explored the possibility that there are also defects in GI smooth muscle itself or shown how these defects progress during development of the diabetic state. In STZ-induced diabetic mice and db/db diabetic mice impaired stomach smooth muscle contractility has been reported to be due to alterations in muscarinic receptor coupling through GTP-binding proteins [95]. Similarly in diabetic BB/W rats a decreased contractile response of stomach smooth muscle resulted from altered intracellular signal transduction through IP3 and PKC pathways [96]. In some severe diabetic cases in both rat models and human patients where hyperglycemia is controlled poorly, gastroparesis occurs that is associated with gastric smooth muscle myopathy [96, 97]. Mechanistically, prolonged hyperglycemia can lead to increased O-glycosylation of proteins as a result of increased flux of glucose through the hexosamine pathway. Increased global O-glycosylation in cardiac and skeletal muscles has been shown to decrease Ca^{2+} sensitivity in these tissues and attenuate contractility [101, 102, 104]. Although the affects of O-glycosylation on colonic contractility have not been explored. Recently it has been shown that that reduction in insulin/IGF-I in diabetic mice causes decreased stem cell factor (SCF) production resulting in smooth muscle atrophy that eventually leads to ICC depletion [87]. These results suggest that myopathy may play a more central role in diabetic gastroenteropathies than previously recognized. They also suggest a role for insulin depletion in addition to hyperglycemia in progression of the smooth muscle dysfunction.

The main goal of the current study was to determine the affects of diabetes on colon smooth muscle structure and function in a type 1 diabetic mouse model

induced by low dose STZ. Animals in this model develop hyperglycemia and hypoinsulinemia rapidly and maintain these changes for several weeks. We observed that STZ-induced diabetic mice have decreased colonic contractility and motility which develops rapidly within 1 week and is maintained for more than 7 weeks. At early time points the decreased contractility is likely a result of impaired Ca^{2+} handling within the colonic smooth muscle cells that subsequently leads to more pronounced Ca^{2+} defects during prolonged exposure to hyperglycemia and hypoinsulinemia.

Methods

Streptozotocin (STZ)-induced diabetic mice. 9-12 week old C57BL6 mice were injected intraperitoneally with freshly prepared streptozotocin (STZ) (Sigma, S0130) at dose 55mg/kg for 5 consecutive days. Mice developed hyperglycemia (>200 mg/dl) within one week after injection and were sacrificed 1 week or 7-8 weeks following the last injection of STZ. Blood glucose levels were measured using an Accu-Chek Aviva glucose measuring kit (Roche). All animal procedures were approved by the Indiana University School of Medicine IACUC committee.

Computed Tomography. For in vivo GI motility measurements, mice were fasted over a 12-hour period then 100 μL of the oral contrast agent Gastrografin (Bracco Diagnostic Inc) diluted with 300 μL saline was given through oral gavage. CT images were subsequently acquired at 3, 5, 9 and 15 hours after administration of the contrast agent. For all scans, an x-ray voltage of 90kVp and an anode current of 100mAs were utilized. CT imaging was performed with a high-speed clinical CT scanner, a Siemens Somatom Sensation-16, capable of obtaining a mouse volumetric image within 1 minute. The image voxel resolution was 300 μx 300 μx 625 μx . A 3D volume rendering was generated using Siemens' image processing workstation equipped with the "Syngo" software. During

imaging, mice were kept anesthetized with 1.5% isoflurane (0.8L oxygen/minute). Between each scan mice were awake and received regular water and food. The GI motility was visualized by comparing images at different time points.

Contractility measurements of colon rings. Colons were dissected and cut into 0.5cm long circular rings. 4 rings from the proximal and 4 from the distal part of the colon (Figure 12a) were placed in Krebs buffer in an organ bath (Kent Scientific) and attached to isometric force transducers. An optimal resting tension of 1.5g was determined empirically following stimulation with 60mM KCl. Colon rings from control and STZ-induced diabetic animals were equilibrated at optimal resting tension in Krebs buffer for 1h and contracted using 60mM KCl. After contraction rings were washed for 30min and the contraction repeated. Samples from each experiment were paired and data expressed as percentage of the KCl induced contraction.

Ca²⁺ imaging. The ratio-metric imaging of Fura-2AM fluorescence was employed to monitor intracellular Ca²⁺ changes in colon strips. Ratio-metric imaging eliminates the artifacts associated with the tissue movement during KCl applications. 1mm wide colon strips were dissected free of epithelia and loaded with Fura-2AM for 5-14 hrs at room temperature in phosphate buffer solution containing 0.901mM Ca²⁺, 0.493mM Mg²⁺, 5.56mM glucose and 0.327mM pyruvate, 40μM Fura-2AM and 1% BSA. The Fura-2AM loaded colon strips were washed in standard external solution containing 145mM NaCl, 2.5mM KCl, 1mM CaCl₂, 1mM MgCl₂, 10mM HEPES and 5.5mM glucose pH7.3 without Fura-2AM and were incubated for additional 1-3hrs at room temperature before the experiment, allowing complete Fura-2AM hydrolysis. Ca²⁺ imaging was performed using a monochromator-based TillPhotronics imaging system attached to an inverted Zeiss microscope equipped with a “Fluor” 2.5x objective and a back-illuminated Andor CCD camera. Fura-2AM was alternatively excited at 345nm and 380nm. The emitted light was collected using a 510nm long-pass

filter. The TillVision software was used to control all fluorescence imaging experiments and to perform the analysis of images. Images were acquired every 5seconds. The background fluorescence was subtracted. The intracellular Ca^{2+} concentration was calculated using the equation $[\text{Ca}^{2+}]_i = K_d \times [(R-R_{\min})/(R_{\max}-R)] \times (F_{\max}(380)/F_{\min}(380))$. The K_d value of 225nM was used. To determine the R_{\max} value, the strips were bathed in a solution containing 135 mM NMDG, 10 mM HEPES, 10mM CaCl_2 , 5.5mM Glucose, 10mM Ionomycin Ca^{2+} salt, pH7.3. The R_{\min} value was determined in a solution containing 145mM NaCl, 10mM EGTA, 10mM HEPES, 5.5mM Glucose, 10mM EGTA, Ca^{2+} -free Ionomycin, pH7.3. High KCl solution contained 145mM KCl, 1mM CaCl_2 , 1mM MgCl_2 , 10mM HEPES, 5.5mM Glucose, pH7.3.

RNA analysis. Mouse colon was dissected and the epithelial layer was removed by mechanical scraping. RNA was extracted from distal colon as described previously [140]. 0.5 μ g of RNA was used as template for reverse transcription (RT). Gene expression levels were measured by quantitative real time PCR using SYBR green PCR master mix (Roche) and a 7500 Real Time PCR system (Applied Biosystems). 5 μ l of 1:5 diluted cDNA was used for each reaction. All PCR reactions were performed in duplicate. Primers used are shown in table 3.

Western blot analysis. Protein from proximal or distal colon was extracted with RIPA lysis buffer. Protein concentrations were determined by using a BCA Protein Assay kit (Pierce). Proteins were fractionated on 5.0, 7.5 or 15% polyacrylamide gels and transferred to nitrocellulose or polyvinyl difluoride membranes. Membranes were then probed with a series of antibodies. Antibodies used for western blotting were against: MLCK (Sigma, clone K36, 1:10,000), SM α -actin (Sigma, clone 3A1, 1:10,000), SM22 α (rabbit polyclonal antibody directed against the peptide CGPDVGRPDRGRLGFQVW, Proteintech, 1:10,000), telokin (1:6,000) [16], SM1, SM2, phospholamban [31], caldesmon (Sigma, clone C21, 1:10,000), GAPDH (Novus, clone 1D4, 1:5,000), PMCA4

ATPase (Thermo Scientific, clone JA9, 1:1,000), SERCA2 (Cell Signaling, 1:1,000), IP3R2 (Santa Cruz, clone C-20, 1:1,000), Cav1.2 (Alomone, 1:200), Cav1.2 (Santa Cruz, clone H-280, 1:1,000), O-linked N-Acetylglucosamine (Thermo Scientific, clone RL2, 1:1,000). Primary antibodies were detected using horseradish peroxidase-conjugated secondary antibodies and visualized and quantitated using chemiluminescence on a G-Box imaging system (Syngene)

Immunohistochemical staining. Tissues were collected from control and diabetic mice, and fixed in 4% paraformaldehyde solution for 24h and processed for paraffin embedding. After embedding 6 μ m sections were cut and stained with hematoxylin and eosin.

In vitro O-glycosylation. To test the direct effects of protein O-glycosylation on smooth muscle contractility colonic smooth muscle rings were incubated with 0.05mM glucosamine in Krebs buffer for 1h. 60mM KCl induced contractile responses were measured before and after glucosamine treatment. After contractility measurements, samples were processed for western blot analyses to confirm that the experimental protocol resulted in globally enhanced O-glycosylation.

MLC phosphorylation. Distal colon was isolated, cut in 0.5cm circular rings and hung in an organ bath as described above for contractility measurements. Tissues were flash frozen in the basal non-contracted state or at the peak of contraction initiated by 60mM KCl stimulation. Myosin light chain phosphorylation levels were measured by western blotting of proteins separated on urea/glycerol gels as described previously [141].

Results

STZ-induced diabetic mice have decreased overall gastrointestinal tract motility. Computed Tomography was used to assess the rate of food transit through the GI tract of control and diabetic animals 7 weeks following STZ injections. At the earliest time point analyzed (0 hour) contrast agent was found mainly in the stomach and was starting to enter the small intestine in both mouse groups (data not shown). Within 3 hours, although some contrast agent reached the rectum in both control and diabetic mice (Figure 11), there was more residual contrast left in the stomach and small intestine of the diabetic animals. After 5 hours contrast agent was seen primarily in the colon and rectum of control mice while in diabetic mice, a significant amount of contrast was still visible throughout the whole of the small and large intestine. In control mice, the contrast agent was completely excreted between 9 and 15 hours post gavage. In contrast, in diabetic mice large amounts of contrast material still remained in the small and large intestine even 15 hours after gavage. These data demonstrate that the overall gastrointestinal transit time in diabetic animals was longer than in control mice. The CT scan data show that motility in diabetic animals is decreased in the stomach as well as small and large intestine resulting in an overall increased GI transit time. These results correlate with patient data showing significant constipation in large proportion of the diabetic human population [74, 75]. In addition, from both CT scans and also direct dissection of the GI tract the intestine appeared dilated in diabetic mice when compared to controls, possibly due to pseudo-obstruction in the lower GI tract.

STZ-induced diabetic mice show decreased colon contractility. To better understand the mechanisms responsible for the decreased motility in diabetic mice we analyzed the contractility of colon rings ex vivo. To avoid neuronal pathway, we analyzed the ability of the rings to contract in response to direct depolarization induced by 60mM KCl. This approach bypasses the

neuromuscular synaptic transmission pathway and thus allows us to directly assess the contractility of the colonic smooth muscle itself. To determine if there were localized or global changes in colonic contractility the colon was divided into 8 segments and the contractility of each segment measured separately (Figure 12A). In diabetic mice, rings from the proximal part of the colon (P1 to P3) did not show any statistically significant changes in contractility when compared to control animals (Figure 12B, C). In contrast, the more central and distal P4 to D2 parts of the colon showed 30-70% decreases in contractility in diabetic mice compared to control mice, with the most pronounced decrease (70%) found in the D4 part (Figure 12B, C). After combining data from all colonic segments the colons from diabetic mice showed a statistically significant decrease in overall colonic contractility as compared to control mice (Figure 12D).

Long term diabetic mice have increased basal intracellular Ca^{2+} levels and decreased Ca^{2+} response to KCl stimulation. To begin to unravel the causes of the contractility defects, we examined changes in intracellular calcium in response to KCl stimulation. Strips of colonic smooth muscle were obtained from the central region of the colon and loaded with Fura-2 for ratio-metric calcium imaging. Ratio-metric measurements showed a large increase in the basal Ca^{2+} levels in strips obtained from long term diabetic mice as compared to control mice (Figure 13A, B). These levels calibrated to approximately 200nM Ca^{2+}_i in control mice and 600nM in diabetic mice (data not shown). In addition, the calcium transient generated in response to KCl stimulation was approximately 60-70% lower in STZ-induced diabetic mice when compared to control mice (Figure 13A, C). Despite the elevated basal intracellular calcium levels seen in the diabetic mice there was no significant change in the basal myosin light chain phosphorylation levels in these mice (Figure 13D).

Long term diabetic animals show significant changes in levels of calcium handling proteins. In order to determine the mechanisms that may lead to the

alteration in basal and KCl-stimulated Ca^{2+} levels we performed qRT-PCR and western blot analysis of a wide panel of proteins known to be important for regulating intracellular calcium levels (Figure 14). This analysis revealed an approximately two-fold increase in SERCA2b (sarcoplasmic reticulum calcium pump) and IP3R2 (IP3 receptor) mRNA levels in long term diabetic mice as compared to control mice (Figure 14A). Cav1.2b (L-type calcium channel), PMCA4 (plasma membrane calcium ATPase), RyR2 (ryanodine receptor 2) and NCX2 (sodium calcium exchanger) mRNA levels also showed a trend toward an increase in diabetic mice, however, due to the variability among animals these changes did not show statistical significance (Figure 14A). In contrast, SERCA2b and IP3R2 protein levels decreased 20-40% in diabetic mice (Figure 14B). Cav1.2b protein levels were not changed in diabetic mice, while PMCA4 protein levels increased by 20% in diabetic mice (Figure 14B). In addition, we did not observe any significant changes in smooth muscle contractile (myosin, actin) or regulatory proteins (caldesmon, SM22 α , telokin) at either the mRNA or protein levels (Figure 14A, D).

Contractility in short term diabetic mice is decreased due to an attenuated intracellular Ca^{2+} response and decreased myosin light chain phosphorylation. The complex and somewhat confounding changes in expression of calcium handling proteins described above, suggest that after 7 weeks of hyperglycemia adaptive changes may have occurred in the diabetic mice in an attempt to compensate for an initial defect. To try to identify which changes may represent the initial defect we analyzed diabetic mice that had been hyperglycemic for a much shorter time (less than 1 week). Mice that have been hyperglycemic for less than 1 week (sacrificed 1 week after the last STZ injection) also showed a decreased contractile response to KCl in the middle portion of the colon (P4 and D4) (Figure 15A). Ratio-metric measurements of intracellular calcium showed no changes in the basal Ca^{2+} levels but a lower Ca^{2+} increase in response to KCl in these diabetic mice as compared to controls (Figure 15B, C).

Collectively, these data suggest that an initial defect in depolarization stimulated Ca^{2+} entry is later confounded by an elevation in basal intracellular Ca^{2+} which occurs following prolonged hyperglycemia. Despite the attenuated calcium response, we observed no significant changes in protein and mRNA levels of the L-type channel, SERCA 2 and IP3R2. A statistically significant but small decrease was detected in PMCA4 protein levels (Figure 15D, E, F). Consistent with the intracellular calcium measurements there was no differences in the basal myosin light chain phosphorylation levels between diabetic and control mice (Figure 15G). However, KCl stimulated myosin light chain phosphorylation levels were lower in diabetic mice as compared to controls (Figure 15G).

Long term hyperglycemic mice have increased global O-glycosylation levels although elevated O-glycosylation in vitro does not significantly affect contractility. Although we did not see any changes in expression of calcium channels or calcium handling proteins in mice which have been hyperglycemic for less than 1 week it is possible that the function of these molecules may be altered. One of the common ways in which hyperglycemia can modify proteins is through elevated O-glycosylation [142]. Previous studies in cardiac and skeletal muscle have shown that STZ-induced diabetic mice have increased global O-glycosylation levels in these tissues that leads to decreased contractility [101, 102, 104]. Consistent with these findings western blot analysis of protein extracted from the middle part of the colon, showed increased O-glycosylation levels in our STZ-induced diabetic mice (Figure 16A). To determine if increased O-glycosylation could lead to decreased colonic contractility we treated colon rings from control mice with glucosamine to increase O-glycosylation levels directly and determined the subsequent affects on contractility. After 1h glucosamine treatment rings had elevated global O-glycosylation levels comparable to those seen in STZ-induced diabetic mice (compare Figure 16A to 16B). Although contractility of glucosamine treated rings was slightly decreased this did not reach statistical significance (Figure 16C).

Long term diabetic mice show increased iNos mRNA levels in the colon smooth muscle layer, but no other signs of inflammation. To rule out the possibility that the attenuated contractility of the colons from diabetic mice is due to a thinner smooth muscle layer, we examined hematoxylin- and eosin-stained cross-sections. Smooth muscle layer thickness and nuclear density (data not shown) were not different between diabetic and control mice (Figure 17A). As inflammatory cytokines are known to attenuate GI smooth muscle contractility [117] and the STZ-diabetic model has been reported to exhibit elevated inflammation, we examined the possible contribution of elevated cytokines in the attenuated contractility observed in the colons from diabetic mice. Immunohistological analysis of macrophages in the colon revealed that there are no significant differences between control and STZ-induced mice. In addition, although qRT-PCR analysis revealed a 4-fold increase in iNos mRNA levels in colon smooth muscle tissues from diabetic mice 7 weeks after STZ treatment no changes were observed after 1 week (Figure 17B). In addition, in the long term diabetic animals there was a 50% decrease in IL1 α levels and no significant changes in TNF α levels (Figure 17E). These data would suggest that there is not a marked inflammatory response in the colon at either 1 or 7 weeks following STZ injection as this would be expected to result in an elevation of several cytokines. However, an increase in NO produced by iNos could be contributing to the attenuated contractility in the long term diabetic mice.

Discussion

Previous studies have demonstrated that diabetes affects GI motility through causing neuronal damage. For example, studies in STZ-induced diabetic rats showed a neuronal defect in the duodenum and colon following a short term hyperglycemic exposure of 7 days [85, 143]. However, few studies have explored possible effects of diabetes directly on colonic smooth muscle. We observed that mice with long term hyperglycemia for 7-8 weeks exhibited a similar impairment in the whole gut transit time to that reported previously in mouse and human studies (Figure 11) [79, 144, 145]. These findings are consistent with constipation being the most common GI disorder observed in human diabetic patients. Results from our ex vivo contractility measurements further demonstrate that in this type 1 diabetic mouse model both short term (less than 1 week) and long term (7-8 weeks) hyperglycemia results in a direct impairment of colonic smooth muscle contractility, independent of any potential neuronal effects (Figures 12 and 15). This impaired contractility is not associated with a general dedifferentiation of colonic smooth muscle as expression levels of smooth muscle contractile proteins were not altered in any of these diabetic mice (Figure 14A, D). The attenuated contractility is also not a result of grossly altered smooth muscle structure as histology sections of the middle part of the colon showed no significant structural changes in the smooth muscle of the colon of STZ-induced diabetic mice (Figure 17A). Perhaps surprisingly, we observed regional differences in the contractile response along the length of the colon. The decreased contractile response to KCl was most pronounced in the middle portion of the colon (P4-D2 in Figure 12). There are a number of possible explanations for this regional variation. For example, the anatomical structure of the colon could be contributing to this phenomena. In the mouse, the middle portion of the colon exhibits a sharp bend as it is positioned in the abdominal cavity. This region also exhibits a steep decrease in its diameter when compared to the more proximal part. It is likely that these combined anatomical features

provide increased resistance to the movement of fecal matter through this region. Alternatively the distinct neural innervation of the proximal (vagal) and distal (pelvic) portions of the colon could be contributing to the regional pathological changes [147, 148] and causing a secondary functional atrophy.

Our observations that the impaired colonic contractility in diabetic mice is associated with an impairment in the depolarization-induced intracellular calcium increase is consistent with previous studies in diabetic rats which also exhibited impaired calcium handling [94, 138]. Moreover, our temporal data suggest that a primary defect in depolarization-induced calcium increases, eventually lead to an elevation in basal intracellular calcium levels following more long term exposure to hyperglycemia (Figures 13 and 15B). By inducing contraction of colonic rings with direct KCl-induced depolarization instead of a natural neurotransmitter ligand such as acetylcholine, or electrical field stimulation of the nerves, we were able to bypass the neuronal pathways and directly assess the function of the colonic smooth muscle. Contractions induced by KCl depolarization occur primarily through voltage dependent opening of L-type Ca^{2+} channels in the sarcolemma and perhaps to a small extent to release of calcium from intracellular stores [146]. The attenuated contractility observed following either 1 week or 7 weeks of hyperglycemia, suggests a direct defect in depolarization-dependent contractility of colonic smooth muscle that likely involves defects in the L-type Ca^{2+} channels (Figures 18, 19). In support of this, short-term diabetic mice exhibited a statistically significant but small decrease in PMCA4 protein levels, but no significant changes in the expression of any other of the L-type Ca^{2+} channel or any other calcium handling proteins (Figures 15, 18). Although statistically significant, the decrease in PMCA4 may not be sufficient to account for the attenuated Ca response. Other possibilities include posttranslational modifications to calcium regulatory proteins. In support of this, previous studies have shown that diabetes can lead to oxidative stress in smooth muscle [149-151] and oxidative stress in cardiac myocytes has been shown to cause nitration

of L-type channels leading to their decreased activity [112, 152]. Whether this occurred in response to STZ-induced hyperglycemia or not will be examined in future studies.

In contrast to short-term diabetic mice, long-term hyperglycemic mice (7-8 weeks) exhibited an elevated basal calcium level in addition to the attenuated KCl-induced calcium increase (Figures 13B, 19). These changes were associated with changes in several calcium handling mRNA and proteins levels. mRNA levels of SERCA2b and IP3R2 were significantly up-regulated and mRNA encoding Cav1.2b, PMCA4, RyR2 and NCX2 trended toward being elevated (Figures 14, 19). In contrast, western blotting revealed a down-regulation of IP3R2 and SERCA2 proteins (Figures 14, 19). These inconsistencies between mRNA and protein levels could be explained by compensatory transcriptional mechanisms occurring in response to downregulated protein levels due to protein posttranslational modifications. This would be consistent with previous studies have shown that diabetes induced oxidative stress can lead to nitration of SERCA [153]. Nitration in turn can attenuate SERCA activity and lead to its degradation resulting in impaired Ca^{2+} uptake into the SR. This could be contributing to the elevated basal calcium levels observed in colon smooth muscle following long term diabetes. Although we observed an increase in basal Ca^{2+} levels in colon from long term diabetic mice these changes did not lead to increased basal MLC phosphorylation (Figures 13D, 19). This result would suggest that the myosin light chain phosphorylation pathway has been desensitized to the calcium signal possibly through activation of the MLC phosphatase or inhibition of the MLC kinase in these mice.

Studies have shown that inflammatory cytokines such as $\text{TNF}\alpha$ [117] can also lead to decreased smooth muscle contractility in the gut but the influence of cytokines in altering GI motility in diabetes has not been examined. In our studies we did not find any evidence of macrophage activation in the colon of diabetic

mice nor could we detect any elevation of TNF α mRNA, and in fact observed a decrease in IL1 α mRNA levels (Figure 17B). We did however, detect higher levels of iNos mRNA in the smooth muscle of long term but not short term diabetic mice (Figure 17B, C). Together these data suggest that the increased iNos expression likely results from long-term oxidative stress rather than from an intestinal inflammatory response.

The diabetic state can lead to several different post-translational modifications of proteins, including nitration and O-glycosylation [142, 154]. Hyperglycemia, in particular leads to increased O-glycosylation of proteins via increased flux through the hexosamine pathway. Consistent with studies in skeletal and cardiac muscles, we detected increased global O-glycosylation levels in colon smooth muscle from STZ-induced diabetic mice. Although O-glycosylation levels were increased in STZ-induced diabetic mice, in vitro studies in which colon rings were treated with N-acetylglucosamine for 1 hour to directly increase levels of O-glycosylation did not show a significant decrease in their contractile response. As we still observed a global increase in O-glycosylated proteins, these findings suggest that increased O-glycosylation levels may not be the main contributor to the decreased contractility observed in STZ-induced diabetic animals.

In summary, our results show that STZ-induced diabetic mice develop decreased colon contractility as early as 7 days after developing hyperglycemia. This decreased contractility is likely caused by an attenuated depolarization-induced calcium increase which leads to decreased myosin light chain phosphorylation and impaired contractility. The primary molecular defect that results in the attenuated calcium increase is most likely an alteration in the activity of L-type Ca²⁺ channels through posttranslational modifications such as nitration or O-glycosylation. In long-term diabetes, we also observed increased basal intracellular Ca²⁺ levels that could be due to a decrease in SERCA2b level leading to decreased Ca²⁺ uptake to the SR. Together these data demonstrate

that in addition to any affects it may have on enteric neural innervation diabetes also has a direct effect on colonic smooth muscle cells that impairs their contractility.

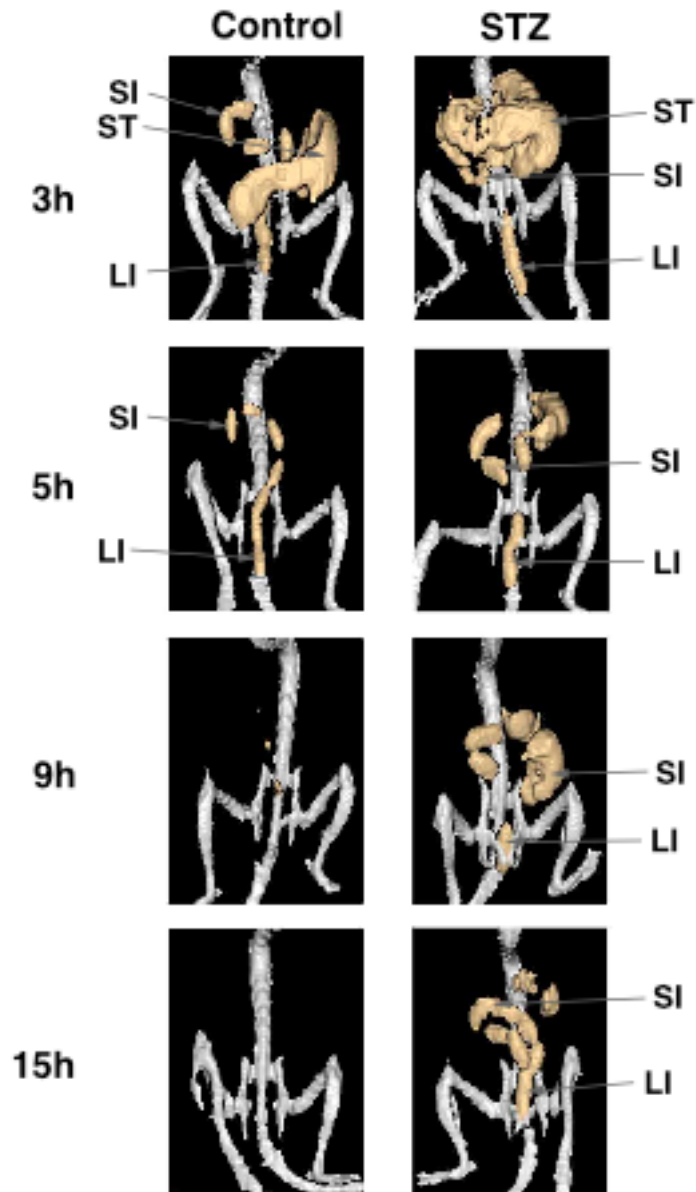


Figure 11. CT scan reveals decreased GI motility in chronic diabetic mice.

At 7-8 weeks after becoming hyperglycemic mice (n=3) were subjected to CT scan and compared to the control littermates injected with saline (n=2). CT images were taken 3, 5, 9, and 15 hours after contrast agent administration. In control mice throughout the scan contrast agent movement was faster and completely excreted after 9-15 hours, while contrast agent still detectable in diabetic mice at 15 hours. ST-stomach, SI-small intestine, LI-large intestine.

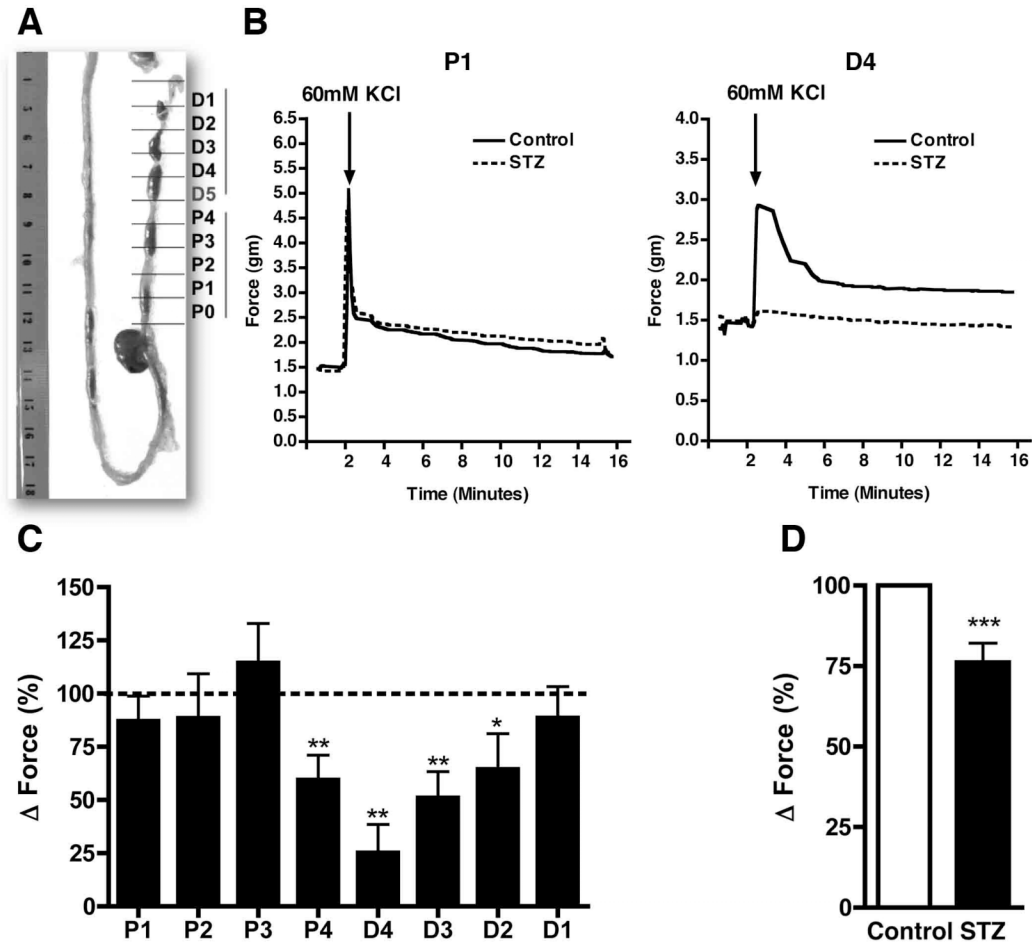


Figure 12. Chronic diabetic mice show decreased colon contractility. At 7-8 weeks after becoming hyperglycemic, mice colons were dissected for contractility measurements. (A) Colons were cut into 0.5 cm circular rings starting from the distal part, where D1 is assigned as the most distal part and P0 is the most proximal part. The proximal (P1-P4) rings and the distal distal (D1-D4) 4 rings of the colon were used for contractility measurements. (B) Representative tracings of colon ring contractility measurements after 60mM KCl stimulation. (C) Quantification of changes in contractility in control and STZ-induced mice of the different parts of the colon P1 (n=10), P2 (n=11), P3 (n=10), P4 (n=12), D4 (n=6), D3 (n=9), D2 (n=11), D1 (n=10). Changes in contractility of control mice are set to 100%. Each column represents the mean of different mice. Error bars represent standard deviation (\pm SD). (* $P < 0.05$, ** $P < 0.005$, Student t-test). (D)

Quantification of the average contractility changes from all colonic rings (proximal and distal) (n=79). Changes in contractility of control mice are set to 100%. (**P<0.0005, Student t-test).

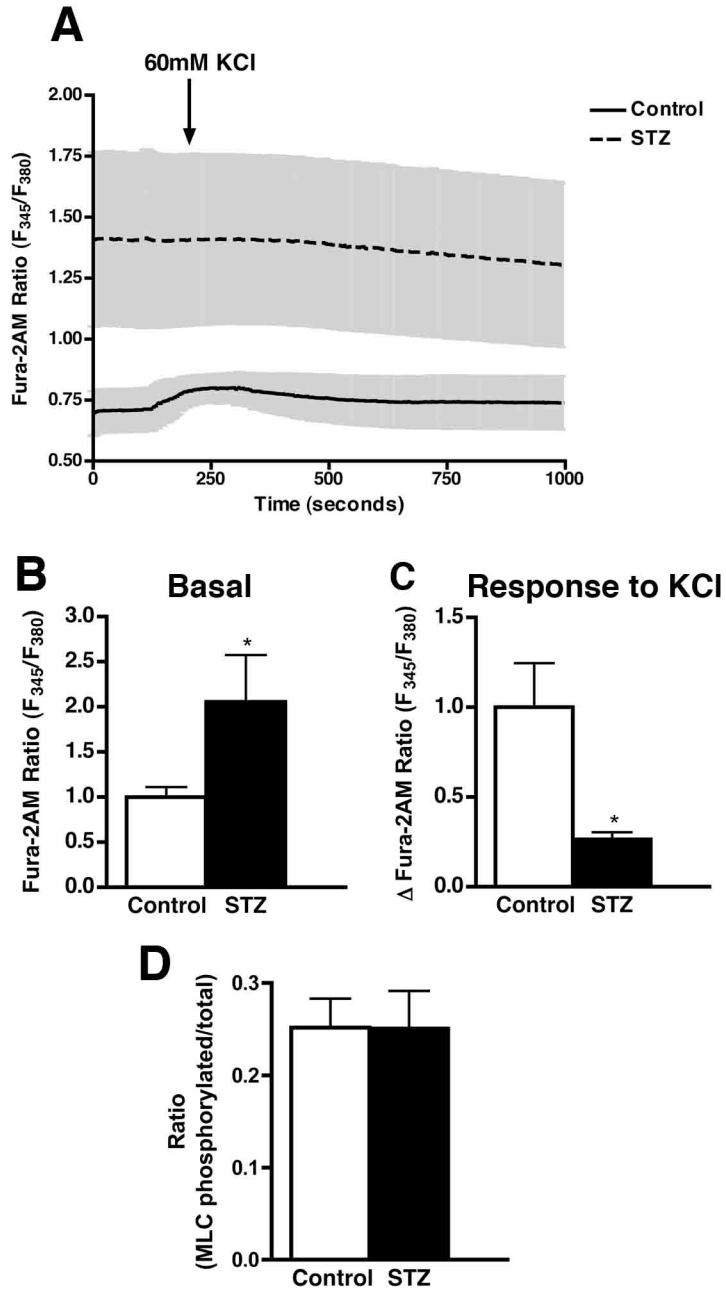


Figure 13. Basal intracellular Ca^{2+} levels are increased while the Ca^{2+} response to 60mM KCl is decreased in the middle part of the colon in chronic diabetic mice. (A) Representative averaged recordings of intracellular Ca^{2+} measured using Fura-2AM over the time. (B) Basal levels of intracellular Ca^{2+} . (C) Changes in intracellular Ca^{2+} in response to 60mM KCl in control and STZ-induced diabetic mice. For (A-C) Each tracing/column represents the mean

of different mice (n=6-8). Error bars represent standard deviation (\pm SD). For (B) and (C) intracellular Ca^{2+} levels of control mice are set to 1. (*P<0.05, Student t-test). (D) Myosin light chain phosphorylation was measured in the middle to distal part of colon (mechanically dissected free of the epithelial mucosa layer) by urea gel electrophoresis coupled to western blotting. MLC phosphorylation was expressed as $\text{MLC}_{\text{phosphorylated}}/\text{MLC}_{\text{total}}$. Each column represents the mean of samples obtained from 4 different mice. Error bars represent standard deviation (\pm SD). (*P<0.05, Student t-test).

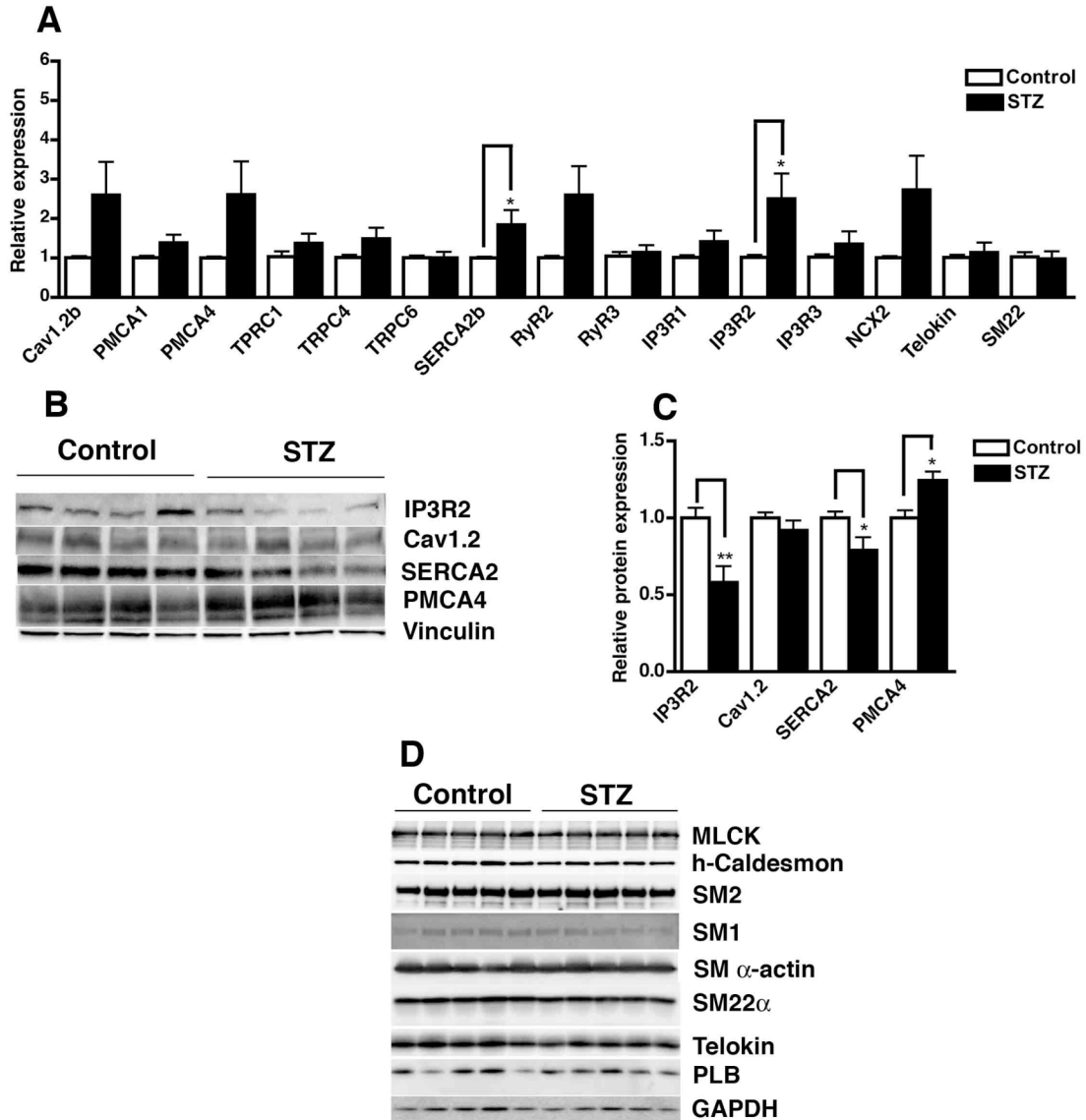


Figure 14. Changes in mRNA levels and protein of calcium handling proteins in chronic diabetic mice. The middle to distal portion of the colon was dissected and cleaned free from the mucosal layer. (A) RNA was isolated using Trizol (Invitrogen) and transcripts were quantitated by real-time RT-PCR. Transcript levels were firstly normalized to *HPRT* internal loading control and then samples from STZ-induced diabetic mouse colons normalized to those obtained from the control group of mice. Relative expression = $2^{-\Delta\Delta Ct}$, where $\Delta\Delta Ct = (Ct_{STZ} - Ct_{HPRT}) - (Ct_{control} - Ct_{HPRT})$. Changes in mRNA levels of control mice

are set to 1. Each column represents the mean data obtained from several different mice (n=4-10). Error bars represent standard deviation (\pm SD). (*P<0.05, Student t-test). (B) Immunoblots of proteins extracted from the colons of control and STZ-induced diabetic mice. (C) Quantification of protein expression following normalizing to vinculin levels as a loading control. Protein levels of control mice are set to 1. Each column represents the mean data obtained from 4 different mice. Error bars represent standard deviation (\pm SD). (*P<0.05, **P<0.005, Student t-test). (D) Smooth muscle contractile proteins are not changed in chronic diabetic mice. Immunoblots of proteins extracted from the middle part of the colon from chronic diabetic and control mice were performed as described in 'C'.

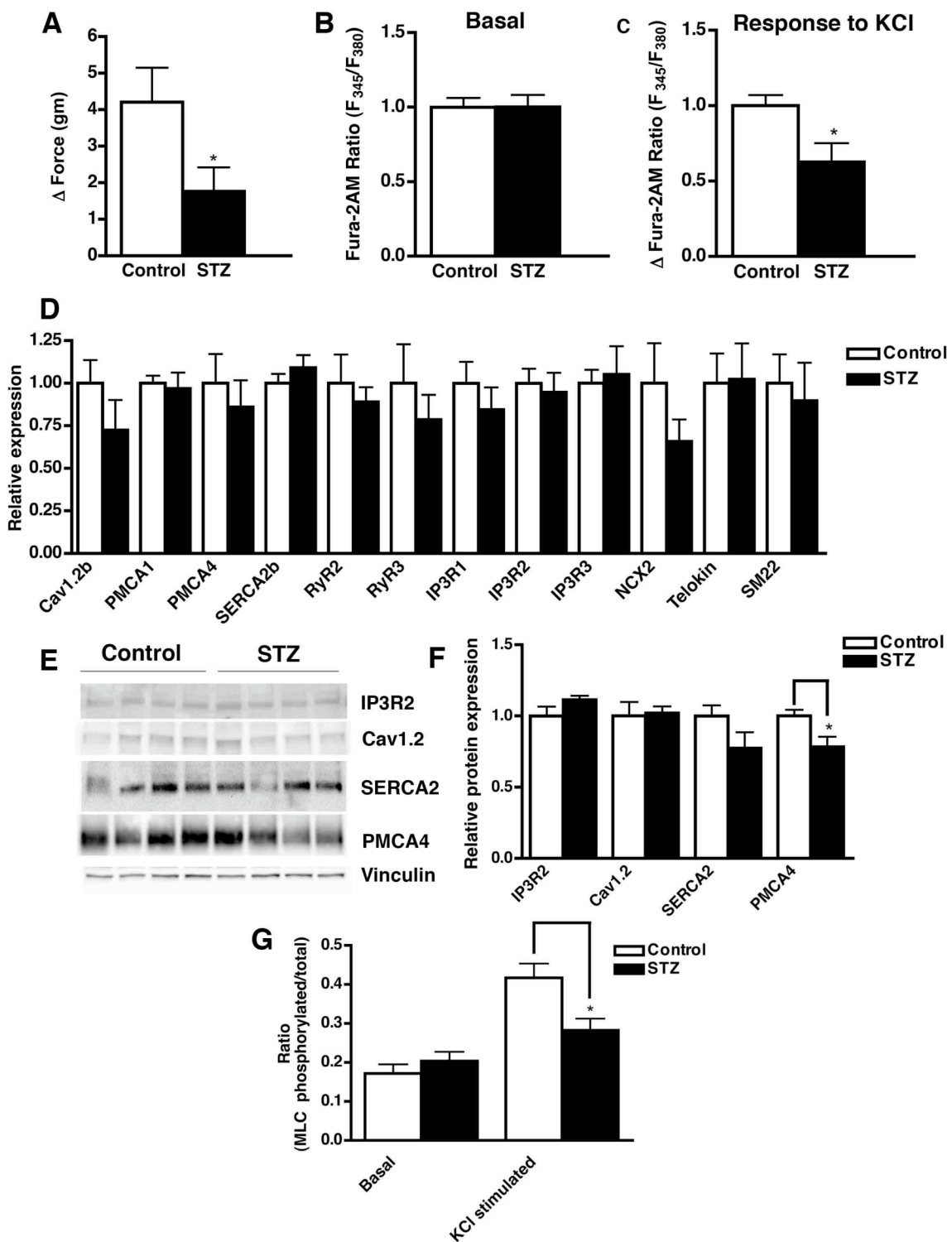


Figure 15. Contractility in short term diabetic mice is decreased due to altered intracellular Ca²⁺ signaling. 1 week after becoming hyperglycemic mice colons were dissected for contractility measurements, Ca²⁺ imaging, mRNA and protein analysis. (A) Quantification of changes in contractility of rings obtained from the middle part of the colon (P4 and D4) combined (n=12). Changes in contractility following KCl stimulation are indicated in grams. (*P<0.05, Student t-test). (B) Basal levels of intracellular Ca²⁺ in the smooth muscle of the middle portion of the colon. (C) Changes in intracellular Ca²⁺ in response to 60mM KCl stimulation of smooth muscle obtained from the middle portion of the colon from control and STZ-induced diabetic mice. Each column in (B) and (C) represents the mean data obtained from several different mice (n=5-6). Error bars represent standard deviation (\pm SD). Intracellular Ca²⁺ levels of control mice are set to 1. (*P<0.05, Student t-test). (D) RNA from the middle to distal part of colon was isolated using Trizol (Invitrogen) and transcripts were quantitated by real-time RT-PCR. Transcript levels were firstly normalized to *Hprt* internal loading control and then samples from STZ-treated mice are expressed relative to those from control mice. Relative expression = $2^{-\Delta\Delta Ct}$, where $\Delta\Delta Ct = (Ct_{STZ} - Ct_{HPRT}) - (Ct_{control} - Ct_{HPRT})$. Each column represents the mean of data obtained from several different mice (n=4-5). Error bars represent standard deviation (\pm SD). (*P<0.05, Student t-test). (E) Immunoblots of proteins extracted from the middle part of the colon of the mice described in panel (C). (F) Quantification of protein expression following normalization to vinculin as an internal control. Protein levels of control mice are set to 1. Each column represents the mean of samples obtained from 8 different mice. Error bars represent standard deviation (\pm SD). (*P<0.05, Student t-test). (G) MLC phosphorylation was measured in colonic muscles rings obtained from short term diabetic and control mice using urea PAGE and western blotting. Levels of MLC phosphorylation were measured in resting rings (basal MLC phosphorylation) and at the peak of a contraction initiated by 60mM KCl. MLC phosphorylation is expressed as $MLC_{phosphorylated}/MLC_{total}$. Each column represents the mean of data obtained from

7-8 different mice. Error bars represent standard deviation (\pm SD). (* $P < 0.05$, Student t-test).

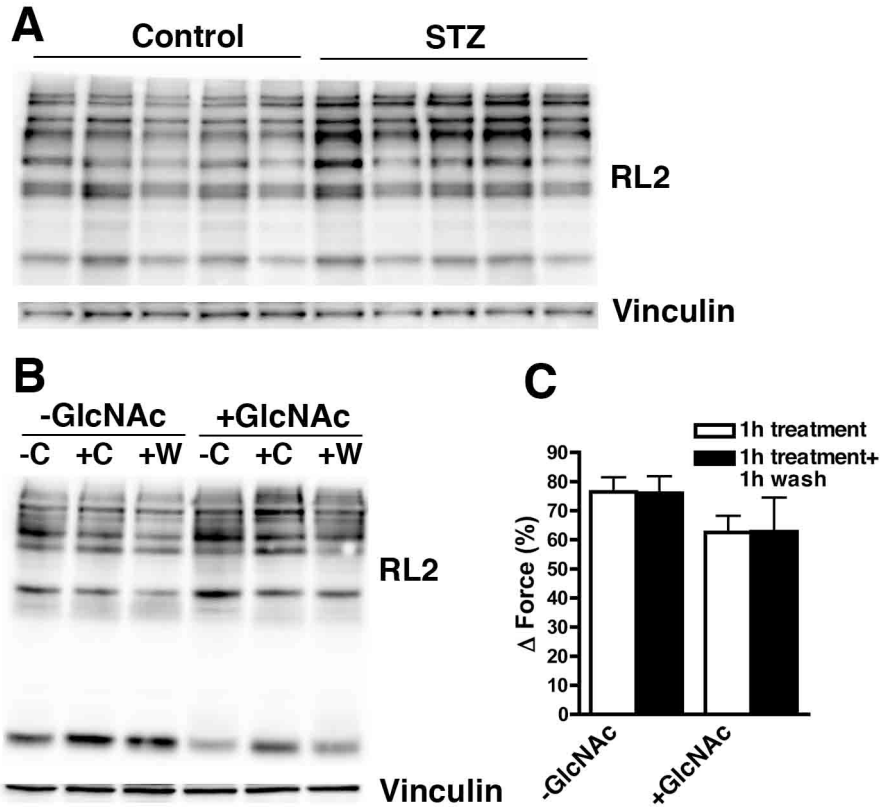


Figure 16. Chronic hyperglycemic mice have increased global O-glycosylation levels while elevated O-glycosylation in vitro does not significantly affect contractility. (A) Immunoblots of proteins extracted from the middle part of the colon of long-term (7 week) diabetic and control mice. (B) The P4 portion of the colon from 12 week old control mice were dissected and hung in organ baths. Samples were treated with glucosamine for 1 hour and collected before contraction (-C), immediately after inducing contraction with KCl (+C) or after contraction followed by a 1 hour washout. Samples then were processed for western blot analysis using the RL2 antibody to detect O-glycosylated proteins. Immunoblots show increased global O-glycosylation levels after glucosamine treatment. (C) Contractility measurements of samples treated as described in 'B'. Changes in contractility following glucosamine treatment are normalized to the changes in contractility before treatment (n=4-8). Error bars represent standard

deviation (\pm SD). -GlcNAc - no glucosamine treatment, +GlcNAc - glucosamine treatment for 1 hour.

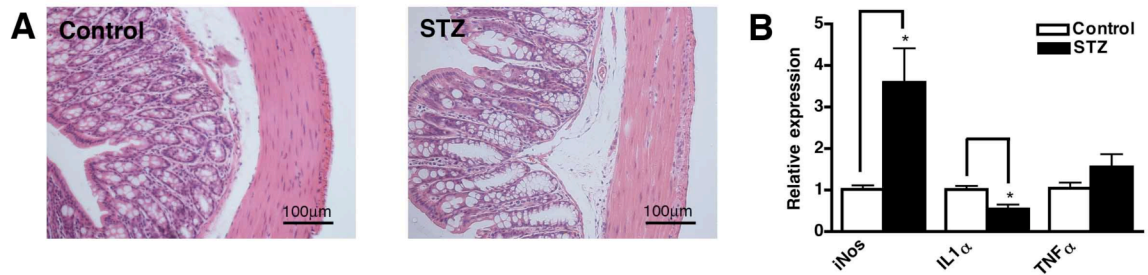


Figure 17. Chronic diabetic mice show increased iNos mRNA levels in the colon smooth muscle layer. RNA was isolated from the colon of chronic diabetic and control mice by using Trizol (Invitrogen) and transcripts were quantitated by real-time RT-PCR. Transcript levels were firstly normalized to *Hprt* internal loading control and then samples from STZ-induced diabetic mouse colons normalized to those obtained from control mice. Relative expression = $2^{-\Delta\Delta Ct}$, where $\Delta\Delta Ct = (Ct_{STZ} - Ct_{HPRT}) - (Ct_{control} - Ct_{HPRT})$. Changes in mRNA levels of control mice are set to 1. Each column represents the mean of different mice (n=5-7). Error bars represent standard deviation (\pm SD). (*P<0.05, **P<0.005, Student t-test).

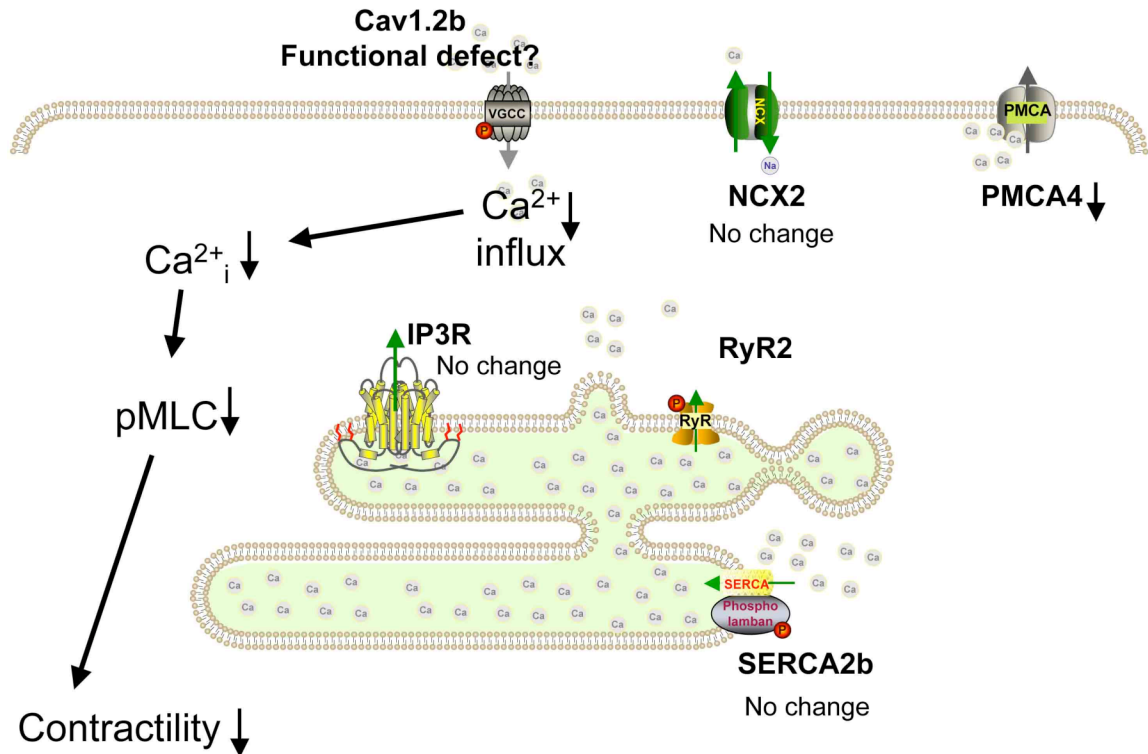


Figure 18. Defects occurring at acute state in STZ-induced diabetic mice. In acute diabetic mice L-type voltage gated channel mRNA and protein levels were not changed. KCl-induced stimulation led to decreased calcium influx suggesting functional defect of the L-type channel. No other transcriptional changes of calcium channels and receptors were observed, while PMCA4 protein levels were significantly decreased and SERCA2 protein showed trend to decrease. Decreased calcium influx leads to decreased myosin light chain phosphorylation and decreased contractility.

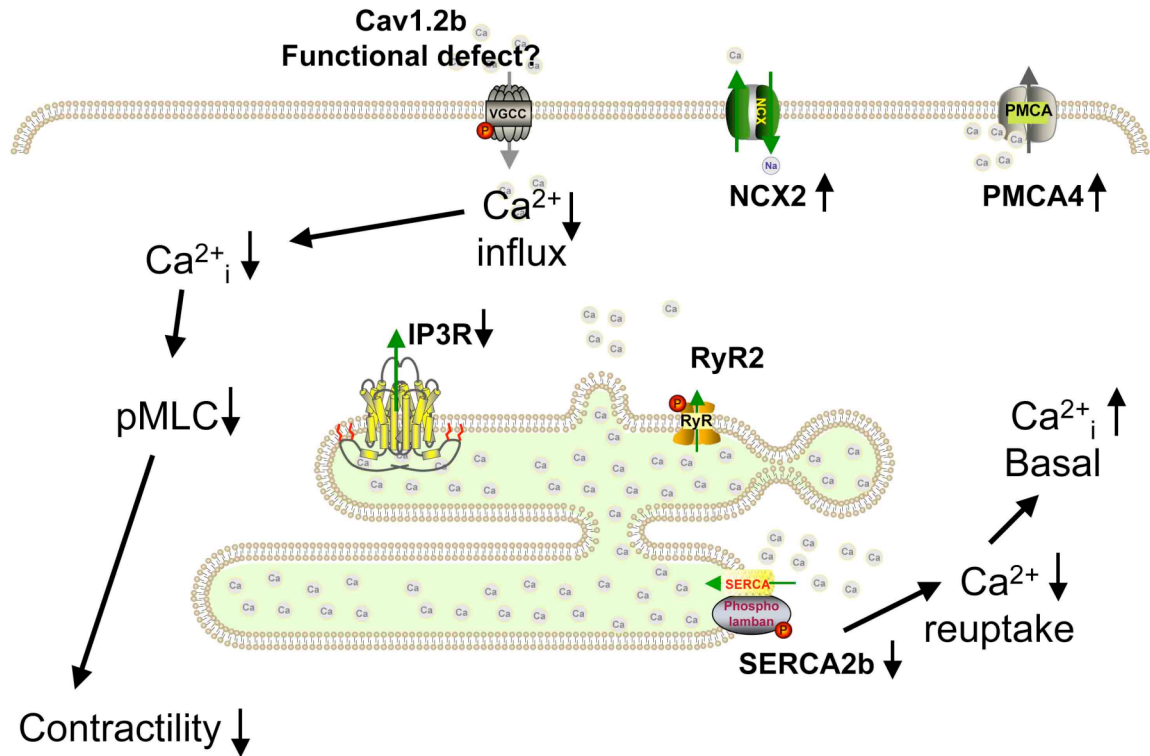


Figure 19. Defects occurring at chronic state in STZ-induced diabetic mice.

In chronic diabetic mice, similar to acute diabetics, L-type voltage gated channel mRNA and protein levels were not changed. KCl-induced stimulation led decreased calcium influx while high basal intracellular calcium levels. SERCA2b mRNA levels were increased while protein levels were decreased. Similarly IP3R mRNA levels were increased while protein levels decreased. PMCA4 mRNA and protein levels were decreased. These results suggest that decreased contractility is due to elevated intracellular calcium levels and altered calcium influx and efflux/uptake to SR. These defects also lead to decreased myosin light chain phosphorylation in response to KCl.

Table 3. Primers used for qRT-PCR.

Primers	Forward	Reverse
Cav1.2b	GCTACCTGGACTGGATCACC	TTCCCTTTCTTCTGATCATGC
PMCA1	TTAGTCTGGGAAGCATTACAAGATGTC AC	CTTCTTCCCCAACAGAACTTCTCC
PMCA4	ACGTCTTCCCACCCAAGGTTT	CCAGCAGCCCACACTCTGTC
TRPC1	TTCAAAGAGCAGAAGGACTG	CAAAGCAGGTGCCAATGAA
TRPC4	GATGATATTACCGTGGGTCCTG	GATTCCACCAGTCATGGATGT
TRPC6	GCAGCTGTTCAGGATGAAAAC	TTCAGCCCATATCATGCCTA
Serca2b	TCGACCAGTCAATTCTTACAGG	CAGGGACAGGGTCAGTATGC
RyR2	TTCAACACGCTCACGGAGTA	TGCCAGGCTCTGCTGATT
RyR3	CTGGCCATCATTCAAGGTCT	GTCTCCATGTCTTCCCGTA
IP3R1	GCACCGGAAGCTGAGAACT	AATTTGTCCGAGTGCCTCAC
IP3R2	GGCTCAGGCAGAAACAATG	CTTCATCATCAAGCTGAACTGG
IP3R3	TGCAGATCCCTTACGACAAGA	ACTGGTGTGTGTAGCGCAGT
NCX2	AAGCAGAAGCACCCGGATA	TGCATAGTACTTGGCGATGC
SM22	CGAAGCCAGTGAAGGTGCCTGAGAAC	CCCAAAGCCATTAGAGTCCTCTGCA CTGC
Telokin	GACACCGCCTGAGTCCAACCTCCG	GGCTTTTTCTCAGCAACAGCCTCC
<i>HPRT</i>	TGGCCCTCTGTGTGCTCAA	TGATCATTACAGTAGCTCTTCAGTC TGA
iNos	GGGCTGTCACGGAGATCA	CCATGATGGTCACATTCTGC
PAR2	GGACCGAGAACCTTGAC	GGAACCCCTTTCCAGTG
IL1a	TGTAATGAAAGACGGCACACC	TCTTCTTTGGGTATTGCTTGG
TNFa	TGCCTATGTCTCAGCCTCTTC	GAGGCCATTTGGGAATTCT
Erg1	GCCGAGCGAACAACCCTAT	CCATCGCCTTCTCATTATTCAGA

CHAPTER IV

CONCLUSIONS AND FUTURE STUDIES

Results from my thesis work have demonstrated that *Hprt* locus targeted single copy transgenes show reproducible appropriate levels and patterns of expression among different founder lines. Telokin promoter-driven transgene expression recapitulated the expression of endogenous telokin in adult and embryonic tissues. Thus, I was able to use the *Hprt*-targeted transgenic approach to further analyze regulatory elements within the telokin promoter. Although previous studies have shown that SM22 α promoter-driven transgenes are restricted to arterial smooth muscle we observed high levels of transgene expression in bladder, gallbladder and veins when these transgenes were targeted to the *Hprt* locus (Figure 8). Thus, *Hprt*-targeted SM22 α transgenes more closely recapitulate endogenous SM22 α expression, which is expressed in all smooth muscle tissues [35, 129, 134]. The lack of transgene expression in GI and reproductive tract smooth muscle cells suggests that additional regulatory elements are required to drive SM22 α expression in these tissues. Moreover, the expression of *Hprt*-targeted SM22 α transgenes but not randomly integrated SM22 α transgenes in bladder, gallbladder and venous smooth muscle cells suggests that chromatin remodeling complexes may be important for regulating SM22 α expression in different smooth muscle tissues. My additional analysis of the telokin promoter showed that a promoter fragment extending from -90 to +180 had a marked decrease in expression when compared to a -190 to +180 promoter (Figure 10). Transgene expression in the GI tract was particularly affected with only a few isolated cells staining positive for β -galactosidase activity (Figure 10). These data suggest that the -190 to -90 region of the telokin promoter is required for high levels of telokin expression particularly in smooth muscle cells of the GI tract. An *Hprt*-targeted telokin promoter-driven transgene

with a mutated CArG box exhibited no detectable β -galactosidase activity demonstrating that the CArG box is required for telokin expression in all smooth muscle tissues in vivo (Table 2). However, the -90 to +180 telokin promoter that contains the CArG box was not sufficient for expressing a transgene at significant levels in the GI tract, reproductive tract or in airway smooth muscle. These findings suggest the CArG box and adjacent AT-rich region are not sufficient for telokin promoter activity in vivo and that SRF and myocardin which interact with this region must cooperate with other factors to drive telokin expression in these tissues. Further studies are needed to determine which transcription factors are required for telokin expression in GI tract. Analysis of the sequence of the -190 to -90 region using rVISTA revealed the presence of conserved putative Sox and SMAD binding sites (Figure 20). SMAD family members have been shown to play a role in GI tract development hence it is tempting to propose that they may be contributing to telokin expression in the GI tract [9, 11, 12]. Sox family members have been shown to play a role in development of GI tract epithelium but their role in GI smooth muscle differentiation is unknown [135, 157]. My preliminary experiments using siRNA mediated silencing of Sox genes in primary cultures of GI smooth muscle cells suggest that Sox 4, 5, 6, 7 and 12 are possible candidates involved in telokin transcriptional regulation (data not shown). As knockdown of Sox genes could be indirectly affecting telokin expression it will be important to show that Sox proteins directly affect telokin transcription. To do this it will be necessary to verify the importance of the Sox binding site within the telokin promoter for directing expression in GI smooth muscle cells. Further studies using *Hprt*-targeted transgenes with the Sox binding site either deleted or mutated are being performed in order to achieve this goal. From in vitro experiments I also determined that SMAD signaling might play a role in regulating telokin expression in vitro, however it is unclear which family members are involved. BMP family members are expressed in mesenchyme and epithelial cells in the developing gut. In the GI tract, the TGF β family member BMP4 plays a significant role during smooth muscle development [9, 10]. BMP4 plays

important roles in regulating both smooth muscle and epithelial proliferation and differentiation [11]. BMP2 can also enhance smooth muscle differentiation in vitro from embryonic stem cells to form contracting gut-like structures that express SM α -actin [12]. To identify whether TGF β family members are important for telokin transcriptional regulation, we are planning to mutate the SMAD binding sites on the telokin promoter and determine whether these mutations lead to decreased promoter activity in the GI tract. If we observe decreased transgene activity, we would use a siRNA-mediated silencing approach together with luciferase assays to determine which TGF β and SMAD family members are involved in regulating telokin transcription. These experiments will be coupled to ChIP assays to demonstrate direct binding of Sox or SMAD proteins to the telokin promoter.

In parallel to my study investigating transcriptional regulation of telokin in GI smooth muscle I was interested in determining if this regulation may be altered in the diabetic state. Previous reports have shown altered colon smooth muscle contractility in diabetic patients and animal models. A study in diabetic rats implied that altered contractility possibly occurs through altered sensitivity to calcium in smooth muscle [94]. As telokin is known to play a role in smooth muscle calcium desensitization, my goal was to determine whether telokin expression is altered in colon smooth muscle of diabetic mice. In a type 1 diabetic mouse model in which STZ was used to destroy the pancreatic beta cells, I found that telokin mRNA and protein levels were not changed. However, from an in vivo study of GI motility in these mice I found that long term hyperglycemia for 7-8 weeks resulted in a delayed whole gut transit time (Figures 11, 19). Results from our ex vivo contractility measurements further demonstrate that in my type 1 diabetic mouse model, both short term (less than 1 week) and long term (7-8 weeks) hyperglycemia resulted in a direct impairment of colonic smooth muscle contractility (Figures 12, 15, 18, 19). As this was not due to changes in telokin expression I was interested in determining the mechanisms resulting in this smooth muscle contractility defect. Colonic rings were stimulated

with KCl to bypass neuronal pathways and directly assess the function of the colonic smooth muscle. The decreased contractile response to KCl was most pronounced in the middle portion of the colon (P4-D2 in Figure 12). These regional pathological changes could possibly be explained by the anatomical structure of the colon or distinct neural innervation of the proximal (vagal) and distal (pelvic) portions of the colon [147, 148]. Further studies showed that the impaired colonic contractility in diabetic mice is associated with an attenuation of the depolarization induced intracellular calcium increase that eventually leads to an elevation in basal intracellular calcium levels after 7 weeks of hyperglycemia (Figures 13c, 19). I also examined the expression of the proteins that are involved in regulation of intracellular calcium levels. In short term diabetic mice I observed statistically significant changes in protein levels of PMCA4 while no changes in the expression of any other proteins (Figure 15). These findings suggest that posttranslational changes, most likely of the L-type calcium channel are likely causing the attenuated calcium response following short term hyperglycemia (Figure 18).

In our studies I did not find any evidence of inflammation related macrophage activation or elevation of $\text{TNF}\alpha$ in colons from diabetic mice while I did detect higher levels of iNos mRNA in the smooth muscle of long term but not short term diabetic mice (Figure 17). Together these data suggest that the increased iNos expression likely results from long term oxidative stress rather than from an intestinal inflammatory response and is thus unlikely to be contributing to the attenuated contractility seen after short term hyperglycemia. I also examined whether hyperglycemia leads to global O-glycosylation and evaluated its possible role in mediating altered contractility. I determined that O-glycosylation levels were increased in STZ-induced diabetic mice. However, my in vitro studies in which colon rings were treated with N-acetylglucosamine for 1 hour to directly increase levels of O-glycosylation, did not show a significant decrease in their contractile response. These findings suggest that increased O-glycosylation levels

may not be the main contributor to the decreased contractility observed in STZ-induced diabetic animals. Alternatively it is possible that the O-glycosylation pathway may need to be activated for a prolonged period in order to effect contractility and my 1 hour incubation may not have been sufficient to achieve this affect.

Overall my data demonstrate that type 1 diabetes leads to a direct defect in GI smooth muscle, however there are many questions that still should be answered before we will be in a position to design and appropriate treatment regime to alleviate these GI symptoms in patients. Diabetes is a multifactorial disease that affects different areas of the GI tract through distinct pathways. I think it would be useful to determine if in my STZ-induced diabetic mice the smooth muscle in other parts of GI tract (small intestine and stomach) have similar defects to those I observed in colon. The most likely explanation for the contractile defect that I observed in the colon of diabetic mice is an altered activity of the L-type channel. In future experiments it would be important to test this hypothesis directly. To do this we would use patch-clamp measurements of single colon smooth muscle cell. By using patch-clamp measurements we would be able to determine resting membrane potential as well as changes in the action potential in STZ-induced mice colons in response to KCl. As Ca^{2+} influx through the L-type calcium channels accounts for the upstroke of the action potentials in GI smooth muscle cells these electrophysiological measurements would enable us to directly measure L-type calcium channel activity.

Results of my study suggest that post-translational modification of L-type channels, that alter channel activity, rather than changes in protein or mRNA levels could account for changes in calcium responses within colonic smooth muscle cells. Previous studies have shown that diabetes can lead to oxidative stress in smooth muscle [149-151] and studies with cardiac myocytes have shown that oxidative stress related nitration of L-type channels leads to their

decreased activity [112, 152]. Nitration in turn can attenuate SERCA activity and lead to its degradation resulting in impaired Ca^{2+} uptake into the SR. Further studies should be done to determine whether nitration of the L-type channel is the main cause for defective calcium signaling in colonic smooth muscle cells. I also observed that at the later stages of diabetes mice had increased levels of iNos in the colonic smooth muscle layer without an increase in other inflammatory markers. These findings suggest that increased NO produced by iNos could be contributing to free radical damage and protein nitration and/or it could be directly inhibiting smooth muscle contractility. Thus, further studies to determine what role oxidative stress plays in increasing iNos production and whether the increased NO contributes to decreased motility either directly or indirectly through posttranslational modification of proteins should be determined.

The colon is a complex organ consisting of a mucosal and submucosal layer, smooth muscle and neurons. To treat diabetes-related complications it would be beneficial to understand how each of these different tissues contribute to motility problems observed in the diabetic state. Many studies have shown diabetes-related motility problems can be caused by neuronal damage. Recent studies have also shown that epithelial cells and microflora residing in the GI tract also can be affected in the diabetic state and in IBD alterations in gut microflora have been shown to lead to altered motility [158, 159]. However, interaction among different cell types in the diabetic state is not well studied. It has been shown that long term hyperglycemia leads to morphological changes in the autonomic nervous system and atrophy of ENS in the stomach and colon leading to motility problems [84, 85, 160]. Moreover, loss of myenteric neurons in STZ-induced diabetic rats has been detected as early as 7 days after the onset of diabetes [85]. In my study I observed decreased motility and altered calcium signaling within colonic smooth muscle itself as early as 1 week after hyperglycemia. Thus, it is still unclear whether neuronal damage occurs first leading to defects in smooth muscle or if these defects occur simultaneously and independently.

Never the less my data suggest that direct affects of diabetes on GI smooth muscle play a more significant role than was previously thought in causing intestinal dysmotility. Determining if the neuronal and muscle defects occur independently during the progression of diabetes will be important for developing more effective treatment rationales for the prevention of GI symptoms in diabetic patients.

Another point of interest would be identifying the main players within the diabetic milieu that cause to GI dysmotility. Studies have shown that short-term hyperglycemia has reversible effects on gut motility in diabetic patients. These studies showed that a rise in blood glucose levels in type 1 diabetic patients for two hours slows down gastric emptying [155, 156]. Studies suggest that uncontrolled hyperglycemia leads to complications of diabetes by causing oxidative stress and neuronal damage in GI tract. One study shows that blood glucose levels rather than the length of diabetes is the main cause for GI dysmotility problems [98]. On the other hand insulin and IGF-1 receptors have been found in stomach smooth muscle and data indicates that they can increase SCF levels which prevents smooth muscle atrophy [87]. These results suggest that insulin depletion could contribute to impaired GI motility by promoting smooth muscle atrophy. It is still unclear whether similar defects occur in the small and large intestine. Also, it is unclear what role hyperglycemia and hypoinsulinemia have on smooth muscle pathophysiology in diabetic colonic smooth muscle.

My study on colon smooth muscle investigated the effects of type 1-like diabetes characterized by hyperglycemia and hypoinsulinemia. However, GI problems occur also in patients with type 2 diabetes in which GI tract motility is also affected and patients suffer from similar symptoms as in type 1 diabetes. In further studies it would be beneficial to determine if similar smooth muscle defects with altered calcium signaling also occur in type 2 diabetic models such as seen in db/db and ob/ob mice. In these mouse models an insulin resistance

develops that leads to hyperglycemia and at least for a period of time hyperinsulinemia. These models may thus be useful in teasing out the relative roles of hyperglycemia and hypoinsulinemia in impairing GI contractility. These mouse models, however, also develop dyslipidemia and obesity which themselves could affect GI motility. The different mouse models also have different degrees of neuronal damage, thus comparing these mice models would be helpful in determining whether neuronal damage leads to smooth muscle defects or if these defects occur simultaneously [78, 161].

Overall, my current study shows that *Hprt*-targeted transgenic mice exhibit a reproducible pattern and level of transgene expression. This approach is thus a useful model for promoter analysis within GI tract smooth muscle. I also determined that the CArG element in the telokin promoter is necessary for telokin expression in all smooth muscle cells while an adjacent region is necessary for telokin expression specifically in the GI tract. My STZ-induced diabetic mice did not show signs of smooth muscle dedifferentiation or altered telokin expression, although they did exhibit impaired colonic contractility. In these mice the colon motility was decreased in part due to altered calcium signaling (Figures 18, 19). This novel finding provides possibilities for new therapeutic targets for motility treatment in diabetics.



Figure 20. Sequence alignment of the telokin promoter. Telokin promoter region -190 to -94 relative to the transcription start site shows putative Sox and SMAD binding sites and regions used for mice T370 and T270 design.

References

1. Altaf, M.A. and M.R. Sood, *The nervous system and gastrointestinal function*. Dev Disabil Res Rev, 2008. **14**(2): p. 87-95.
2. Lomax, A.E., K.A. Sharkey, and J.B. Furness, *The participation of the sympathetic innervation of the gastrointestinal tract in disease states*. Neurogastroenterol Motil. **22**(1): p. 7-18.
3. Webb, R.C., *Smooth muscle contraction and relaxation*. Adv Physiol Educ, 2003. **27**(1-4): p. 201-6.
4. Murthy, K.S., *Signaling for contraction and relaxation in smooth muscle of the gut*. Annu Rev Physiol, 2006. **68**: p. 345-74.
5. McHugh, K.M., *Molecular analysis of smooth muscle development in the mouse*. Dev Dyn, 1995. **204**(3): p. 278-90.
6. McHugh, K.M., *Molecular analysis of gastrointestinal smooth muscle development*. J Pediatr Gastroenterol Nutr, 1996. **23**(4): p. 379-94.
7. Ramalho-Santos, M., D.A. Melton, and A.P. McMahon, *Hedgehog signals regulate multiple aspects of gastrointestinal development*. Development, 2000. **127**(12): p. 2763-72.
8. Sukegawa, A., et al., *The concentric structure of the developing gut is regulated by Sonic hedgehog derived from endodermal epithelium*. Development, 2000. **127**(9): p. 1971-80.
9. Roberts, D.J., et al., *Sonic hedgehog is an endodermal signal inducing Bmp-4 and Hox genes during induction and regionalization of the chick hindgut*. Development, 1995. **121**(10): p. 3163-74.
10. Roberts, D.J., et al., *Epithelial-mesenchymal signaling during the regionalization of the chick gut*. Development, 1998. **125**(15): p. 2791-801.
11. Batts, L.E., et al., *Bmp signaling is required for intestinal growth and morphogenesis*. Dev Dyn, 2006. **235**(6): p. 1563-70.
12. Torihashi, S., et al., *The expression and crucial roles of BMP signaling in development of smooth muscle progenitor cells in the mouse embryonic gut*. Differentiation, 2009. **77**(3): p. 277-89.
13. Cervantes, S., T.P. Yamaguchi, and M. Hebrok, *Wnt5a is essential for intestinal elongation in mice*. Dev Biol, 2009. **326**(2): p. 285-94.
14. Geske, M.J., et al., *Fgf9 signaling regulates small intestinal elongation and mesenchymal development*. Development, 2008. **135**(17): p. 2959-68.
15. Vandekerckhove, J. and K. Weber, *At least six different actins are expressed in a higher mammal: an analysis based on the amino acid sequence of the amino-terminal tryptic peptide*. J Mol Biol, 1978. **126**(4): p. 783-802.
16. Gallagher, P.J. and B.P. Herring, *The carboxyl terminus of the smooth muscle myosin light chain kinase is expressed as an independent protein, telokin*. J Biol Chem, 1991. **266**(35): p. 23945-52.

17. Herring, B.P. and A.F. Smith, *Telokin expression is mediated by a smooth muscle cell-specific promoter*. Am J Physiol, 1996. **270**(6 Pt 1): p. C1656-65.
18. Kim, S., et al., *A serum response factor-dependent transcriptional regulatory program identifies distinct smooth muscle cell sublineages*. Mol Cell Biol, 1997. **17**(4): p. 2266-78.
19. Li, L., et al., *Expression of the SM22alpha promoter in transgenic mice provides evidence for distinct transcriptional regulatory programs in vascular and visceral smooth muscle cells*. J Cell Biol, 1996. **132**(5): p. 849-59.
20. Moessler, H., et al., *The SM 22 promoter directs tissue-specific expression in arterial but not in venous or visceral smooth muscle cells in transgenic mice*. Development, 1996. **122**(8): p. 2415-25.
21. Choudhury, N., et al., *Telokin mediates Ca²⁺-desensitization through activation of myosin phosphatase in phasic and tonic smooth muscle*. J Muscle Res Cell Motil, 2004. **25**(8): p. 657-65.
22. Khromov, A.S., et al., *Smooth muscle of telokin-deficient mice exhibits increased sensitivity to Ca²⁺ and decreased cGMP-induced relaxation*. Proc Natl Acad Sci U S A, 2006. **103**(7): p. 2440-5.
23. Komatsu, S., et al., *Translocation of telokin by cGMP signaling in smooth muscle cells*. Am J Physiol Cell Physiol, 2002. **283**(3): p. C752-61.
24. Walker, L.A., et al., *Site-specific phosphorylation and point mutations of telokin modulate its Ca²⁺-desensitizing effect in smooth muscle*. J Biol Chem, 2001. **276**(27): p. 24519-24.
25. Wu, X., et al., *Acceleration of myosin light chain dephosphorylation and relaxation of smooth muscle by telokin. Synergism with cyclic nucleotide-activated kinase*. J Biol Chem, 1998. **273**(18): p. 11362-9.
26. Zhang, J.C., et al., *Analysis of SM22alpha-deficient mice reveals unanticipated insights into smooth muscle cell differentiation and function*. Mol Cell Biol, 2001. **21**(4): p. 1336-44.
27. Feil, S., F. Hofmann, and R. Feil, *SM22alpha modulates vascular smooth muscle cell phenotype during atherogenesis*. Circ Res, 2004. **94**(7): p. 863-5.
28. Je, H.D. and U.D. Sohn, *SM22alpha is required for agonist-induced regulation of contractility: evidence from SM22alpha knockout mice*. Mol Cells, 2007. **23**(2): p. 175-81.
29. Rozenblum, G.T. and M. Gimona, *Calponins: adaptable modular regulators of the actin cytoskeleton*. Int J Biochem Cell Biol, 2008. **40**(10): p. 1990-5.
30. Wang, C.L., *Caldesmon and the regulation of cytoskeletal functions*. Adv Exp Med Biol, 2008. **644**: p. 250-72.
31. Herring, B.P., et al., *Telokin expression is restricted to smooth muscle tissues during mouse development*. Am J Physiol Cell Physiol, 2001. **280**(1): p. C12-21.

32. Herring, B.P. and A.F. Smith, *Telokin expression in A10 smooth muscle cells requires serum response factor*. Am J Physiol, 1997. **272**(4 Pt 1): p. C1394-404.
33. Hoggatt, A.M., G.M. Simon, and B.P. Herring, *Cell-specific regulatory modules control expression of genes in vascular and visceral smooth muscle tissues*. Circ Res, 2002. **91**(12): p. 1151-9.
34. Li, L., et al., *SM22 alpha, a marker of adult smooth muscle, is expressed in multiple myogenic lineages during embryogenesis*. Circ Res, 1996. **78**(2): p. 188-95.
35. Lees-Miller, J.P., D.H. Heeley, and L.B. Smillie, *An abundant and novel protein of 22 kDa (SM22) is widely distributed in smooth muscles. Purification from bovine aorta*. Biochem J, 1987. **244**(3): p. 705-9.
36. Xu, R., et al., *Human SM22 alpha BAC encompasses regulatory sequences for expression in vascular and visceral smooth muscles at fetal and adult stages*. Am J Physiol Heart Circ Physiol, 2003. **284**(4): p. H1398-407.
37. Miano, J.M., *Serum response factor: toggling between disparate programs of gene expression*. J Mol Cell Cardiol, 2003. **35**(6): p. 577-93.
38. Arsenian, S., et al., *Serum response factor is essential for mesoderm formation during mouse embryogenesis*. Embo J, 1998. **17**(21): p. 6289-99.
39. Weinhold, B., et al., *Srf(-/-) ES cells display non-cell-autonomous impairment in mesodermal differentiation*. Embo J, 2000. **19**(21): p. 5835-44.
40. Angstenberger, M., et al., *Severe intestinal obstruction on induced smooth muscle-specific ablation of the transcription factor SRF in adult mice*. Gastroenterology, 2007. **133**(6): p. 1948-59.
41. Mericskay, M., et al., *Inducible mouse model of chronic intestinal pseudo-obstruction by smooth muscle-specific inactivation of the SRF gene*. Gastroenterology, 2007. **133**(6): p. 1960-70.
42. Miano, J.M., et al., *Restricted inactivation of serum response factor to the cardiovascular system*. Proc Natl Acad Sci U S A, 2004. **101**(49): p. 17132-7.
43. Zilberman, A., et al., *Evolutionarily conserved promoter region containing CArG*-like elements is crucial for smooth muscle myosin heavy chain gene expression*. Circ Res, 1998. **82**(5): p. 566-75.
44. Mack, C.P. and G.K. Owens, *Regulation of smooth muscle alpha-actin expression in vivo is dependent on CArG elements within the 5' and first intron promoter regions*. Circ Res, 1999. **84**(7): p. 852-61.
45. Miano, J.M., et al., *Serum response factor-dependent regulation of the smooth muscle calponin gene*. J Biol Chem, 2000. **275**(13): p. 9814-22.
46. Hirschi, K.K., et al., *Transforming growth factor-beta induction of smooth muscle cell phenotype requires transcriptional and post-transcriptional control of serum response factor*. J Biol Chem, 2002. **277**(8): p. 6287-95.

47. Rensen, S.S., et al., *Expression of the smoothelin gene is mediated by alternative promoters*. Cardiovasc Res, 2002. **55**(4): p. 850-63.
48. Strobeck, M., et al., *Binding of serum response factor to CArG box sequences is necessary but not sufficient to restrict gene expression to arterial smooth muscle cells*. J Biol Chem, 2001. **276**(19): p. 16418-24.
49. Manabe, I. and G.K. Owens, *CArG elements control smooth muscle subtype-specific expression of smooth muscle myosin in vivo*. J Clin Invest, 2001. **107**(7): p. 823-34.
50. Chen, J., et al., *Myocardin: a component of a molecular switch for smooth muscle differentiation*. J Mol Cell Cardiol, 2002. **34**(10): p. 1345-56.
51. Du, K.L., et al., *Myocardin is a critical serum response factor cofactor in the transcriptional program regulating smooth muscle cell differentiation*. Mol Cell Biol, 2003. **23**(7): p. 2425-37.
52. Jasin, M., M.E. Moynahan, and C. Richardson, *Targeted transgenesis*. Proc Natl Acad Sci U S A, 1996. **93**(17): p. 8804-8.
53. Hark, A.T., et al., *CTCF mediates methylation-sensitive enhancer-blocking activity at the H19/Igf2 locus*. Nature, 2000. **405**(6785): p. 486-9.
54. Kaffer, C.R., A. Grinberg, and K. Pfeifer, *Regulatory mechanisms at the mouse Igf2/H19 locus*. Mol Cell Biol, 2001. **21**(23): p. 8189-96.
55. Bronson, S.K., et al., *Single-copy transgenic mice with chosen-site integration*. Proc Natl Acad Sci U S A, 1996. **93**(17): p. 9067-72.
56. Cvetkovic, B., et al., *Appropriate tissue- and cell-specific expression of a single copy human angiotensinogen transgene specifically targeted upstream of the HPRT locus by homologous recombination*. J Biol Chem, 2000. **275**(2): p. 1073-8.
57. Evans, V., et al., *Targeting the Hprt locus in mice reveals differential regulation of Tie2 gene expression in the endothelium*. Physiol Genomics, 2000. **2**(2): p. 67-75.
58. Guillot, P.V., et al., *Targeting of human eNOS promoter to the Hprt locus of mice leads to tissue-restricted transgene expression*. Physiol Genomics, 2000. **2**(2): p. 77-83.
59. Minami, T., et al., *Differential regulation of the von Willebrand factor and Flt-1 promoters in the endothelium of hypoxanthine phosphoribosyltransferase-targeted mice*. Blood, 2002. **100**(12): p. 4019-25.
60. Vivian, J.L., W.H. Klein, and P. Hasty, *Temporal, spatial and tissue-specific expression of a myogenin-lacZ transgene targeted to the Hprt locus in mice*. Biotechniques, 1999. **27**(1): p. 154-62.
61. Doetschman, T., N. Maeda, and O. Smithies, *Targeted mutation of the Hprt gene in mouse embryonic stem cells*. Proc Natl Acad Sci U S A, 1988. **85**(22): p. 8583-7.
62. Owens, G.K., M.S. Kumar, and B.R. Wamhoff, *Molecular regulation of vascular smooth muscle cell differentiation in development and disease*. Physiol Rev, 2004. **84**(3): p. 767-801.

63. Chen, J., et al., *Regulation of SRF/CArG-dependent gene transcription during chronic partial obstruction of murine small intestine*. Neurogastroenterol Motil, 2008. **20**(7): p. 829-42.
64. Chacko, S., et al., *Contractile protein changes in urinary bladder smooth muscle following outlet obstruction*. Adv Exp Med Biol, 1999. **462**: p. 137-53.
65. Hirota, J.A., et al., *Airway smooth muscle in asthma: phenotype plasticity and function*. Pulm Pharmacol Ther, 2009. **22**(5): p. 370-8.
66. Kanematsu, A., A. Ramachandran, and R.M. Adam, *GATA-6 mediates human bladder smooth muscle differentiation: involvement of a novel enhancer element in regulating alpha-smooth muscle actin gene expression*. Am J Physiol Cell Physiol, 2007. **293**(3): p. C1093-102.
67. Taplin, C.E. and J.M. Barker, *Autoantibodies in type 1 diabetes*. Autoimmunity, 2008. **41**(1): p. 11-8.
68. Surampudi, P.N., J. John-Kalarickal, and V.A. Fonseca, *Emerging concepts in the pathophysiology of type 2 diabetes mellitus*. Mt Sinai J Med, 2009. **76**(3): p. 216-26.
69. Deshpande, A.D., M. Harris-Hayes, and M. Schootman, *Epidemiology of diabetes and diabetes-related complications*. Phys Ther, 2008. **88**(11): p. 1254-64.
70. Huysman, E. and C. Mathieu, *Diabetes and peripheral vascular disease*. Acta Chir Belg, 2009. **109**(5): p. 587-94.
71. Intagliata, N. and K.L. Koch, *Gastroparesis in type 2 diabetes mellitus: prevalence, etiology, diagnosis, and treatment*. Curr Gastroenterol Rep, 2007. **9**(4): p. 270-9.
72. Levey, A.S., et al., *Chronic kidney disease, diabetes, and hypertension: what's in a name?* Kidney Int. **78**(1): p. 19-22.
73. Rayner, C.K. and M. Horowitz, *Gastrointestinal motility and glycemic control in diabetes: the chicken and the egg revisited?* J Clin Invest, 2006. **116**(2): p. 299-302.
74. Feldman, M. and L.R. Schiller, *Disorders of gastrointestinal motility associated with diabetes mellitus*. Ann Intern Med, 1983. **98**(3): p. 378-84.
75. Maleki, D., et al., *Pilot study of pathophysiology of constipation among community diabetics*. Dig Dis Sci, 1998. **43**(11): p. 2373-8.
76. Duchon, L.W., et al., *Pathology of autonomic neuropathy in diabetes mellitus*. Ann Intern Med, 1980. **92**(2 Pt 2): p. 301-3.
77. Yagihashi, S. and A.A. Sima, *Diabetic autonomic neuropathy in the BB rat. Ultrastructural and morphometric changes in sympathetic nerves*. Diabetes, 1985. **34**(6): p. 558-64.
78. Schmidt, R.E., et al., *Non-obese diabetic mice rapidly develop dramatic sympathetic neuritic dystrophy: a new experimental model of diabetic autonomic neuropathy*. Am J Pathol, 2003. **163**(5): p. 2077-91.

79. Yamamoto, T., et al., *Disturbed gastrointestinal motility and decreased interstitial cells of Cajal in diabetic db/db mice*. J Gastroenterol Hepatol, 2008. **23**(4): p. 660-7.
80. Schmidt, R.E., S.B. Plurad, and C.W. Modert, *Experimental diabetic autonomic neuropathy characterization in streptozotocin-diabetic Sprague-Dawley rats*. Lab Invest, 1983. **49**(5): p. 538-52.
81. Tougas, G., et al., *Evidence of impaired afferent vagal function in patients with diabetes gastroparesis*. Pacing Clin Electrophysiol, 1992. **15**(10 Pt 2): p. 1597-602.
82. He, C.L., et al., *Loss of interstitial cells of cajal and inhibitory innervation in insulin-dependent diabetes*. Gastroenterology, 2001. **121**(2): p. 427-34.
83. Yoneda, S., et al., *Enhanced colonic peristalsis by impairment of nitrergic enteric neurons in spontaneously diabetic rats*. Auton Neurosci, 2001. **92**(1-2): p. 65-71.
84. Fregonesi, C.E., et al., *Quantitative study of the myenteric plexus of the stomach of rats with streptozotocin-induced diabetes*. Arq Neuropsiquiatr, 2001. **59**(1): p. 50-3.
85. Furlan, M.M., S.L. Molinari, and M.H. Miranda Neto, *Morphoquantitative effects of acute diabetes on the myenteric neurons of the proximal colon of adult rats*. Arq Neuropsiquiatr, 2002. **60**(3-A): p. 576-81.
86. Anitha, M., et al., *GDNF rescues hyperglycemia-induced diabetic enteric neuropathy through activation of the PI3K/Akt pathway*. J Clin Invest, 2006. **116**(2): p. 344-56.
87. Horvath, V.J., et al., *Reduced stem cell factor links smooth myopathy and loss of interstitial cells of cajal in murine diabetic gastroparesis*. Gastroenterology, 2006. **130**(3): p. 759-70.
88. Long, Q.L., et al., *Gastro-electric dysrhythm and lack of gastric interstitial cells of cajal*. World J Gastroenterol, 2004. **10**(8): p. 1227-30.
89. Ordog, T., et al., *Remodeling of networks of interstitial cells of Cajal in a murine model of diabetic gastroparesis*. Diabetes, 2000. **49**(10): p. 1731-9.
90. Wang, X.Y., et al., *Loss of intramuscular and submuscular interstitial cells of Cajal and associated enteric nerves is related to decreased gastric emptying in streptozotocin-induced diabetes*. Neurogastroenterol Motil, 2009. **21**(10): p. 1095-e92.
91. Nowak, T.V., et al., *Structural and functional characteristics of muscle from diabetic rodent small intestine*. Am J Physiol, 1990. **258**(5 Pt 1): p. G690-8.
92. Forrest, A., et al., *Increase in stretch-induced rhythmic motor activity in the diabetic rat colon is associated with loss of ICC of the submuscular plexus*. Am J Physiol Gastrointest Liver Physiol, 2008. **294**(1): p. G315-26.
93. Wang, C.L., et al., *Type 1 diabetes attenuates the modulatory effects of endomorphins on mouse colonic motility*. Neuropeptides, 2008. **42**(1): p. 69-77.

94. Forrest, A., A. Molleman, and M. Parsons, *The responses to manipulation of extracellular and intracellular calcium are altered in the streptozotocin-diabetic rat colon and ileum*. Eur J Pharmacol, 2005. **509**(1): p. 77-83.
95. Soulie, M.L., et al., *Impairment of contractile response to carbachol and muscarinic receptor coupling in gastric antral smooth muscle cells isolated from diabetic streptozotocin-treated rats and db/db mice*. Mol Cell Biochem, 1992. **109**(2): p. 185-8.
96. Takahashi, T., et al., *Impaired intracellular signal transduction in gastric smooth muscle of diabetic BB/W rats*. Am J Physiol, 1996. **270**(3 Pt 1): p. G411-7.
97. Moscoso, G.J., M. Driver, and R.J. Guy, *A form of necrobiosis and atrophy of smooth muscle in diabetic gastric autonomic neuropathy*. Pathol Res Pract, 1986. **181**(2): p. 188-94.
98. Bytzer, P., et al., *Prevalence of gastrointestinal symptoms associated with diabetes mellitus: a population-based survey of 15,000 adults*. Arch Intern Med, 2001. **161**(16): p. 1989-96.
99. Comer, F.I. and G.W. Hart, *O-Glycosylation of nuclear and cytosolic proteins. Dynamic interplay between O-GlcNAc and O-phosphate*. J Biol Chem, 2000. **275**(38): p. 29179-82.
100. Hart, G.W., et al., *O-GlcNAcylation of key nuclear and cytoskeletal proteins: reciprocity with O-phosphorylation and putative roles in protein multimerization*. Glycobiology, 1996. **6**(7): p. 711-6.
101. Clark, R.J., et al., *Diabetes and the accompanying hyperglycemia impairs cardiomyocyte calcium cycling through increased nuclear O-GlcNAcylation*. J Biol Chem, 2003. **278**(45): p. 44230-7.
102. Hedou, J., et al., *O-linked N-acetylglucosaminylation is involved in the Ca²⁺ activation properties of rat skeletal muscle*. J Biol Chem, 2007. **282**(14): p. 10360-9.
103. Konrad, R.J. and J.E. Kudlow, *The role of O-linked protein glycosylation in beta-cell dysfunction*. Int J Mol Med, 2002. **10**(5): p. 535-9.
104. Ramirez-Correa, G.A., et al., *O-linked GlcNAc modification of cardiac myofilament proteins: a novel regulator of myocardial contractile function*. Circ Res, 2008. **103**(12): p. 1354-8.
105. Good, P.F., et al., *Protein nitration in Parkinson's disease*. J Neuropathol Exp Neurol, 1998. **57**(4): p. 338-42.
106. He, C., H.C. Choi, and Z. Xie, *Enhanced tyrosine nitration of prostacyclin synthase is associated with increased inflammation in atherosclerotic carotid arteries from type 2 diabetic patients*. Am J Pathol. **176**(5): p. 2542-9.
107. Rabbani, N., et al., *Increased glycation and oxidative damage to apolipoprotein B100 of LDL cholesterol in patients with type 2 diabetes and effect of metformin*. Diabetes. **59**(4): p. 1038-45.

108. Singer, II, et al., *Expression of inducible nitric oxide synthase and nitrotyrosine in colonic epithelium in inflammatory bowel disease*. Gastroenterology, 1996. **111**(4): p. 871-85.
109. Smith, M.A., et al., *Widespread peroxynitrite-mediated damage in Alzheimer's disease*. J Neurosci, 1997. **17**(8): p. 2653-7.
110. Zou, M.H., R. Cohen, and V. Ullrich, *Peroxynitrite and vascular endothelial dysfunction in diabetes mellitus*. Endothelium, 2004. **11**(2): p. 89-97.
111. Ceriello, A., *Oxidative stress and diabetes-associated complications*. Endocr Pract, 2006. **12 Suppl 1**: p. 60-2.
112. Kang, M., G.R. Ross, and H.I. Akbarali, *The effect of tyrosine nitration of L-type Ca²⁺ channels on excitation-transcription coupling in colonic inflammation*. Br J Pharmacol. **159**(6): p. 1226-35.
113. Kang, M., G.R. Ross, and H.I. Akbarali, *COOH-terminal association of human smooth muscle calcium channel Ca(v)1.2b with Src kinase protein binding domains: effect of nitrotyrosylation*. Am J Physiol Cell Physiol, 2007. **293**(6): p. C1983-90.
114. Bauer, A.J., *Mentation on the immunological modulation of gastrointestinal motility*. Neurogastroenterol Motil, 2008. **20 Suppl 1**: p. 81-90.
115. Mikkelsen, H.B., J.O. Larsen, and H. Hadberg, *The macrophage system in the intestinal muscularis externa during inflammation: an immunohistochemical and quantitative study of osteopetrotic mice*. Histochem Cell Biol, 2008. **130**(2): p. 363-73.
116. Horie, A., et al., *Proinflammatory cytokines suppress the expression level of protease-activated receptor-2 through the induction of iNOS in rat colon*. J Vet Med Sci, 2009. **71**(12): p. 1609-15.
117. Kinoshita, K., et al., *Role of TNF-alpha in muscularis inflammation and motility disorder in a TNBS-induced colitis model: clues from TNF-alpha-deficient mice*. Neurogastroenterol Motil, 2006. **18**(7): p. 578-88.
118. Schmidt, J., et al., *Proinflammatory role of leukocyte-derived Egr-1 in the development of murine postoperative ileus*. Gastroenterology, 2008. **135**(3): p. 926-36, 936 e1-2.
119. Kalff, J.C., et al., *Role of inducible nitric oxide synthase in postoperative intestinal smooth muscle dysfunction in rodents*. Gastroenterology, 2000. **118**(2): p. 316-27.
120. Turler, A., et al., *Leukocyte-derived inducible nitric oxide synthase mediates murine postoperative ileus*. Ann Surg, 2006. **244**(2): p. 220-9.
121. Manabe, I. and G.K. Owens, *The smooth muscle myosin heavy chain gene exhibits smooth muscle subtype-selective modular regulation in vivo*. J Biol Chem, 2001. **276**(42): p. 39076-87.
122. Li, L., et al., *Expression of the SM22a promoter in transgenic mice provides evidence for distinct transcriptional regulatory programs in vascular and visceral smooth muscle cells*. J. Cell Biol., 1996. **132**: p. 849-859.

123. Chang, D.F., et al., *Cysteine-rich LIM-only proteins CRP1 and CRP2 are potent smooth muscle differentiation cofactors*. Dev Cell, 2003. **4**(1): p. 107-18.
124. Li, S., et al., *The serum response factor coactivator myocardin is required for vascular smooth muscle development*. Proc Natl Acad Sci U S A, 2003. **100**(16): p. 9366-70.
125. Oh, J., J.A. Richardson, and E.N. Olson, *Requirement of myocardin-related transcription factor-B for remodeling of branchial arch arteries and smooth muscle differentiation*. Proc Natl Acad Sci U S A, 2005. **102**(42): p. 15122-7.
126. Li, J., et al., *Myocardin-related transcription factor B is required in cardiac neural crest for smooth muscle differentiation and cardiovascular development*. Proc Natl Acad Sci U S A, 2005. **102**(25): p. 8916-21.
127. Herring, B.P., et al., *Targeted expression of SV40 large T-antigen to visceral smooth muscle induces proliferation of contractile smooth muscle cells and results in megacolon*. J Biol Chem, 1999. **274**(25): p. 17725-32.
128. Li, L., et al., *Expression of the SM22a promoter in transgenic mice provides evidence for distinct transcriptional regulatory programs in vascular and visceral smooth muscle cells*. Journal of Cell Biology, 1996. **132**: p. 849-859.
129. Camoretti-Mercado, B., et al., *Expression and cytogenetic localization of the human SM22 gene (TAGLN)*. Genomics, 1998. **49**(3): p. 452-7.
130. Wang, Z., et al., *Myocardin is a master regulator of smooth muscle gene expression*. Proc Natl Acad Sci U S A, 2003. **100**(12): p. 7129-34.
131. Herring, B.P., et al., *Regulation of myosin light chain kinase and telokin expression in smooth muscle tissues*. Am J Physiol Cell Physiol, 2006.
132. Yin, F., et al., *130-kDa smooth muscle myosin light chain kinase is transcribed from a CARG-dependent, internal promoter within the mouse mylk gene*. Am J Physiol Cell Physiol, 2006. **290**(6): p. C1599-609.
133. Herring, B.P., S. Dixon, and P.J. Gallagher, *Smooth muscle myosin light chain kinase expression in cardiac and skeletal muscle*. Am J Physiol Cell Physiol, 2000. **279**(5): p. C1656-64.
134. Li, L., et al., *SM22 alpha, a marker of adult smooth muscle, is expressed in multiple myogenic lineages during embryogenesis*. Circ. Research, 1996. **78**(2): p. 188-95.
135. Moniot, B., et al., *SOX9 specifies the pyloric sphincter epithelium through mesenchymal-epithelial signals*. Development, 2004. **131**(15): p. 3795-804.
136. Zhou, J. and B.P. Herring, *Mechanisms responsible for the promoter-specific effects of myocardin*. J Biol Chem, 2005. **280**(11): p. 10861-9.
137. Yoshida, T., et al., *Myocardin is a key regulator of CARG-dependent transcription of multiple smooth muscle marker genes*. Circ Res, 2003. **92**(8): p. 856-64.

138. Forrest, A. and M. Parsons, *The enhanced spontaneous activity of the diabetic colon is not the consequence of impaired inhibitory control mechanisms*. *Auton Autacoid Pharmacol*, 2003. **23**(3): p. 149-58.
139. Chandrasekharan, B., et al., *Colonic motor dysfunction in human diabetes is associated with enteric neuronal loss and increased oxidative stress*. *Neurogastroenterol Motil*. **23**(2): p. 131-e26.
140. Rodenberg, J.M., et al., *Regulation of serum response factor activity and smooth muscle cell apoptosis by chromodomain helicase DNA-binding protein 8*. *Am J Physiol Cell Physiol*. **299**(5): p. C1058-67.
141. Gunst, S.J., W.T. Gerthoffer, and M.H. al-Hassani, *Ca²⁺ sensitivity of contractile activation during muscarinic stimulation of tracheal muscle*. *Am J Physiol*, 1992. **263**(6 Pt 1): p. C1258-65.
142. Copeland, R.J., J.W. Bullen, and G.W. Hart, *Cross-talk between GlcNAcylation and phosphorylation: roles in insulin resistance and glucose toxicity*. *Am J Physiol Endocrinol Metab*, 2008. **295**(1): p. E17-28.
143. Furlan, M.M., et al., *Number and size of myenteric neurons of the duodenum of adult rats with acute diabetes*. *Arq Neuropsiquiatr*, 1999. **57**(3B): p. 740-5.
144. Wegener, M., et al., *Gastrointestinal transit disorders in patients with insulin-treated diabetes mellitus*. *Dig Dis*, 1990. **8**(1): p. 23-36.
145. Iber, F.L., et al., *Relation of symptoms to impaired stomach, small bowel, and colon motility in long-standing diabetes*. *Dig Dis Sci*, 1993. **38**(1): p. 45-50.
146. Ratz, P.H., et al., *Regulation of smooth muscle calcium sensitivity: KCl as a calcium-sensitizing stimulus*. *Am J Physiol Cell Physiol*, 2005. **288**(4): p. C769-83.
147. Takahashi, T. and C. Owyang, *Regional differences in the nitrergic innervation between the proximal and the distal colon in rats*. *Gastroenterology*, 1998. **115**(6): p. 1504-12.
148. Tong, W.D., et al., *Effects of autonomic nerve stimulation on colorectal motility in rats*. *Neurogastroenterol Motil*. **22**(6): p. 688-93.
149. Beshay, E. and S. Carrier, *Oxidative stress plays a role in diabetes-induced bladder dysfunction in a rat model*. *Urology*, 2004. **64**(5): p. 1062-7.
150. Ferrini, M.G., et al., *The Genetic Inactivation of Inducible Nitric Oxide Synthase (iNOS) Intensifies Fibrosis and Oxidative Stress in the Penile Corpora Cavernosa in Type 1 Diabetes*. *J Sex Med*.
151. Poladia, D.P. and J.A. Bauer, *Oxidant driven signaling pathways during diabetes: role of Rac1 and modulation of protein kinase activity in mouse urinary bladder*. *Biochimie*, 2004. **86**(8): p. 543-51.
152. Ross, G.R., M. Kang, and H.I. Akbarali, *Colonic inflammation alters Src kinase-dependent gating properties of single Ca²⁺ channels via tyrosine nitration*. *Am J Physiol Gastrointest Liver Physiol*. **298**(6): p. G976-84.

153. Vangheluwe, P., et al., *Modulating sarco(endo)plasmic reticulum Ca²⁺ ATPase 2 (SERCA2) activity: cell biological implications*. Cell Calcium, 2005. **38**(3-4): p. 291-302.
154. Chirino, Y.I., M. Orozco-Ibarra, and J. Pedraza-Chaverri, *[Role of peroxynitrite anion in different diseases]*. Rev Invest Clin, 2006. **58**(4): p. 350-8.
155. Fraser, R.J., et al., *Hyperglycaemia slows gastric emptying in type 1 (insulin-dependent) diabetes mellitus*. Diabetologia, 1990. **33**(11): p. 675-80.
156. Schvarcz, E., et al., *Physiological hyperglycemia slows gastric emptying in normal subjects and patients with insulin-dependent diabetes mellitus*. Gastroenterology, 1997. **113**(1): p. 60-6.
157. Blache, P., et al., *SOX9 is an intestine crypt transcription factor, is regulated by the Wnt pathway, and represses the CDX2 and MUC2 genes*. J Cell Biol, 2004. **166**(1): p. 37-47.
158. Verdu, E.F. and S.M. Collins, *Microbial-gut interactions in health and disease. Irritable bowel syndrome*. Best Pract Res Clin Gastroenterol, 2004. **18**(2): p. 315-21.
159. Musso, G., R. Gambino, and M. Cassader, *Interactions between gut microbiota and host metabolism predisposing to obesity and diabetes*. Annu Rev Med. **62**: p. 361-80.
160. Schmidt, R.E., *Neuropathology and pathogenesis of diabetic autonomic neuropathy*. Int Rev Neurobiol, 2002. **50**: p. 257-92.
161. Schmidt, R.E., et al., *Experimental rat models of types 1 and 2 diabetes differ in sympathetic neuroaxonal dystrophy*. J Neuropathol Exp Neurol, 2004. **63**(5): p. 450-60.

Curriculum vitae

Ketrija Touw

EDUCATION

- 2005-2011 Ph.D., Department of Cellular and Integrative Physiology, Indiana University, Indianapolis, Indiana, USA
Minor: Diabetes and Obesity
- 1999-2000 M.S. student, Human and Animal Physiology, Department of Biology, University of Latvia, Riga, Latvia
- 1995-1999 B.S., Biology, University of Latvia, Riga, Latvia

PROFESSIONAL EXPERIENCE

- 2003-2005 Research Technician, Department of Physiology, Indiana University School of Medicine, Indianapolis, Indiana, USA
- 1999-2000 Research Technician, Department of Medical Chemistry, Latvian Institute of Organic Synthesis, Riga, Latvia
- 1998-1999 Undergraduate Researcher, Institute of Biology, Salaspils, Latvia

TEACHING EXPERIENCE

- 2009 Human Physiology, F503: Stomach lecture

AWARDS

- 2011 Indiana Physiological Society Abstract Award
- 2008 Takeda Travel Award from the APS Gastrointestinal and Liver Section
- 2008 IU School of Medicine Graduate Student Travel Award
- 2007-2010 T32 Diabetes and Obesity training grant
- 2007 Moenkhaus Physiology Graduate Fellowship for Academic Excellence
- 2006 Moenkhaus Physiology Graduate Fellowship for Academic Excellence

MANUSCRIPTS

Touw K., Chakraborty S., Zhang W., Obukhov A.G., Tune J.D., Gunst S.J., Herring B.P. "Type 1 diabetes leads to altered calcium signaling in chronic and acute diabetic mice." (Under editorial review)

Rodenberg J.M., Hoggatt A.M., Chen M., **Touw K.**, Jones R., Herring B.P. "Regulation of serum response factor activity and smooth muscle cell apoptosis by chromodomain helicase DNA-binding protein 8." *Am J Physiol Cell Physiol.* Nov;299(5):C1058-67. 2010

Touw K., Hoggatt A.M., Simon G. and Herring B.P. "*Hprt*-targeted transgenes provide new insights into smooth muscle-restricted promoter activity." *Am J Physiol Cell Physiol*. Mar;292(3):C1024-32. 2007

ABSTRACTS

Ketrija Touw, Saikat Chakraborty, Wenwu Zhang, Alexander Obukhov, Johnathan Tune, Susan Gunst, Paul Herring. "The effects of Type 1 diabetes on colon smooth muscle." Poster Presentation. Experimental Biology 2011, Washington D.C.

Ketrija Touw, Saikat Chakraborty, Wenwu Zhang, Alexander Obukhov, Johnathan Tune, Susan Gunst, Paul Herring. "Type 1 diabetes leads to altered calcium signaling in chronic and acute diabetic mice." Poster Presentation. Indiana Physiological Society Meeting. February 5, 2011. Indianapolis, IN

Ketrija Touw, Johnathan D. Tune, B. Paul Herring. "Diabetes effects on colon smooth muscle." Poster Presentation. Department of Cellular and Integrative Physiology Statewide Retreat. October 2, 2009. Indianapolis, IN

Ketrija Touw, Johnathan D. Tune, B. Paul Herring. "Diabetes effects on colon smooth muscle" CTSI poster session presentation, September 16, 2009. Indianapolis, IN

Ketrija Touw, Jiliang Zhou, and B. Paul Herring. "Transcriptional regulation of GI smooth muscle in normal and diabetic mice." Poster Presentation. Department of Cellular and Integrative Physiology Statewide Retreat. October 17, 2008. Indianapolis, IN

Ketrija Touw, Jiliang Zhou, and B. Paul Herring. "Transcriptional regulation of GI smooth muscle in normal and diabetic mice." Poster Presentation. Experimental Biology Meeting. April 2008. San Diego, CA

Ketrija Touw, April M. Hoggatt, Gina Simon and B. Paul Herring. "Transcriptional regulation of GI smooth muscle." Poster Presentation. Department of Cellular and Integrative Physiology Statewide Retreat. August 2007. Indianapolis, IN

Ketrija Touw, April M. Hoggatt, Gina Simon and B. Paul Herring. "*Hprt*-targeted transgenes provide new insights into smooth muscle-restricted promoter activity." Poster Presentation. Department of Cellular and Integrative Physiology Statewide Retreat. August 2006. Indianapolis, IN

B. Paul Herring, **Ketrija Touw**, April Hoggatt, Julia Azriel, Jiliang Zhou, Omar El-Mounayri. "Smooth muscle cell-restricted expression of telokin." *Endothelium* (2004), **10**, 357

Paul Herring, **Ketrija Touw**, April Hoggatt, Julia Azriel, Omar El-Mounayri, Jiliang Zhou and Feng Yin. "Mechanisms of smooth muscle cell-restricted gene expression." *Cardiovascular Pathology* (2004) 13, Issue 3, Supplement 1, p12

PRESENTATIONS

"Diabetes induced changes in colon smooth muscle" IUSM Physiology Department seminar series. June 2009

"Transcriptional regulation of GI smooth muscle in normal and diabetic mice" Sigma Xi Graduate Research Competition. May 2008

"Transcriptional regulation of GI smooth muscle in health and disease" IUSM Physiology Department Thesis Proposal. December 2007

"Transcriptional regulation of telokin in GI smooth muscle" IUSM Physiology Department seminar series. May 2007

"*Hprt* targeted mice reveal distinct regulatory modules that control Telokin and *SM22 α* expression" Sigma Xi Graduate Research Competition. June 2006

PROFESSIONAL SOCIETIES

2009-2010 American Physiology Society

PROFESSIONAL SERVICE

2009 Mentor for NIH T35 "Short term training for minority students"

2007-2009 Cellular and Integrative Physiology Graduate Student representative to IU School of Medicine 2007-2009

2007-2008 Student mentor for incoming students

2007-2008 Judging panelist for Student Travel Grant Competition

2007 Student mentor for Physiology F503 class Fall semester